Macroscopic Dislocation Modelling

Stephen Patrick Tighe
Hertford College
Oxford

Thesis submitted for the degree of Doctor of Philosophy

Michaelmas Term 1992

Abstract

Work-hardened metals typically possess large numbers of dislocations in complex three-dimensional configurations about which little is known theoretically. Here these large numbers of dislocations are accounted for by means of a dislocation density tensor, which is obtained by applying an averaging process to families of discrete dislocations. Some simple continuous distributions are examined and an analogy is drawn with solenoids in electromagnetism before the question of the equilibrium of dislocation configurations is studied. It is then proved that the only finite, simply-connected distribution of dislocations in equilibrium in the absence of applied stresses are ones in which all components of stress vanish everywhere. Some examples of these zero stress everywhere (ZSE) distributions are then given, and the concept of 'plastic distortion' is used to facilitate their interpretation as rotations of the crystal lattice.

Plastic distortion can also be understood as a distribution of infinitesimal dislocation loops ('Kroupa loops'), and this idea is used in Chapter 4 to investigate the dislocation distributions which correspond to elastic inclusions.

The evolution, under an applied stress, of some simple ZSEs is analysed, and the idea of 'polarisation' is introduced, again in analogy with electromagnetism. Finally, a mechanism is conjectured for the onset of plastic flow.

Acknowledgements

I would like to thank my supervisors Dr. J.R. Ockendon and Dr. S.D. Howison for their support and advice, and also Dr. A.K. Head for many helpful discussions and for encouragement. Additionally, I would like to thank Professor E. Kröner for inspiration, and Professor G. Herrmann for his assistance.

My colleagues, especially Jon Chapman, Jonathan Evans, Chris Huntingford, Brian Hunton, John Morgan and Michael Peake, have my gratitude both for academic help freely given, and for their friendship.

I would also like to thank my family and friends for their unstinting support and encouragement.

The financial support of the Science and Engineering Research Council is also gratefully acknowledged.

Contents

Chapter 1

Introduction

The discovery of the crystallinity of metals led to the recognition that plastic deformation was the result of the shearing of one part of a crystal with respect to another. This eventually resulted in the postulation by Orowan (1934), Polanyi (1934) and Taylor (1934) of the edge dislocation as an explanation of plastic shear. Many years prior to this, Volterra (1907) and others (see Love 1927) considered the elastic properties of homogeneous, isotropic cylinders which had been cut, strained and welded together again to produce bodies which were 'internally' strained - that is, strained in the absence of external stresses. However, it was not until after the work of Orowan, Polanyi and Taylor, that the relation between the studies of internally strained elastic continua and crystal dislocations was noticed.

In common with these early advances, most of the attention devoted since then to the theory of dislocations has concerned single dislocations or simple two-dimensional arrays. However, experiment confirms that plastic deformation produces complicated three-dimensional distributions of dislocations. A description of static equilibrium arrangements, and of the evolution of such distributions is the goal of a macroscopic theory of dislocation plasticity, to which this thesis aims to contribute.

The mathematical model (for static problems) used here will be essentially that of Kröner (1958), and cast within the framework of linear isotropic elasticity. An added ingredient is the condition for equilibrium - that the force on a dislocation, as given by Peach & Koehler (1950), should be zero.

Later in this chapter the aims of the theory are discussed in greater detail, and a review of linear elasticity is given. The basic concepts relating to the creation

and motion of dislocations are then explained and a survey of previous discrete and continuum models of dislocation behaviour is presented before the properties of single dislocations are considered. The stress fields of isolated straight line dislocations are derived, and the idea of incompatibility is introduced. This is then generalised, and Kröner's theory of stress functions is developed in order to obtain the stress field of a curved dislocation.

The introduction, in Chapter 2, of a dislocation density tensor incorporates into the model a description of large numbers of dislocations. This is done by means of an averaging process in which discrete dislocations are approximated by a continuous distribution. The stress, strain and incompatibility are each given in terms of the dislocation density tensor, and some simple examples of continuous distributions are presented.

The central theme of the thesis will concern configurations of dislocations for which every component of the stress tensor vanishes. These zero stress everywhere (ZSE) distributions correspond to a state of minimum (that is, zero) elastic strain energy, and so are likely to be found in real materials. In addition, in Chapter 3, it is proved that, though for equilibrium only one component of stress need be zero, and then only where there are dislocations, those distributions which occupy a simply-connected, spatially bounded region, and which are in self-equilibrium (that is, in equilibrium under zero applied stress) must be of ZSE type.

Kröner's (1955) idea of "plastic distortion" is the subject matter of Chapter 4. Unlike Kröner, however, who proceeded from incompatibility, plastic distortion is here developed from what will be known as "total displacement" - a generalised function interpretation of Burgers' (1939) expression for the displacement field of a dislocation. Plastic distortion is then used to give a geometrical interpretation of the ZSEs encountered previously, and an alternative method of proof of the theorem mentioned above is presented.

Finally, the responses to an applied stress of some simple ZSEs are analysed in Chapter 5, and some conjectures are presented concerning the behaviour of more general distributions with a view to explaining the onset of plastic deformation.

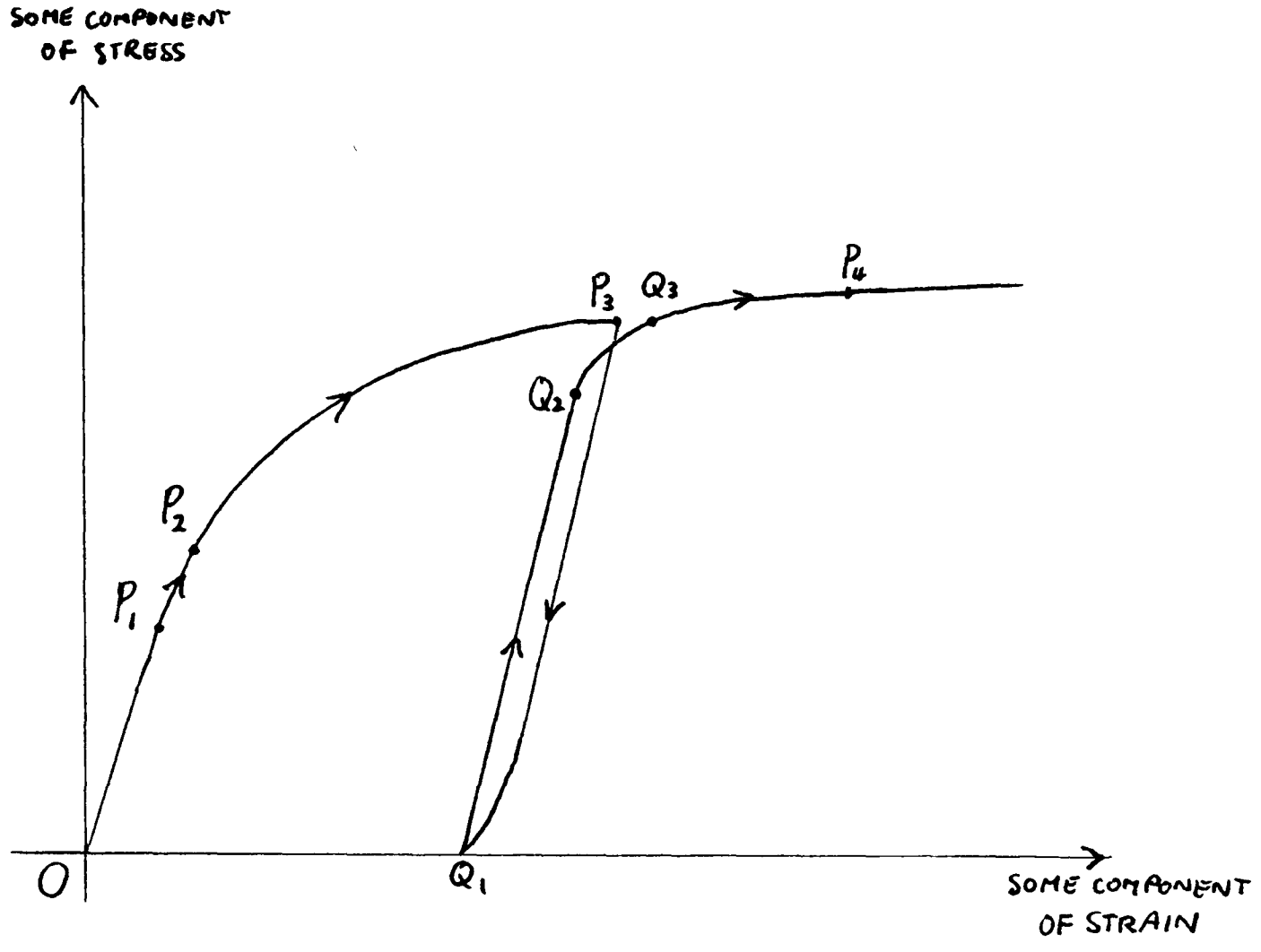

Figure 1.1: Stress-strain diagram for a typical crystalline metal under load.

1.1 The Stress-Strain Curve

The relation between the stress and strain in a typical crystalline metal is represented schematically in Fig. 1.1. Initially, as the applied load is increased, the specimen responds linearly, and if the load is removed the original shape of the specimen will be regained. Thus, along OP_1 Hooke's law holds, and the point P_1, at which Hooke's law ceases to model the behaviour of the material, is known as the proportional limit. Between P_1 and P_2 the stress-strain relation is not linear, but the metal is, nevertheless, still elastic. Beyond the point P_2 the specimen suffers an irreversible deformation. P_2 is thus known as the yield point, and the stress corresponding to P_2 is the yield stress.

Between P_2 and P_3 the gradient of the stress-strain curve usually decreases, so that the strain increases rapidly with a small increase in stress. If at P_3 the specimen is unloaded, it does so linearly and elastically, although with a small plastic component just prior to complete removal of the load at Q_1.

If the material is then reloaded, the process repeats itself, with the specimen obeying Hooke's law between Q_1 and Q_2, which is the new elastic limit. The

material yields at Q_3 and plastically deforms along Q_3P_4, which is an extrapolation of the curve between P_2 and P_3. As the material is repeatedly loaded, unloaded and reloaded, the proportional limit can be seen to increase. This phenomenon is known as work-hardening.

In this thesis we will be concerned mainly with the state of the material at points on the strain axis (such as Q_1) when the material is unloaded although it has been previously strained. The state of the material at the yield stress (such as Q_2) will be touched upon in Chapter 5.

1.2 Review of Linear Elasticity

It is assumed that the materials we are dealing with obey the laws of linear elasticity theory away from any dislocations. Cartesian axes will be used throughout and we define the Lagrangian coordinates of a typical point $\boldsymbol{X}$ in the material by

$$X_i = X_i(x_1, x_2, x_3) \qquad (i = 1, 2, 3),$$

where (x_1, x_2, x_3) is the reference position of the particle now at $\boldsymbol{X}$. The Einstein summation convention will be used; that is, we sum over repeated indices. Also, all indices will take the values 1, 2 and 3 unless otherwise stated.

The components of displacement are denoted by u_i. Differentiation will be denoted by a comma, so that differentiation with respect to x_j, for example, will be written

$$u_{i,j} = \frac{\partial u_i}{\partial x_j},$$

and differentiation with respect to x'_j will be denoted

$$u_{i,j'} = \frac{\partial u_i}{\partial x'_j}.$$

Bold and suffix notation will be used interchangeably both for vectors and second order tensors. Where there is ambiguity, the precise version in suffix notation will be given.

The components of the strain tensor are defined as

$$e_{ij} = \frac{1}{2}(u_{i,j} + u_{j,i}), \tag{1.1}$$

wherever single-valued differentiable displacements u_i exist. Given such a displacement field $\boldsymbol{u}$ the strain components are easily calculated. However, for a given strain, a displacement field satisfying (1.1) may not exist. This is effectively because the second derivatives of $\boldsymbol{u}$ may not be continuous, so that the equations

$$\frac{\partial^2 u_1}{\partial x_1 \partial x_2} = \frac{\partial^2 u_1}{\partial x_2 \partial x_1}, \qquad \frac{\partial^2 u_2}{\partial x_1 \partial x_3} = \frac{\partial^2 u_2}{\partial x_3 \partial x_1}, \text{ etc.},$$

may not hold. The conditions for a single-valued displacement field to exist can be written

$$\varepsilon_{ikl}\varepsilon_{jmn}e_{ln,km} = 0 \qquad (i \leq j), \tag{1.2}$$

and these are known as the compatibility equations. The necessity of such equations can be established by cross-differentiation of equation (1.1), and their sufficiency may be shown as follows. Suppose we define the rotation

$$\omega_i = \frac{1}{2}\varepsilon_{ikl}u_{l,k}.$$

Then, by (1.1) we must have the relation

$$\omega_{i,n} = \varepsilon_{ikl}e_{ln,k},$$

if ω_i and e_{ln} are derived from continuous, single-valued, differentiable displacements u_i. Now, the rotation ω_i must itself be continuous and single-valued. Thus, the integral

$$\omega_i(B) - \omega_i(A) = \int_A^B \varepsilon_{ikl}e_{ln,k}dx_n,$$

which is the difference in value of the rotation between the points A and B, must be path-independent. In other words the curl of the integrand must vanish, which gives (1.2).

Since we will not be considering dynamic problems, nor problems involving body forces, the conditions for translational equilibrium are written in the form

$$\sigma_{ij,j} = 0, \tag{1.3}$$

where σ_{ij} are the components of the stress tensor.

The stress and strain components are related by Hooke's law, which, in an isotropic solid, is written

$$\sigma_{ij} = 2\mu e_{ij} + \lambda e_{kk}\delta_{ij}, \tag{1.4}$$

with inverse relation

$$e_{ij} = \frac{1}{2\mu}\left(\sigma_{ij} - \frac{\nu}{\nu+1}\sigma_{kk}\delta_{ij}\right), \tag{1.5}$$

where δ_{ij} is the Kronecker delta, λ and μ are the Lamé constants, the bulk and shear modulus respectively, and ν is Poisson's ratio: $\nu = \frac{\lambda}{2(\lambda+\mu)}$.

In cases where the strains are compatible (that is, (1.2) is satisfied), we can make two further statements concerning the stress and strain. Substituting (1.4) into (1.3) gives

$$2\mu e_{ij,j} + \lambda e_{kk,i} = 0.$$

Replacing $\boldsymbol{e}$ by (1.1), we obtain

$$(\lambda+\mu)u_{i,ij} + \mu\nabla^2 u_j = 0, \tag{1.6}$$

which in vector notation is

$$(\lambda+\mu)\boldsymbol{\nabla}(\boldsymbol{\nabla}.\boldsymbol{u}) + \mu\nabla^2\boldsymbol{u} = 0,$$

and is known as Navier's equation. Differentiating (1.6) with respect to x_j and adding gives

$$\nabla^2 u_{j,j} = \nabla^2 e_{jj} = 0, \tag{1.7}$$

and so from Hooke's law

$$\nabla^2\sigma_{kk} = (2\mu+3\lambda)\nabla^2 e_{kk} = 0.$$

Taking the Laplacian of (1.6) and using (1.7) gives

$$\nabla^4 u_j = 0,$$

and so from (1.1)

$$\nabla^4 e_{ij} = 0,$$

which, from (1.4) leads to

$$\nabla^4\sigma_{ij} = 0. \tag{1.8}$$

Thus, all the stress components are everywhere biharmonic functions.

1.3 Basic Concepts Concerning Discrete Dislocations

1.3.1 Definition

Dislocations can be envisaged physically in one of two ways.

(i). As a crystal defect. At the atomic level a dislocation is a curve of misfit of atoms. As we shall see shortly, there are two types of dislocation - the 'screw' and the 'edge'. The screw dislocation is somewhat complicated to envisage at this level, and so attention will be concentrated here on the edge dislocation, an example of which is given in Fig. 1.2(b). Real dislocation sources are discussed below, but for conceptual purposes an edge dislocation may be thought to have been created by the insertion into the crystal of an extra sheet of atoms, which covers a half-plane as shown in Fig. 1.2. The dislocation line is then the boundary of the half-plane - that is, the line through X perpendicular to the plane of the paper - and we may deduce certain properties from this definition. Being the boundary of a half-plane, the dislocation line must not end in the material - a property which all dislocations share. Also, the displacement caused by the insertion of the sheet of atoms can be seen to be constant along the line of the dislocation because the sheet has a uniform thickness. This displacement can be more precisely defined in terms of a 'Burgers circuit'. A closed circuit SABCF is drawn which encloses the dislocation line in Fig. 1.2(b), the same circuit is then drawn in the perfect reference lattice and the closure failure **FS** is known as the 'Burgers vector'.

(ii). Considering the material as an elastic continuum rather than a crystal with an ordered lattice, dislocations may be created through the 'cut-and-weld' procedure. Straight line dislocations are depicted in Fig. 1.3. We take a cylinder of metal and cut it along a half-plane whose boundary is the axis of the cylinder. The two faces of the cut are displaced relative to each other by a vector $\boldsymbol{B}$, and are then welded together again, leaving the body in a state of self-stress. This displacement is equivalent to the Burgers vector mentioned above. If $\boldsymbol{B}$ is parallel to the axis then a screw dislocation is produced; if $\boldsymbol{B}$ is perpendicular to the axis, an edge dislocation is formed.

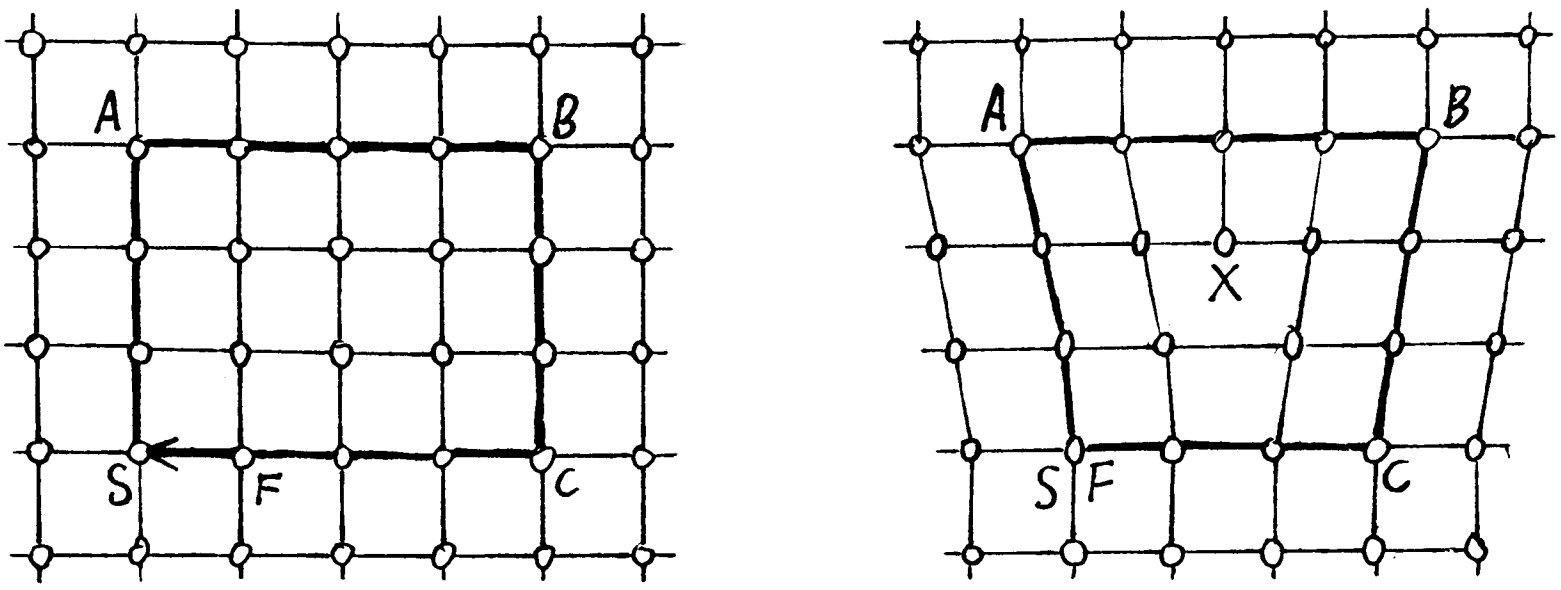

Figure 1.2: (a) Perfect lattice; (b) Lattice with extra half-plane of atoms, consisting of those rows of atoms above X. SABCF is the Burgers circuit, with the closure failure $\boldsymbol{FS}$ in (a) being equal to the Burgers vector.

In a similar fashion curved dislocations can be viewed as being created by cutting along a surface whose boundary is the curve, displacing the two faces of the cut relative to one another and then welding. Overlapping material would of course need to be removed and any gaps filled in with extra material.

On completion of the cut-and-weld procedure, we notice that across the cut surface there is a finite jump, equal to $\boldsymbol{B}$, in the displacement $\boldsymbol{u}$ from the reference state. Thus du_i is no longer a perfect derivative, and the line integral of the displacements around a closed curve γ, which links the dislocation as in Fig. 1.4, is no longer zero, but equal to the Burgers vector

$$B_i = \oint_\gamma du_i = \oint_\gamma u_{i,j} dx_j. \tag{1.9}$$

The integral is taken round γ in a clockwise right-handed sense relative to $\boldsymbol{\tau}$, a unit tangent vector assigned to the dislocation line.

We will be concerned with those dislocations which are created by displacing the two faces of the cut surface by a constant vector relative to each other, and which thus have a constant Burgers vector. A curved dislocation will therefore have, at every point of its line, a component of Burgers vector which is tangent to the line and a component perpendicular to the line. Hence, a curved dislocation has a linear combination of edge and screw character.

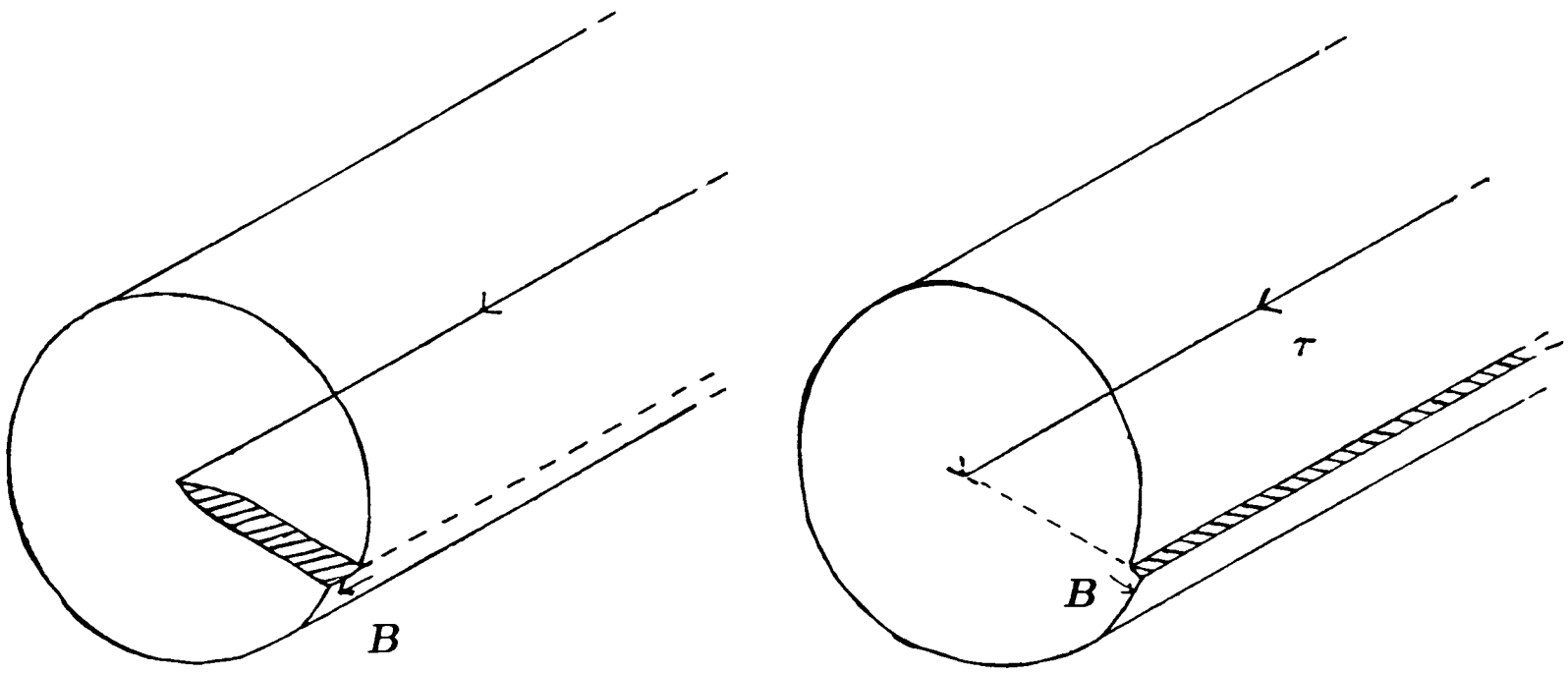

(a) (b)

Figure 1.3: A cylinder of the crystal showing the geometry of, (a) a screw dislocation; (b) an edge dislocation.

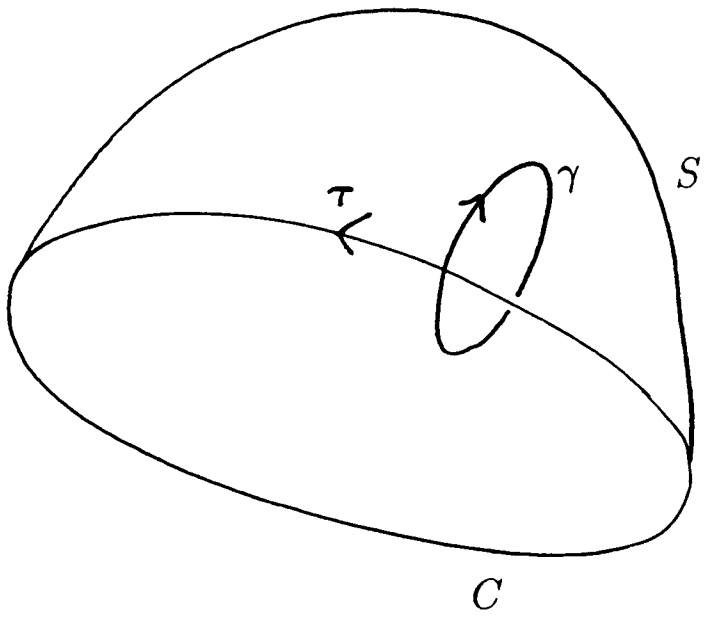

Figure 1.4: A dislocation line linked by a curve γ, which is the boundary of a surface S.

From the cut-and-weld procedure, it is clear that a dislocation, being the boundary of the cut surface, cannot end in the material, and, as stated above, the dislocations we will consider will have Burgers vectors which are constant along the dislocation line. In fact, it can be proved in more general circumstances (see Nabarro 1967) that, in order for the stresses and strains to be continuous away from the dislocation line, the relative displacement of the two faces of the cut must be a rigid body displacement - that is, a translation or a rigid body rotation.

Of these two definitions of a dislocation most use will be made of the second, based on the cut-and-weld procedure, as this allows us access to the tools of the continuum theory of elasticity. However, as our goal is a model of dislocation plasticity, which is a consequence of the crystalline nature of metals, we wish to incorporate into the continuum model certain aspects of dislocation behaviour which are determined by the crystal lattice.

1.3.2 Dislocation Dynamics and Slip Planes

One such aspect of the influence of the crystal lattice is the motion of a dislocation. Fig. 1.5 depicts the movement through the crystal lattice of an edge dislocation under the influence of an applied shear stress. Away from the dislocation the atom spacings are uniform, whereas close to the dislocation they are not. This ensures that atom 1, in breaking free of atom 3 and attaching to atom 2, moves only a small distance (though large compared to the displacement of other atoms) while the extra half-plane is shifted from x to y. As the dislocation continues to glide and this process is repeated, neighbouring atoms such as 1 and 3 are displaced relative to each other by the Burgers vector. Thus the direction of slip for an edge dislocation is, by necessity, parallel to the Burgers vector, and for a dislocation with an edge component slip will take place in the plane spanned by $\boldsymbol{B}$ and $\boldsymbol{\tau}$. This plane is known as the *slip* (or *glide*) plane. In the case of screw dislocations for which the tangent and Burgers vectors are parallel, the slip plane is not unique[1] but in what follows the plane chosen as slip plane will be explicitly stated.

[1] In practice pure screw dislocations are unlikely to occur; most dislocations are curved though they may have straight segments of pure screw character. It is therefore reasonable to speak of the slip plane of a screw dislocation.

Figure 1.5: Movement of an edge dislocation under an applied stress, indicated by arrows. (Hull & Bacon 1984).

A *slip system* is defined as a family of slip planes, whose unit normal is $\boldsymbol{m}$, say, together with those dislocations lying in these slip planes, each of whose Burgers vector is $\boldsymbol{B}$, say.

In what follows it will be assumed that the possible slip planes are those planes parallel to the coordinate planes, so that in each slip plane there are two Burgers vectors, parallel to the two coordinate axes that lie in that particular plane. In terms of the crystal lattice this implies a 'simple cubic' structure which, although unrealistic[2] as no metal has such a lattice, is adopted for simplicity. In addition, it will be assumed that glide dislocations are under consideration[3] unless it is stated otherwise, and that if they move they do so in their slip planes.

There is another type of dislocation motion, called 'climb', in which the dislocation moves out of its slip plane normal to the Burgers vector. There are two types of climb – positive and negative. Positive climb occurs when, for example, the row of atoms A, normal to the plane of the paper in Fig. 1.5(c), is removed. This may be due to diffusion of vacancies to A, or the appearance of interstitial atoms at A and their diffusion away. Negative climb can occur either by interstitial atoms diffusing to A, or the formation of a vacancy at A and its diffusion away.

[2]Real crystal systems will be discussed in Chapter 3 in the context of von Mises criterion for general plastic deformation of a crystal.

[3]Though some results will also apply to more general scenarios.

Figure 1.6: Cross-sectional view of the creation of a prismatic dislocation. (a) A 'disc' of atoms is removed; (b) The lattice rearranges to compensate for the gap, and the dislocation is now the boundary of the disc. (Hull & Bacon 1984).

1.3.3 Prismatic Dislocations

Thus far it has been implicitly assumed that a dislocation and its Burgers vector lie in the same plane, and we will continue to assume this unless otherwise stated. However, it is possible that a Burgers vector does not lie in the plane of the dislocation. A dislocation whose Burgers vector is perpendicular to the plane of the loop is known as a *prismatic* dislocation and can be thought of as being created by the removal (as shown in Fig. 1.6) or addition of a disc of atoms. The dislocation is then the boundary of the disc, and its slip surface is the cylinder whose generators are parallel to the Burgers vector. Prismatic dislocations arise, in practice, from an accumulation of vacancies, for example after rapid quenching of a crystal from a high temperature. It is possible for prismatic dislocations to expand (or contract) in the plane of the loop, but they must do so by climb.

As can be seen from Fig. 1.5, and as will be shown more explicitly when the 'force' on a dislocation is calculated, those dislocations whose Burgers vectors lie in the plane of the loop are moved by shear stresses (and are known as slip dislocations), whereas prismatic dislocations respond to compressive stresses. Most plastic deformation is the result of shear stresses, and this is why we will be concerned primarily with slip dislocations.

Figure 1.7: The Frank-Read Source. (Nabarro 1967).

1.3.4 Creation and Annihilation of Dislocations

Dislocations may be created through a number of different mechanisms. The Frank-Read source is one of the best known and is depicted in Fig. 1.7.

BC is a segment of a dislocation that lies in a plane which intersects the plane of the paper in the line through B and C. At B and C the dislocation is pinned by an unspecified barrier, which may consist of dislocation intersections, composite jogs (segments of dislocations connecting parts of the same dislocation on different slip planes) etc. (see Hull & Bacon 1984 for further details of these and other barriers). When a stress is applied,BC moves from 1 through to 4, at which stage two parts of the same dislocation are about to meet and form a single large loop together with the original segment BC, as in 5. (See Dash 1956, for example, where experimental evidence is provided for Frank-Read sources.)

The Bardeen-Herring source (Bardeen & Herring 1952) is similar to that of the Frank-Read source but involves a climb process instead of glide. Among other mechanisms for creation of dislocations is that of cross-slip, where a screw segment of a dislocation moves out of the slip plane of the dislocation and into another plane called the cross-slip plane. Double cross-slip occurs when the screw segment then moves into a slip plane parallel to the original slip plane (Fig. 1.8).

Large numbers of dislocations are created at grain boundaries (boundaries separating differently orientated crystal regions) through each of these mechanisms.

Figure 1.8: Double cross-slip. The Burgers vector $\boldsymbol{B}$ is parallel to BG. The screw segment moves from the plane ABHG into BCFG and finally CDEF which is parallel to ABHG. (Nabarro 1967).

Due to the difference in orientation of neighbouring grains, dislocations in one grain may not be able to pass through to the next, and a 'pile-up' may result, creating large stress concentrations which induce the emission of dislocations from the sources already described. (See Li 1963, Hirth 1972, Malis & Tangri 1979 for example).

A dislocation is annihilated when it meets its exact opposite or when it meets the surface of the material. It is clear from Fig. 1.5 that if two half-sheets of atoms (one, as shown, lying above the dotted line, another lying below the line) meet, a perfect lattice will be the result. As shown in Fig. 1.5(d), when the dislocation reaches the edge of the material there is no interior deformation and so no internal stresses.

1.4 The 'Force' on a Dislocation

A dislocation cannot experience a Newtonian force since such a force is a product of mass and acceleration, whereas it is not meaningful to speak of mass in this context. However, as we have seen (Section 1.3.2), a dislocation will move when in the presence of an appropriate component of stress. If the stress acting on

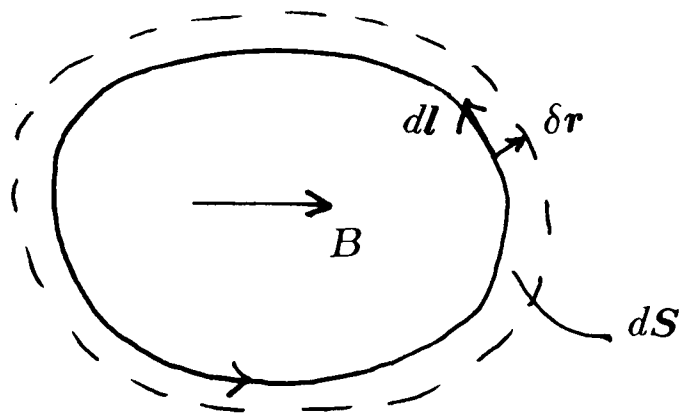

Figure 1.9: An element of dislocation line $d\boldsymbol{l}$ sweeps out an area $d\boldsymbol{S}$ on moving a distance $\delta\boldsymbol{r}$.

the dislocation is an external stress (that is, due to other dislocations or applied tractions at the boundary of the material) then the work done in moving the dislocation can be thought of as arising from a force per unit length along the dislocation line.

Suppose that the element of the dislocation line $d\boldsymbol{l}$ is displaced by an amount $\delta\boldsymbol{r}$, in the presence of a stress field $\boldsymbol{\sigma}^{Tot}$ which does not include the stress field of the dislocation itself but which does include the stress due to all other sources. Then, as shown in Fig. 1.9, the element sweeps out an area

$$d\boldsymbol{S} = \delta\boldsymbol{r} \wedge d\boldsymbol{l},$$

the direction of $d\boldsymbol{S}$ being (according to the right-hand rule) out of the plane of the paper. The traction force exerted on (say) the upper face of the elemental area $d\boldsymbol{S}$ is equal to

$$\boldsymbol{\sigma}^{Tot}.d\boldsymbol{S},$$

and, since the upper face of $d\boldsymbol{S}$ is moved relative to the lower face by an amount $\boldsymbol{B}$, the work done *by* the external stresses on the dislocation line element is

$$(\boldsymbol{\sigma}^{Tot}.\boldsymbol{B}).d\boldsymbol{S} = (\boldsymbol{\sigma}^{Tot}.\boldsymbol{B}).(\delta\boldsymbol{r} \wedge d\boldsymbol{l}).$$

Consequently, the increase in strain energy of the dislocation, which is the work done *against* the external stresses, is

$$\begin{aligned} \delta W &= -(\boldsymbol{\sigma}^{Tot}.\boldsymbol{B}).(\delta\boldsymbol{r} \wedge d\boldsymbol{l}) \\ &= \delta\boldsymbol{r}.((\boldsymbol{\sigma}^{Tot}.\boldsymbol{B}) \wedge d\boldsymbol{l}). \end{aligned} \tag{1.10}$$

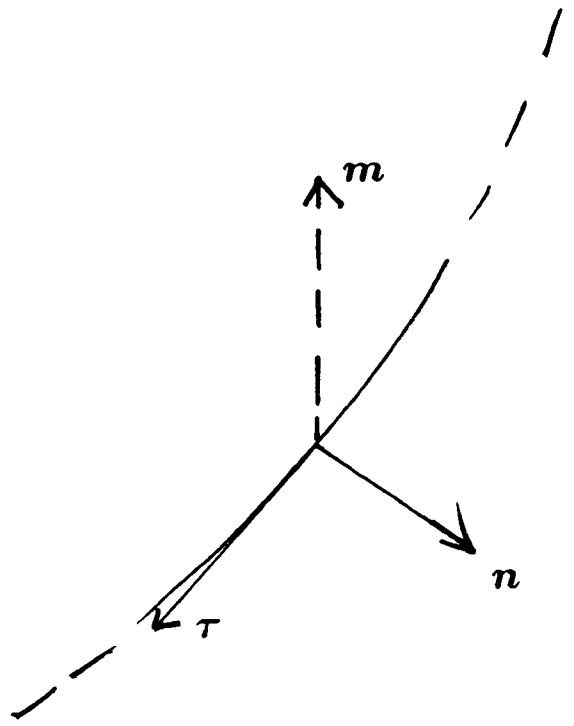

Figure 1.10: Definition of the vectors $\boldsymbol{n}, \boldsymbol{m}, \boldsymbol{\tau}$.

Now, if the 'force per unit length' is $\boldsymbol{F}$, then

$$\delta W = (\boldsymbol{F} dl).\delta \boldsymbol{r}, \tag{1.11}$$

and so, comparing (1.10) with (1.11), we arrive at Peach & Koehler's (1950) expression for the force per unit length on a dislocation as

$$\boldsymbol{F} = (\boldsymbol{\sigma}^{Tot}.\boldsymbol{B}) \wedge \boldsymbol{\tau}, \tag{1.12}$$

where $\boldsymbol{\tau}$ is the unit tangent vector to the dislocation.

The set $(\boldsymbol{n}, \boldsymbol{m}, \boldsymbol{\tau})$ of mutually orthogonal unit vectors is used, where $\boldsymbol{n}$ is the unit normal to the dislocation in the slip plane, $\boldsymbol{m}$ is the unit normal to the slip plane, and

$$\boldsymbol{\tau} \times \boldsymbol{n} = \boldsymbol{m},$$

as in Fig. 1.10. From (1.12) we then have that

$$\boldsymbol{F}.\boldsymbol{n}(\boldsymbol{x}) = B_j \sigma_{ij}^{Tot} m_i(\boldsymbol{x}), \tag{1.13}$$

$$\boldsymbol{F}.\boldsymbol{m}(\boldsymbol{x}) = -B_j \sigma_{ij}^{Tot} n_i(\boldsymbol{x}), \tag{1.14}$$

$$\boldsymbol{F}.\boldsymbol{\tau}(\boldsymbol{x}) = 0, \tag{1.15}$$

where $\boldsymbol{x}$ lies on the dislocation line.

It should be noted that the stress $\boldsymbol{\sigma}^{Tot}$ in (1.12) excludes the stress due to the dislocation itself. Later (Chapter 3) we will be considering the self-equilibrium of continuous dislocation distributions so that the force acting on the dislocations is that due solely to the dislocations themselves. In this case equation (1.12) will be assumed to be the correct expression for the force on the grounds that, since the distribution is continuous, the dislocation through any point is infinitesimal, and hence the stress due to that dislocation is negligible.

1.4.1 Mobility Laws

The relationship between the force on a dislocation and the speed of the dislocation must be assumed from experimental results, as there is no microscopic justification for any of the mobility laws used in the literature. We follow Stein & Low (1960), Head (1972a), for example, and postulate that

$$V_n = A|\boldsymbol{F}.\boldsymbol{n}|^{a-1}\boldsymbol{F}.\boldsymbol{n}, \tag{1.16}$$

where V_n is the velocity in the direction of the normal $\boldsymbol{n}$ to the dislocation, and A and a are positive constants which depend on the properties of the material. We will make use of this law in Chapter 5, when we consider the evolution of dislocation distributions under an applied stress.

1.5 Review of Previous Discrete and [4]Continuum Models

Though the literature, both theoretical and experimental, devoted to the study of dislocations is vast, little progress has been made towards a mathematical interpretation of work-hardening in terms of dislocations. This is largely due to the complexities introduced by the three-dimensionality of the resultant dislocation distributions, and the fact that little can be inferred from experimental studies except that electron micrographs commonly show a pattern of regions of high and low densities of dislocations (see, for example, Kuhlman-Wilsdorf 1987).

[4]The word 'continuum' is used here to denote the presence of large numbers of dislocations rather than large numbers of atoms, as in 'elastic continuum'.

Simple arrays of discrete dislocations have been widely studied. Eshelby, Frank & Nabarro (1951) considered a set of identical dislocations confined to a certain portion of a single slip plane. A method was given for finding the equilibrium arrangement of the dislocations under an applied stress, and it was shown that their positions were given by the roots of a certain set of orthogonal polynomials. The evolution of such a distribution has also been investigated (Kanninen & Rosenfield 1969, Rosenfield & Kanninen 1970, Head 1972 a,b).

When the number of dislocations produced during plastic deformation is very large, it is not feasible to model each one individually, and an averaging process must be used. If a group of infinitely long and parallel dislocations each lying in the same slip plane is represented in this way by a number density, the configuration is known as a 'dislocation sheet'. Head & Louat (1955) investigated the static equilibrium distribution of a dislocation sheet and their results were compared to those of Eshelby et al. (1951) by Mitchell et al. (1965). It was shown that the continuum approximation (first introduced by Eshelby in 1949) is accurate to within 2 percent when there are twenty dislocations in the equilibrium configuration. The time evolution of the dislocation sheet has been studied by Rosenfield (1971), Head (1973), Head & Wood (1973 a,b), Ockendon & Ockendon (1983) and Wood & Head (1974, 1984).

Dislocation sheets have been useful in the modelling of pile-ups (Ockendon & Ockendon 1983); a 'pile-up' is said to occur when a planar array of dislocations is blocked by some obstacle such as a grain boundary or a locked dislocation. The modelling of cracks has also been aided by the study of dislocation sheets. Indeed, the mathematical problems are identical in that any real crack can be modelled with a fictitious dislocation distribution[5] (Lardner 1974). For example, a body containing a crack in the form of an infinite plane strip occupying the region $y = 0$, $-a < x < a$, under an externally applied constant shear stress σ_{yz}, is in the same state of stress as it would be if, under the same loading, the half of the strip $a > x > 0$ were occupied by a continuous distribution of edge dislocations of one sign, and edge dislocations of the opposite sign occupied the other half of the strip $0 > x > -a$ in such a way that the dislocations were in equilibrium.

[5]Note, however, that real cracks in metals produce real dislocations, and that these two ideas should not be confused.

The idea of the dislocation sheet has been generalised by Head et al. (1987) who considered a very special two-dimensional continuous distribution. Some exact steady and unsteady solutions were found in which the applied stress was spatially linear and the boundary of the distribution was an ellipse. We will see in Chapter 2 how some of their results can be derived from the present approach. For the special case of a rectangular domain, Caffarelli & Friedman (1988) have shown that the model of Head et al. can be formulated in terms of variational inequalities, and that a solution exists.

More sophisticated mathematical models have been proposed to describe the three-dimensional networks which are commonly found in metals. Nye (1953) introduced the dislocation density tensor which Kröner (1958) adopted in his kinematic approach; this was the first systematic continuum theory of dislocation densities, and was based on the idea of 'incompatibility' (Moriguchi 1947), which will be discussed shortly. In order to solve the equations of incompatibility, Kröner (1958) introduced stress functions in a manner analogous to the use of the vector potential in electromagnetism. Indeed, a screw dislocation has very similar properties to a line current, the major difference between the two being that like dislocations repel each other, whereas identical line currents attract. The analogy between continuous distributions of dislocations and currents will be explored in Chapter 2.

Other models have involved widely differing approaches. Kadić & Edelen (1982), for example, have used the ideas of gauge invariance to formulate a continuum theory of materials with, among other defects, dislocations. On the other hand, a phenomenological approach is adopted by Pilecki (1977) and Walgraef & Aifantis (1985a,b,c), who considered the formation and stability of dislocation patterns in one, two and three dimensions.

A number of authors have considered arrays of discrete dislocations which produce no long-range stresses (that is, configurations whose stress fields decay exponentially with distance from the array (see Nabarro 1967)). Nye (1953) derived the relationship between the dislocation density and lattice curvature for zero stress distributions. Frank (1955), in determining the nature of dislocation arrays forming hexagonal networks, assumed that it was reasonable to consider the case when no long-range stresses were present, and Bilby et al. (1958) also restricted their

discussion of single glide and plane strain to bodies containing dislocation arrangements of this type. In the continuum limit the stress tensor of such distributions is identically zero and they will play a central role in this work. Mura (1989) called these distributions 'impotent' and compared them to experimentally observed low-energy configurations. Here, as mentioned in the Introduction, such distributions will be known as zero stress everywhere (ZSE) distributions.

1.6 The Mathematical Representation of Single Dislocations

1.6.1 Incompatibility

As can be seen from the cut-and-weld definition (Section 1.3.1*(ii)*), the displacement $\boldsymbol{u}$ can no longer be continuous and single-valued wherever dislocations exist. Thus the definition (1.1) of the strain loses its meaning at certain parts of the material. This also means that the compatibility equations (1.2) are no longer always satisfied, and generally we have, instead of zero on the right-hand side,

$$-\varepsilon_{ikl}\varepsilon_{jmn}e_{ln,km} = \eta_{ij}. \tag{1.17}$$

The function $\boldsymbol{\eta}$, known as the 'incompatibility tensor', is a source function for the strain field and vanishes in 'good', that is, undislocated, material.

1.6.2 The Delta Function

Prior to deriving the expression for the stress components of a curved dislocation we consider the case of the single screw dislocation and the single edge dislocation, and find the incompatibility in these cases. We will require the use of the Dirac distribution (or delta function) $\delta(x_i)$, $i = 1, 2, 3$, which is defined by the linear mapping from 'good' functions $\Gamma(x)$, where $x \epsilon \Re$, (see Lighthill 1980) to the reals:

$$\int_{-\infty}^{\infty} \delta(t' - t)\Gamma(t')dt' = \Gamma(t). \tag{1.18}$$

Similarly, the two-dimensional delta function $\delta(x_1)\delta(x_2)$ is defined by the mapping

$$\int_{-\infty}^{\infty}\int_{-\infty}^{\infty} \delta(t_1' - t_1)\delta(t_2' - t_2)\ \Gamma(t_1', t_2')\ dt_1'dt_2' = \Gamma(t_1, t_2),$$

and the three-dimensional delta function $\delta(x_1)\delta(x_2)\delta(x_3) = \delta(\boldsymbol{x})$, by

$$\int \delta(\boldsymbol{t}' - \boldsymbol{t})\Gamma(\boldsymbol{t}')dV = \Gamma(\boldsymbol{t}),$$

the integral being over the whole space.

The derivative of the delta function, $\delta'(x)$, is defined by the mapping

$$\int_{-\infty}^{\infty} \delta'(t' - t)\Gamma(t')dt' = -\Gamma'(t).$$

1.6.3 The Screw Dislocation

From the cut-and-weld procedure (Section 1.3.1*(ii)*) used to visualise the creation of the screw dislocation, it is clear that the material is in a state of anti-plane strain, and hence that the only nonzero components of strain are $e_{13} = e_{31}$ and $e_{23} = e_{32}$. Thus, the components of displacement are $u_1 = u_2 = 0$, $u_3 = u_3(x, y) \neq 0$, and from equation (1.9) we have

$$B = \oint_\gamma du_3,$$

around the arbitrary circuit γ, and hence, away from the dislocation, we use definition (1.1) to write this as

$$B = 2 \oint_\gamma e_{13}dx_1 + e_{23}dx_2, \tag{1.19}$$

which, on using Green's theorem in the plane, becomes

$$e_{23,1} - e_{13,2} = \frac{B}{2}\delta(x_1)\delta(x_2). \tag{1.20}$$

Partially differentiating this with respect to x_1 and x_2 gives respectively

$$e_{23,11} - e_{13,21} = \frac{B}{2}\delta'(x_1)\delta(x_2), \tag{1.21}$$

and

$$e_{23,12} - e_{13,22} = \frac{B}{2}\delta(x_1)\delta'(x_2). \tag{1.22}$$

Comparing these with equation (1.17) we see that for a screw dislocation

$$\eta_{13} = -\frac{B}{2}\delta(x_1)\delta'(x_2), \tag{1.23}$$

$$\eta_{23} = \frac{B}{2}\delta'(x_1)\delta(x_2), \tag{1.24}$$

and all other components of $\boldsymbol{\eta}$ are zero.

Equation (1.20) may be written

$$\sigma_{23,1} - \sigma_{13,2} = \mu B \delta(x_1)\delta(x_2), \tag{1.25}$$

by use of Hooke's law (1.4). (The legitimacy of using Hooke's law here will be discussed shortly).

The equilibrium equation (1.3) in this case is

$$\sigma_{13,1} + \sigma_{23,2} = 0 \tag{1.26}$$

everywhere. Thus we may write

$$\begin{aligned} \sigma_{13} &= -\phi_{,2}, \\ \sigma_{23} &= \phi_{,1}. \end{aligned}$$

for some function ϕ. Substituting these expressions into (1.25) we find that ϕ must satisfy

$$\nabla^2 \phi = \mu B \delta(x_1)\delta(x_2), \tag{1.27}$$

whose radially symmetric solution is

$$\phi = \frac{\mu B}{2\pi} \log(x_1^2 + x_2^2)^{1/2}. \tag{1.28}$$

This gives the components of stress as

$$\sigma_{13} = -\frac{\mu B}{2\pi} \frac{x_2}{x_1^2 + x_2^2}, \tag{1.29}$$

$$\sigma_{23} = \frac{\mu B}{2\pi} \frac{x_1}{x_1^2 + x_2^2}. \tag{1.30}$$

These stress components have an infinite value at the dislocation line, and so raise the question as to the validity of using Hooke's law in (1.20), since the stress-strain relation is linear only for small strains, as shown in Fig. 1.1. In practice the strains close to a dislocation (within the distance of a few atom spacings, known as the dislocation 'core') are high, although not infinite, and Hooke's law does indeed break down in this region. Nevertheless, it is also true that, even in regions of high dislocation density, the dislocations are separated by distances many times greater than a typical core width, and so Hooke's law is valid in most of the material. Consequently, it is assumed that (1.29, 1.30) are reasonable approximations to the stresses due to a screw dislocation.

1.6.4 The Edge Dislocation

An isolated, infinitely long and straight edge dislocation in an infinite isotropic solid with Burgers vector $(B,0,0)$, lying along the x_3-axis, corresponds to a state of plane strain, as can be seen from the cut-and-weld definition in Section 1.3.1 *(ii)*. Thus, the only components of strain which vanish are $e_{13} = e_{31}$, $e_{23} = e_{32}$. From equation (1.9)

$$B = \oint_\gamma du_1, \tag{1.31}$$

around the arbitrary circuit γ, and hence, away from the dislocation, we use definition (1.1) to write this as

$$B = \oint_\gamma e_{11}dx_1 + (2e_{12} - u_{2,1})dx_2. \tag{1.32}$$

Since γ is arbitrary, we obtain

$$2e_{12,1} - u_{2,11} - e_{11,2} = B\delta(x_1)\delta(x_2),$$

on using Green's theorem in the plane. Differentiating this with respect to x_2 gives

$$2e_{12,12} - e_{22,11} - e_{11,22} = B\delta(x_1)\delta'(x_2). \tag{1.33}$$

Comparing this with equation (1.17) we see that for an edge dislocation

$$\eta_{33} = B\delta(x_1)\delta'(x_2), \tag{1.34}$$

with all other components of $\boldsymbol{\eta}$ being zero.

Writing (1.33) in terms of stress components by means of Hooke's law (1.4), making use of the relationship $\sigma_{33} = \nu(\sigma_{11} + \sigma_{22})$ and of the equilibrium equations (1.3) (which in this case imply that the components of stress may be expressed in terms of the second derivatives of a stress function χ, the Airy stress function), leads us to the equation

$$\nabla^4\chi = -\frac{2\mu B}{1-\nu}\delta(x_1)\delta'(x_2). \tag{1.35}$$

Substituting

$$\chi = -2\psi_{,2},$$

gives

$$\nabla^4\psi = -\frac{\mu B}{1-\nu}\delta(x_1)\delta(x_2), \tag{1.36}$$

whose radially symmetric solution is

$$\psi = \frac{\mu B}{8\pi(1-\nu)}(x_1^2 + x_2^2)\log(x_1^2 + x_2^2)^{1/2}. \tag{1.37}$$

The components of stress are then

$$\sigma_{11} = -\frac{\mu B}{2\pi(1-\nu)}\frac{x_2(3x_1^2 + x_2^2)}{(x_1^2 + x_2^2)^2}, \tag{1.38}$$

$$\sigma_{22} = \frac{\mu B}{2\pi(1-\nu)}\frac{x_2(x_1^2 - x_2^2)}{(x_1^2 + x_2^2)^2}, \tag{1.39}$$

$$\sigma_{12} = \sigma_{21} = \frac{\mu B}{2\pi(1-\nu)}\frac{x_1(x_1^2 - x_2^2)}{(x_1^2 + x_2^2)^2}. \tag{1.40}$$

1.6.5 The Curved Dislocation

The stress field of an arbitrary curved dislocation was first derived by Peach & Koehler in 1950 by differentiating the components of displacement as given by Burgers (1939). We will follow the approach of Kröner (1958), who achieved the same result by means of the introduction of stress functions. Firstly, we need to establish the incompatibility tensor of a loop dislocation by generalising the results for screws and edges.

For the screw dislocation with $\boldsymbol{\tau} = (0,0,1)$, $\boldsymbol{B} = (0,0,B)$, we can rewrite equations (1.23) and (1.24) as

$$\eta_{13} = -\frac{1}{2}[\varepsilon_{123}\tau_3 B_3 \delta(x_1)\delta(x_2)]_{,2}, \tag{1.41}$$

and

$$\eta_{23} = -\frac{1}{2}[\varepsilon_{213}\tau_3 B_3 \delta(x_1)\delta(x_2)]_{,1}. \tag{1.42}$$

For the edge dislocation with $\boldsymbol{\tau} = (0,0,1)$, $\boldsymbol{B} = (B,0,0)$, we can write equation (1.34) as

$$\eta_{33} = -[\varepsilon_{321}\tau_3 B_1 \delta(x_1)\delta(x_2)]_{,2}. \tag{1.43}$$

Since an arbitrary curved dislocation has a linear combination of screw and edge character, we may, on the basis of the above three equations, write the incompatibility tensor of an arbitrary curved dislocation as

$$\eta_{ij} = -[\varepsilon_{jmn}\tau_i B_n \delta(x_p - x'_p)\delta(x_{p+1} - x'_{p+1})]^S_{,m}, \tag{1.44}$$

for $i,j = 1,2,3$, $i \leq j$, where $p \neq i$, $i+1$ and if $p = 3$ then $x_{p+1} = x_1$, and the point $\boldsymbol{x}'$ lies on the dislocation. Here, the superscript 'S' denotes the 'symmetric part'.

We can write the incompatibility tensor in terms of the stress tensor by substituting the expression for the strain components (1.5) in terms of the stress components into equation (1.17). (A more useful form of the incompatibility tensor is given in Appendix A.1). This gives

$$\sigma_{ij,kk} + \sigma_{kk,ij} - (\sigma_{jk,ki} + \sigma_{ki,jk}) + (\sigma_{kl,kl} - \sigma_{kk,ll})\delta_{ij} - \frac{\nu}{\nu+1}(\sigma_{kk,ij} - \sigma_{kk,ll}\delta_{ij}) = 2\mu\eta_{ij}. \tag{1.45}$$

Again we justify the use of Hooke's law by the argument given earlier (p.22).

If the material is in equilibrium under no body force, then, employing (1.3), (1.45) reduces to

$$\sigma_{ij,kk} + \frac{1}{\nu+1}(\sigma_{kk,ij} - \sigma_{kk,ll}\delta_{ij}) = 2\mu\eta_{ij}. \tag{1.46}$$

Our aim now is to solve (1.46) for $\boldsymbol{\sigma}$ in terms of $\boldsymbol{\eta}$ and then substitute for $\boldsymbol{\eta}$ from (1.44). First, we note that since $\boldsymbol{\sigma}$ is a symmetric, second rank tensor, and (1.3) holds, then we may write

$$\sigma_{ij} = -\varepsilon_{ikl}\varepsilon_{jmn}\psi_{ln,km}, \tag{1.47}$$

(see Appendix A.2), where $\boldsymbol{\psi}$ is also a symmetric second rank tensor[6].

This is a generalisation of the stress functions ϕ for screw dislocations, and ψ for edge dislocations. The diagonal elements of $\boldsymbol{\psi}$ are Morera's stress functions, and the off-diagonal elements are Maxwell's stress functions (see Love 1927, §56).

Substituting (1.47) into (1.46) gives a cumbersome expression for $\boldsymbol{\eta}$ and yet we may expect, on the basis of the Airy stress function equation (1.36) for edge dislocations, that we may generalise to obtain $\boldsymbol{\eta}$ as the result of operating with the biharmonic operator ∇^4 on a stress function. This is indeed the case, and to see why we follow Kröner (see de Wit 1960, p.271) and introduce a different stress function $\boldsymbol{\chi}$, defined by

$$\psi_{ij} = 2\mu\left(\chi_{ij} + \frac{\nu}{1-\nu}\chi_{kk}\delta_{ij}\right),$$

[6]This result corresponds to that for vectors which says that a divergence-free vector may be written as the curl of a vector potential.

so that we may write

$$\sigma_{ij} = -2\mu\varepsilon_{ikl}\varepsilon_{jmn}\left(\chi_{ln} + \frac{\nu}{1-\nu}\chi_{pp}\delta_{ln}\right)_{,km}. \tag{1.48}$$

Then, when expression (1.48) is substituted into (1.46), the following equation is obtained:

$$\chi_{ij,kkll} - (\chi_{jk,kill} + \chi_{ki,jkll}) + \frac{1}{1+\nu}\chi_{kl,klij} + \frac{\nu}{1+\nu}\chi_{kl,klmm}\delta_{ij} = \eta_{ij}. \tag{1.49}$$

There are six components of $\boldsymbol{\psi}$ (and $\boldsymbol{\chi}$), but, since the six stress components σ_{ij} derived from them satisfy the three equations (1.3), only three components of $\boldsymbol{\psi}$ (and $\boldsymbol{\chi}$) are independent. $\boldsymbol{\psi}$ or $\boldsymbol{\chi}$ can therefore be made to satisfy three other conditions, and this we do by taking the side condition

$$\chi_{ij,j} = 0, \tag{1.50}$$

which can always be done (see Appendix A.3). Using (1.50), (1.49) becomes

$$\chi_{ij,kkll} = \eta_{ij}.$$

The solution of this which vanishes at infinity is

$$\chi_{ij}(\boldsymbol{x}) = -\frac{1}{8\pi}\int \eta_{ij}(\boldsymbol{x}')RdV', \tag{1.51}$$

where $R = (X_iX_i)^{\frac{1}{2}}$, $X_i = x_i - x_i'$. It follows automatically from (1.17) that

$$\eta_{ij,j} = 0. \tag{1.52}$$

This is the continuity equation, which states that the incompatibility is solenoidal. In the case of a dislocation it states that the dislocation will not stop in the material, but will form a closed loop, as was mentioned when the definition of a dislocation was given (Section 1.3.1). From (1.51) and (1.52) it follows, by integration by parts, the surface integral vanishing at infinity, that

$$\chi_{ij,j}(\boldsymbol{x}) = 0, \tag{1.53}$$

in agreement with the side condition (1.50).

Thus, the formula for the stress is simplified, using (1.50), to

$$\sigma_{ij} = 2\mu\left[\chi_{ij,kk} + \frac{1}{1-\nu}(\chi_{kk,ij} - \chi_{kk,ll}\delta_{ij})\right], \tag{1.54}$$

which, in terms of the incompatibility, becomes

$$\sigma_{ij} = -\frac{\mu}{4\pi}\int \eta_{ij}R_{,ll} + \frac{1}{1-\nu}\eta_{kk}(R_{,ij} - R_{,ll}\delta_{ij})dV'$$

after two integrations by parts. Substituting the expression (1.44) for the incompatibility gives (using the property of the delta function (1.18))

$$\sigma_{ij}(\boldsymbol{x}) = \frac{\mu B_n}{4\pi}\oint_C \left\{\frac{1}{2}R_{,mll}(\varepsilon_{jmn}dx'_i + \varepsilon_{imn}dx'_j) + \frac{\varepsilon_{kmn}}{1-\nu}(R_{,mij} - R_{,mll}\delta_{ij})dx'_k\right\}, \tag{1.55}$$

where C is the dislocation loop. It is easy to see from this formula that as one approaches the dislocation line, that is, as $|\boldsymbol{X}| \to 0$, we have $\sigma_{ij}(\boldsymbol{x}) = O(1/|\boldsymbol{X}|)$, and as $|\boldsymbol{x}| \to \infty$ we have $\sigma_{ij}(\boldsymbol{x}) = O(1/|\boldsymbol{x}^3|)$.

Using (1.5) we may write

$$e_{ij}(\boldsymbol{x}) = \frac{B_n}{8\pi}\oint_C \left\{R_{,mll}\left(\frac{1}{2}\varepsilon_{jmn}dx'_i + \frac{1}{2}\varepsilon_{imn}dx'_j - \varepsilon_{kmn}\delta_{ij}dx'_k\right) + \frac{2(\lambda+\mu)}{\lambda+2\mu}\varepsilon_{kmn}R_{,mij}dx'_k\right\}, \tag{1.56}$$

and from (1.17)

$$\eta_{ij}(\boldsymbol{x}) = \frac{B_n}{8\pi}\oint_C R_{,kkllm}(\varepsilon_{jmn}dx'_i)^S - (\varepsilon_{imn}R_{,jkllm})^S dx'_k. \tag{1.57}$$

Chapter 2

Continuous Dislocation Distributions

Having considered the properties of single dislocations, we now wish to generalise our results in order that they should more closely represent 'real' distributions; this means principally that we must take account of the large number density of dislocations. This is done by means of an averaging process. Firstly, the general case is considered, and the dislocation density tensor introduced. The relationship between the density tensor and the incompatibility tensor is then derived, and the equations for the continuum model are presented. Some simple continuous distributions comprised solely of screw or edge dislocations are examined as a means of illustrating the averaging process, and their stress fields are derived.

A less trivial example of a cylindrical sheet is presented, and the special case of the elliptical shape is highlighted in order to show how the results of Head et al. (1987) may be derived from the present approach.

2.1 Homogenisation

We make the assumption that in a highly dislocated body the dislocations are assembled in families, each of which is smoothly varying; that is, in the vicinity of any particular point, the members of each family have nearly-parallel tangents and have precisely equal Burgers vectors.

By a limiting process in which $\boldsymbol{B}$ and the average lateral separation of the dislocations, say ϵ, both tend to zero, with $|\boldsymbol{B}| = O(\epsilon)$, we define a dislocation

density tensor $\boldsymbol{\alpha}$ for each family by

$$\alpha_{in} = \omega \tau_i b_n, \tag{2.1}$$

where $\boldsymbol{\tau}$ is the unit tangent field of the family, $\boldsymbol{b}$ is the unit Burgers vector (i.e. it is such that $\boldsymbol{B} = \hat{b}\boldsymbol{b}$ with $\hat{b} = |\boldsymbol{B}|$), and $\omega = \lim_{\epsilon,\hat{b}\to 0}(\hat{b}/\epsilon)$ is the number density of dislocations per unit area crossing a plane normal to $\boldsymbol{\tau}$. (Examples of this limiting procedure will be given for some simple cases later in this chapter). Note that in general $\boldsymbol{\alpha}$ is not a symmetric tensor. If several families are present, $\boldsymbol{\alpha}$ for the ensemble is calculated by summing the contributions from each family.

Because dislocations cannot begin or end in the material, the net "dislocation flux" out of any region of dislocated material is zero. Hence $\boldsymbol{\nabla}.(\omega\boldsymbol{\tau}) = 0$ and, since $\boldsymbol{b}$ is constant along the dislocation lines, we have

$$\alpha_{in,i} = 0. \tag{2.2}$$

This says that the divergence of $\boldsymbol{\alpha}$ is zero in the sense that $\boldsymbol{\alpha}$ may be considered to be composed of three vectors, each of which has zero divergence, and hence means that $\boldsymbol{\alpha}$ can be written as a "curl", the implications of which are discussed in Chapter 4. It should be noted that (2.2) holds even in the unsteady case which is discussed in Chapter 5, and for which the full equations are presented in Appendix A.8.

The relationship between the incompatibility and dislocation density tensors can now be derived. In the limit described above, (1.44) becomes

$$\begin{aligned} \eta_{ij} &= -(\varepsilon_{jmn}\tau_i b_n \omega)^S_{,m} \\ &= -(\varepsilon_{jmn}\alpha_{in,m})^S. \end{aligned} \tag{2.3}$$

From this equation it is clear that if $\boldsymbol{\alpha} = \mathbf{0}$, then $\boldsymbol{\eta} = \mathbf{0}$. However, the converse is not true, and there are certain non-trivial dislocation configurations which give zero incompatibility. These situations will figure prominently in subsequent chapters.

By averaging $\boldsymbol{B}$ as above, one can also write (for a continuous distribution) the equations equivalent to (1.55) and (1.56). We obtain

$$\sigma_{ij} = \frac{\mu}{4\pi}\int\left\{(\varepsilon_{jmn}\alpha_{in,m'})^S R_{,ll} + \frac{2(\lambda+\mu)}{\lambda+2\mu}\varepsilon_{kmn}\alpha_{kn,m'}(R_{,ij} - R_{,ll}\delta_{ij})\right\}dV, \tag{2.4}$$

and

$$e_{ij} = \frac{1}{8\pi} \int \left\{ ((\varepsilon_{jmn}\alpha_{in,m'})^S - \delta_{ij}\varepsilon_{kmn}\alpha_{kn,m'})R_{,ll} + \frac{2(\lambda+\mu)}{\lambda+2\mu}\varepsilon_{kmn}R_{,ij}\alpha_{kn,m'} \right\} dV, \tag{2.5}$$

where the integrations are performed over the whole space (or, equivalently, over the dislocated volume).

2.2 The Continuum Model

In view of the assortment of relations introduced and derived in Chapter 1, it is at this point worthwhile to collect together the various equations which describe our model for the case of static equilibrium. For one dislocation family, there are eight independent quantities representing six components of stress and two components of dislocation density. To model these quantities we have three independent equations from (1.3), and one from (2.2). By substituting (2.3) into (1.46), another set of equations can be derived for $\boldsymbol{\alpha}$, namely

$$-(\varepsilon_{jmn}\alpha_{in,m})^S = \frac{1}{2\mu}\left(\sigma_{ij,kk} + \frac{2(\lambda+\mu)}{\lambda+2\mu}(\sigma_{kk,ij} - \sigma_{kk,ll}\delta_{ij})\right). \tag{2.6}$$

Although these are six equations relating $\boldsymbol{\alpha}$ and $\boldsymbol{\sigma}$, using (2.2) in (2.6) implies that

$$\nabla^2\sigma_{ij,i} = 0,$$

and hence, assuming that $\boldsymbol{\nabla}.\boldsymbol{\sigma}$ vanishes at infinity, that (1.3) holds. In summary, therefore, (2.2) and (2.6) provide seven independent equations for the eight unknowns, and we thus need one more scalar equation to close the model. This is supplied by consideration of possible dislocation motion. Thus it is asserted that, for equilibrium, the force given by (1.13) should be zero wherever there are dislocations with Burgers vector $\boldsymbol{B}$.

In summary, the model can be written:

$$\begin{aligned} -(\varepsilon_{jmn}\alpha_{in,m})^S &= \frac{1}{2\mu}\left(\sigma_{ij,kk} + \frac{2(\lambda+\mu)}{\lambda+2\mu}(\sigma_{kk,ij} - \sigma_{kk,ll}\delta_{ij})\right) \\ \alpha_{in,i} &= 0 \\ b_j\sigma_{ij}^{Tot}m_i &= 0. \end{aligned} \tag{2.7}$$

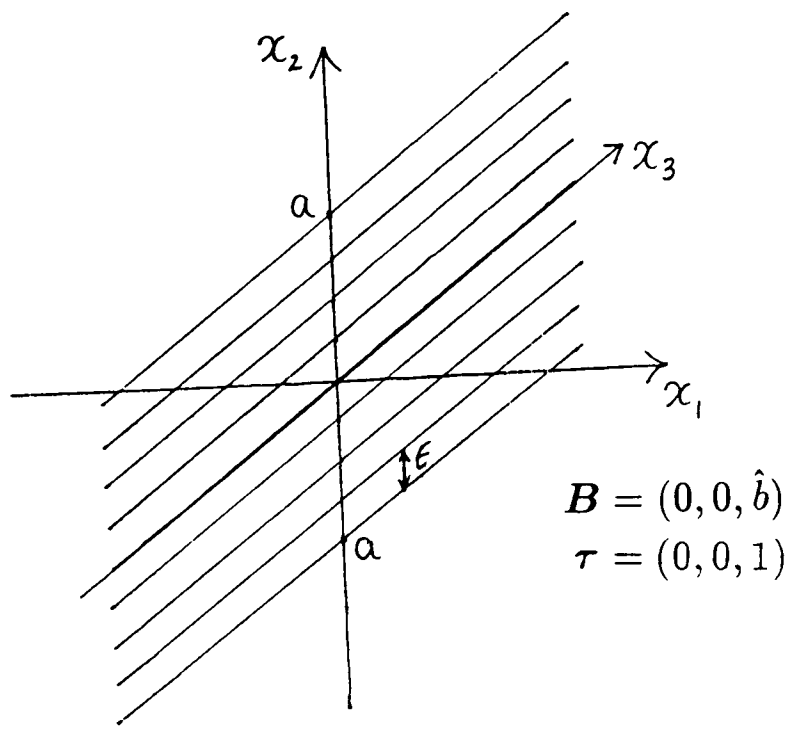

Figure 2.1: A row of screw dislocations.

This model consists of eight equations for eight unknowns, but it is a complicated system for which several boundary conditions need to be appended before one could expect there to be a unique solution. Nevertheless, as we shall see in the next chapter, one can still deduce important results concerning equilibrium distributions.

2.3 Special Distributions

2.3.1 A Sheet of Screws

Consider a row of straight, infinitely long screw dislocations each with Burgers vector $\boldsymbol{B} = (0, 0, \hat{b})$, lying in the $x_1 = 0$ plane, in the strip $-a \leq x_2 \leq a$, parallel to the x_3-axis, at a distance ϵ apart. The only nonzero component of the dislocation density tensor is

$$\alpha_{33} = \sum_{n=-a/\epsilon}^{a/\epsilon} \hat{b}\delta(x_1)\delta(x_2 - n\epsilon).$$

To find the dislocation density tensor for the corresponding continuous distribution we let $\hat{b}, \epsilon \to 0$ in such a way that $\hat{b}/\epsilon \to$ a finite value, Ω, say. Thus we

have

$$\alpha_{33} = \lim_{\substack{\hat{b},\epsilon\to 0 \\ \hat{b}/\epsilon\to\Omega}} \sum_{n=-a/\epsilon}^{a/\epsilon} \frac{\hat{b}}{\epsilon}\epsilon\delta(x_1)\delta(x_2 - n\epsilon)$$

$$= \int_{-a}^{a} \Omega\delta(x_1)\delta(x_2 - N)dN,$$

where $N = n\epsilon$. Consequently, for an infinite sheet of screws we take $a \to \infty$ and obtain

$$\alpha_{33} = \Omega\delta(x_1),$$

so that, in the notation of equation (2.1), $\tau_3 = b_3 = 1$, $\omega = \Omega\delta(x_1)$.

To calculate the components of stress due to this sheet we use the stress components of an individual screw dislocation (1.29 and 1.30) and follow a similar procedure to that above.

Hence, for a continuous distribution of screws occupying the strip $|x_2| \leq a$ of the $x_1 = 0$ plane,

$$\sigma_{13} = -\frac{\mu\Omega}{2\pi}\int_{-a}^{a} \frac{x_2 - N}{x_1^2 + (x_2 - N)^2}dN. \tag{2.8}$$

So, for an infinite sheet of screws

$$\sigma_{13} = -\frac{\mu\Omega}{2\pi}\int_{-\infty}^{\infty} \frac{x_2 - N}{x_1^2 + (x_2 - N)^2}dN = 0. \tag{2.9}$$

Similarly,

$$\sigma_{23} = \frac{\mu\Omega}{2\pi}\int_{-\infty}^{\infty} \frac{x_1}{x_1^2 + (x_2 - N)^2}dN \tag{2.10}$$

$$= \begin{cases} \mu\Omega/2 & x_1 > 0 \\ -\mu\Omega/2 & x_1 < 0. \end{cases} \tag{2.11}$$

Thus there is a jump in the value of σ_{23} across the sheet.

On the sheet of screws itself the integrals (2.9, 2.10) do not exist and so the stress cannot be calculated there. Later, however, we will be considering the equilibrium of continuum dislocation configurations and it will be necessary to know whether or not a sheet of screws exerts a force on itself. One may determine that no such force is exerted by observing that the 23-component of stress of a screw dislocation (which is that which would move the dislocations according to the Peach-Koehler formula (1.12)), as given by (1.30), is zero in the $x_1 = 0$ plane.

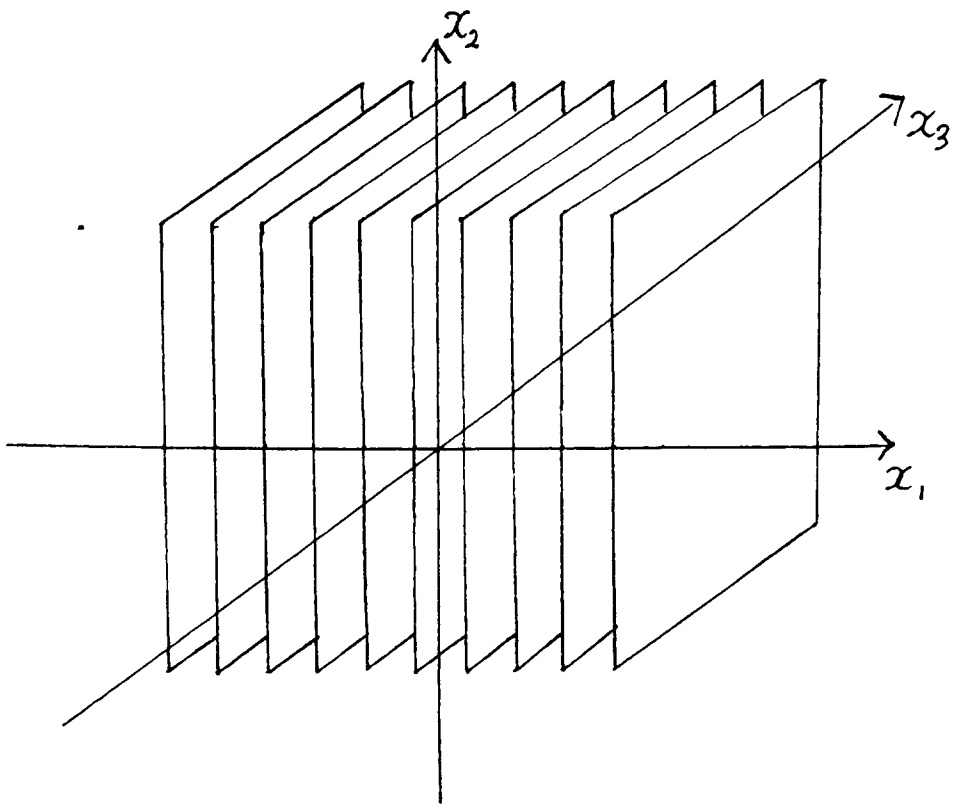

Figure 2.2: A Slab of Screw Dislocations

Thus the 23-component of stress at any point on the sheet, due to the dislocations which do not pass through that point, is zero. This justifies the assertion that the stress on a dislocation sheet, due to itself, is zero.

If the sheet of screws had a variable density $\Omega(N)$ then it would not be so straightforward to evaluate the stress components, as it was to evaluate (2.9, 2.10). Nevertheless, it is possible in this case to derive, in general, the limiting values of σ_{13} and σ_{23} as the dislocation sheet is approached. The result for σ_{13} is provided by

$$\lim_{x_1 \to 0\pm} \int_{-\infty}^{\infty} \frac{(x_2 - N)\Omega(N)}{x_1^2 + (x_2 - N)^2} dN = \pm \fint_{-\infty}^{\infty} \frac{\Omega(N)}{x_2 - N} dN,$$

where the bar on the integrand signifies that the Cauchy Principal Value is to be taken. For σ_{23} one can show that

$$\lim_{x_1 \to 0\pm} \int_{-\infty}^{\infty} \frac{x_1 \Omega(N)}{x_1^2 + (x_2 - N)^2} dN = \pm \pi \Omega(x_2).$$

2.3.2 A 'Slab' of Screw Dislocations

We now consider a set of sheets of dislocations of the above type, lying in the planes $x_1 =$ constant, between $x_1 = -c$ and $x_1 = c$, each a distance ϵ/c apart. In a limiting process similar to that above, we allow ϵ to tend to zero, and obtain what shall be called a 'slab' of dislocations. The only nonzero component of the

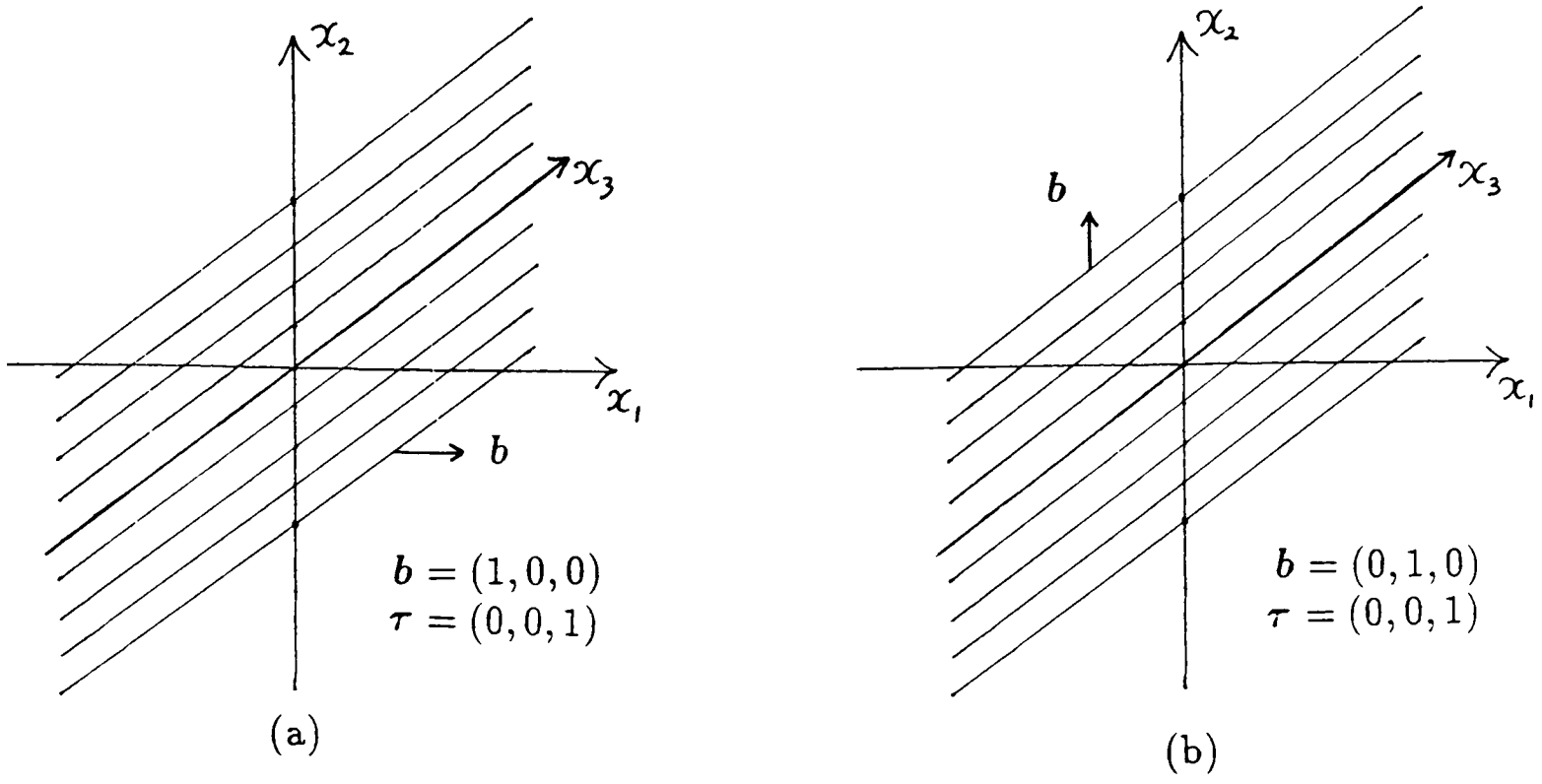

Figure 2.3: Two possibilities for sheets of edge dislocations.

dislocation density tensor is

$$\alpha_{33} = \Omega(H(c - x_1) - H(-c - x_1)),$$

where H is the Heaviside function, defined by

$$H(x) = \begin{cases} 1 & x > 0 \\ 0 & x < 0. \end{cases}$$

The stress tensor also has only one nonzero component, given by

$$\sigma_{23} = \begin{cases} -\mu\Omega c & x_1 \leq -c \\ \mu\Omega x_1 & -c < x_1 < c \\ \mu\Omega c & x_1 \geq c. \end{cases} \tag{2.12}$$

2.3.3 A Sheet of Edges

If we have a sheet of infinitesimal edge dislocations, each parallel to the x_3-axis, lying in the $x_1 = 0$ plane, with tangent vector $\boldsymbol{\tau} = (0,0,1)$, then we have two essentially different choices (in the sense that all other choices are linear combinations of these two) for the unit Burgers vector $\boldsymbol{b}$. We can take $\boldsymbol{b}$ to be parallel to the x_1-axis as in Fig. 2.3(a) and hence to be orthogonal to the sheet, or we can take it to be parallel to the sheet of dislocations.

(a) Let us first consider the situation depicted in Fig. 2.3(a). The components of stress due to a single, infinitely long and straight dislocation lying along the

x_3-axis with Burgers vector $(\hat{b}, 0, 0)$ are given by equations (1.38, 1.39, 1.40). Integrating these as we did for the sheet of screws in the limiting case, we find that all the components of stress are everywhere zero, and the only nonzero component of the dislocation density tensor is

$$\alpha_{31} = \Omega\delta(x_1).$$

(b) For the situation of Fig. 2.3(b) we write the appropriate components of stress for a single edge dislocation and integrate as usual to find that the nonzero components of stress due to this sheet are

$$\sigma_{11} = \begin{cases} -\mu\Omega/(1-\nu) & x_1 > 0 \\ 0 & x_1 = 0 \\ \mu\Omega/(1-\nu) & x_1 < 0, \end{cases} \tag{2.13}$$

and

$$\sigma_{33} = \nu(\sigma_{11} + \sigma_{22}) = \nu\sigma_{11}. \tag{2.14}$$

In this case

$$\alpha_{32} = \Omega\delta(x_1),$$

and all other α_{ij} are zero.

It should be borne in mind that the sheets of edges and screws are infinite distributions whose properties are likely to differ markedly form those of finite distributions. In particular, since the stress fields of the sheets of screws and edges are zero on the sheets themselves, these distributions are in equilibrium, whereas a finite distribution which is, locally, a sheet of screws or edges is unlikely to be in equilibrium.

2.3.4 A Slab of Edge Dislocations

Any slab of edge dislocations composed of sheets of edges as in (a) above will produce zero stress everywhere, and dislocation density

$$\alpha_{31} = \Omega(H(c - x_1) - H(-c - x_1)).$$

A slab of edges occupying the strip $-c \leq x_1 \leq c$, which we think of as being composed of sheets of edges as in case (b) above, will give a stress field whose

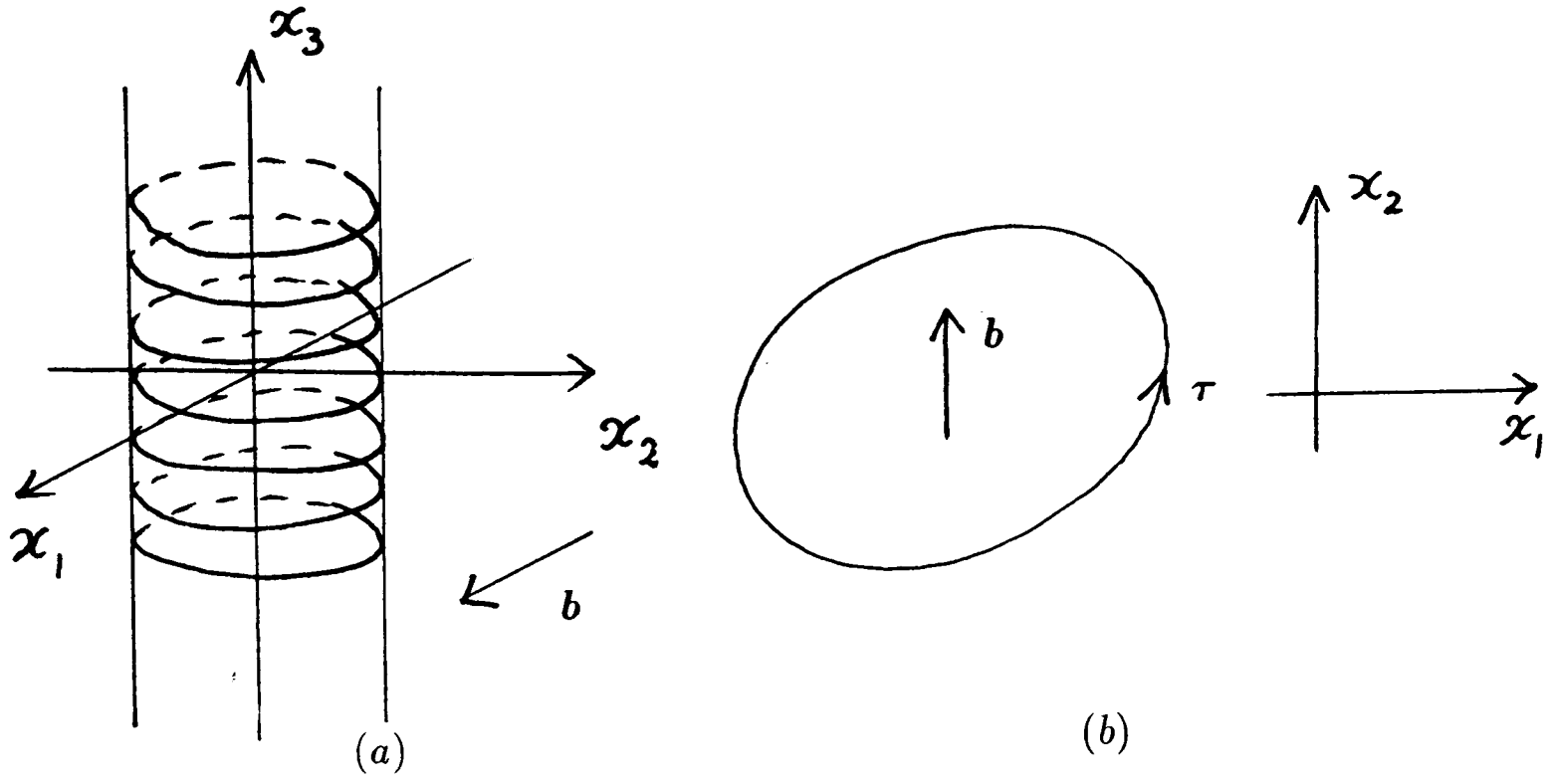

Figure 2.4: (a) Cylindrical sheet; (b) Cross-section of cylinder.

nonzero components are

$$\sigma_{11} = \frac{\sigma_{33}}{\nu} = \frac{2\mu\Omega}{1-\nu} \begin{cases} -c & x_1 \geq c \\ -x_1 & -c < x_1 < c \\ c & x_1 \leq -c\,. \end{cases} \tag{2.15}$$

The dislocation density tensor has nonzero component

$$\alpha_{32} = \Omega(H(c - x_1) - H(-c - x_1)),$$

2.4 The Cylindrical Sheet

A less trivial example of a continuous distribution of dislocations is when the sheet lies on the surface of a cylinder, rather than covering a plane. Consider a set of loop dislocations lying in parallel slip planes whose normal is $\boldsymbol{m} = (0, 0, -1)$, and which have Burgers vector $\boldsymbol{B} = (0, \hat{b}, 0)$. Suppose also that they lie on the surface of a cylinder as in Fig. 2.4(a). The stress field of one of these dislocations is given by the Peach-Koehler formula (1.55). The component of stress which would move the dislocations is, according to (1.13), the 23-component. For the loop in the x_1x_2-plane (1.55) gives

$$\sigma_{23} = \sigma_{32} = \frac{\mu\hat{b}}{4\pi} \oint_C \frac{1}{2} R_{,1kk} dx_2' - \frac{1}{1-\nu} R_{,233} dx_1',$$

where, we recall, $R = (X_iX_i)^{\frac{1}{2}}$, $X_i = x_i - x_i'$. Allowing the separation of the slip

planes ϵ and the strength of the dislocations $\hat{b}$ to tend to zero, as usual, so that $\lim_{\epsilon,\hat{b}\to 0}(\hat{b}/\epsilon) = \Omega$, the total 23-component of stress for the cylinder becomes

$$\sigma_{23}^{cyl} = -\frac{\mu\Omega}{4\pi}\int_{-\infty}^{\infty}\left(\oint_C \frac{1}{2}R_{,1kk}dx_2' - \frac{1}{1-\nu}R_{,233}dx_1'\right)dx_3'. \tag{2.16}$$

The minus sign is necessary because the normal to the slip plane is in the negative x_3 direction and so the jump in the displacement across the plane of the dislocation loop, $\hat{\boldsymbol{b}}$, is positive as the plane of the loop is crossed in the negative x_3 direction. Thus (2.16) becomes

$$\sigma_{23}^{cyl} = -\frac{\mu\Omega}{2\pi}\oint_C \frac{X_1}{X_1^2+X_2^2}dx_2'. \tag{2.17}$$

In general, this integral cannot be evaluated analytically, but if the curve C is an ellipse, then progress can be made. It is known from the work of Eshelby (1957) that the ellipse is special, and Jaswon & Bhargava (1961) have shown that Eshelby's integral results (which are in fact given for the three-dimensional case of the ellipsoid) can be explicitly determined in two dimensions by means of complex variable techniques. Using the same principle, it is found (see Appendix A.4) that for the ellipse C

$$\sigma_{23}^{cyl}(x_1,x_2) = \mu\Omega\begin{cases} b/(a+b) & (x_1,x_2) \text{ inside } C \\ (ab/c^2)\,\mathcal{R}\{1-z/(z^2-c^2)^{1/2}\} & (x_1,x_2) \text{ outside } C, \end{cases} \tag{2.18}$$

where $z = x_1 + ix_2$ and $\mathcal{R}$ denotes the 'real part'. The only other nonzero component of $\boldsymbol{\sigma}$ for the cylinder is

$$\sigma_{13}^{cyl}(x_1,x_2) = \frac{\mu\Omega}{2\pi}\oint_C \frac{X_1}{X_1^2+X_2^2}dx_1', \tag{2.19}$$

which can be evaluated similarly to give

$$\sigma_{13}^{cyl}(x_1,x_2) = \mu\Omega\begin{cases} 0 & (x_1,x_2) \text{ inside } C \\ (-ab/c^2)\,\mathcal{I}\{1-z/(z^2-c^2)^{1/2}\} & (x_1,x_2) \text{ outside } C, \end{cases} \tag{2.20}$$

where $\mathcal{I}$ denotes the 'imaginary part'.

These results for the ellipse correspond to Eshelby's results for the ellipsoid in that the stress inside the ellipse is constant. Eshelby, however, was considering the case of an ellipsoidal "inclusion" - a region in an elastic material which has undergone a "stress-free transformation strain" - whereas our results are for a distribution of dislocations confined to a surface. It will be seen in Chapter 4 that the two different approaches are in fact equivalent.

To determine the real and imaginary parts of the complex function in (2.18), we introduce confocal coordinates through

$$z = c\cosh(\xi + i\eta) = c(\cosh\xi\cos\eta + i\sinh\xi\sin\eta), \tag{2.21}$$

to obtain

$$1 - \frac{z}{(z^2 - c^2)^{1/2}} = \frac{\cos^2\eta + \sinh\xi\cosh\xi - \cosh^2\xi}{\cos^2\eta - \cosh^2\xi} - i\frac{\sin\eta\cos\eta}{\cos^2\eta - \cosh^2\xi}. \tag{2.22}$$

Note that

$$1 - \frac{z}{(z^2 - c^2)^{1/2}} = \frac{2}{e^{2(\xi+i\eta)} + 1},$$

which behaves like $e^{-2\xi}$ as $\xi \to \infty$. From (2.21) we have that, as $\xi \to \infty$, $|z|^2 \sim e^{2\xi}$, and so the stress indeed decays like the inverse square of the distance as the distance approaches infinity.

This result should not occasion surprise - the far field stress of a two-dimensional patch of screw dislocations of constant density should decay like the inverse of the distance (since that is the behaviour of the stress components of the discrete screw dislocation) and, as we shall see shortly, the cylindrical sheet can be thought of as the 'derivative' of the constant density patch of screw dislocations.

2.5 Two-Dimensional Distributions

2.5.1 A Patch of Screws

The integrands of equations (2.17, 2.19) call to mind the expressions (1.29, 1.30) for the stress components of a screw dislocation, and indeed, comparing (1.29, 1.30) to (2.17, 2.19), and bearing in mind (A.13), it can be seen that (2.17) and (2.19) represent the stress field of a distribution of screw dislocations lying on the cylinder,

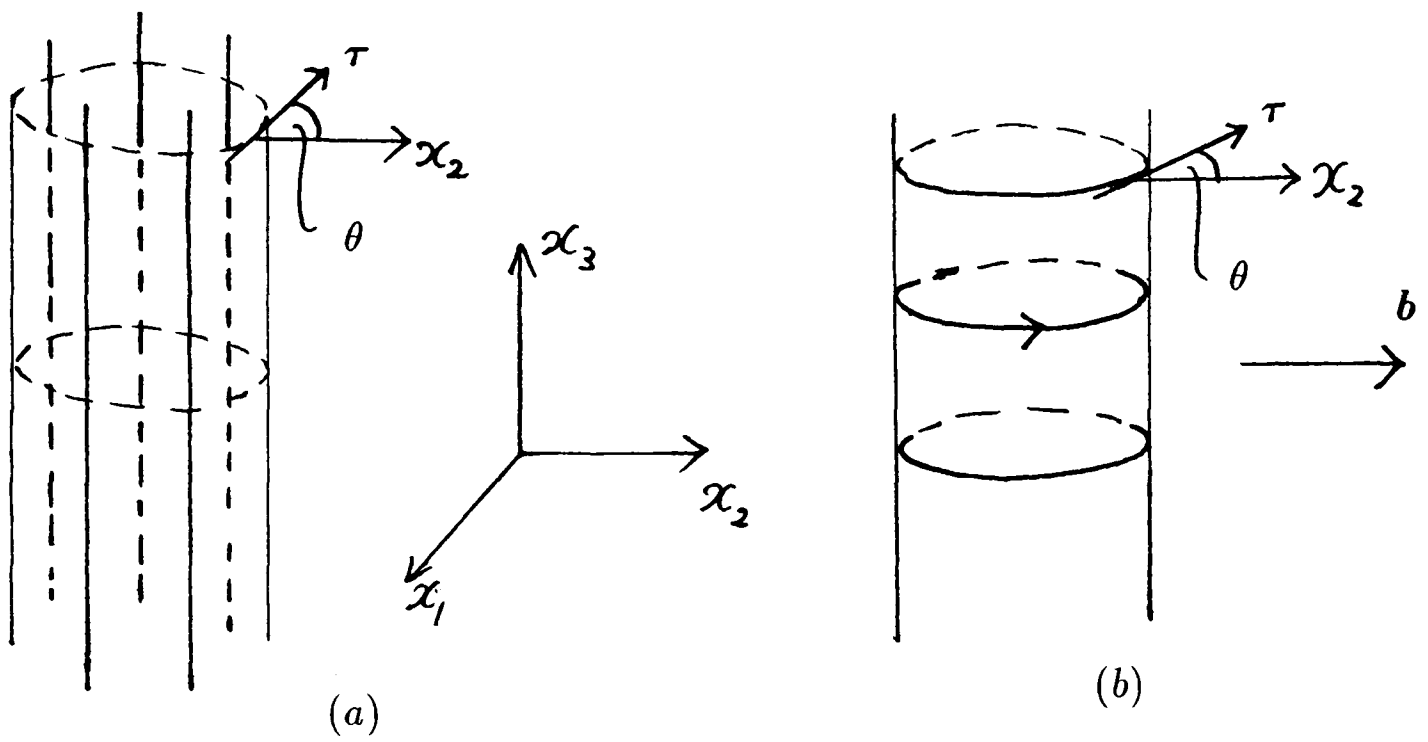

Figure 2.5: (a) Screw dislocations of density $\alpha_{33} = -\Omega\cos\theta$; (b) Loop dislocations of the b_2m_3 family with screw component $\alpha_{22} = \Omega\cos\theta$, edge component $\alpha_{12} = \Omega\sin\theta$.

of density $\alpha_{33} = -\Omega\cos\theta$, where θ is the angle between the tangent to the curve C and the x_2-axis. This density is minus the density of the α_{22} component of the loop dislocations of the b_2m_3 family, and the two distributions are equivalent as far as their stress fields are concerned. We will return to this point in the succeeding chapter. Note also that this equivalence shows that the cylindrical sheet of loops corresponds to a state of anti-plane strain in the material.

Head et al. (1987) also considered two-dimensional elliptic regions, although the dislocation distributions concerned were of pure screws and edges rather than loops as in our case, and were spread throughout a two-dimensional patch rather than being confined to the surface of a cylinder. Nevertheless, in the light of the previous paragraph, it is not surprising that the two situations are related.

The stress field of a distribution of screws of constant density Ω, whose cross-section is a region A, is given by the area integrals

$$\sigma_{23}^{A} = \frac{\mu\Omega}{2\pi}\iint_A \frac{X_1}{X_1^2+X_2^2}dx_1'dx_2', \tag{2.23}$$

$$\sigma_{13}^{A} = -\frac{\mu\Omega}{2\pi}\iint_A \frac{X_2}{X_1^2+X_2^2}dx_1'dx_2'. \tag{2.24}$$

In order to use the results already derived, we differentiate (2.23) and (2.24) with respect to x_1 to obtain

$$\sigma_{23,1}^{A} = -\frac{\mu\Omega}{2\pi}\iint_A \frac{\partial}{\partial x_1'}\frac{X_1}{X_1^2+X_2^2}dx_1'dx_2',$$

$$\sigma^A_{13,1} = \frac{\mu\Omega}{2\pi}\iint_A \frac{\partial}{\partial x'_1}\frac{X_2}{X_1^2+X_2^2}dx'_1dx'_2.$$

Applying Green's theorem in the plane gives

$$\sigma^A_{23,1} = -\frac{\mu\Omega}{2\pi}\oint_C \frac{X_1}{X_1^2+X_2^2}dx'_2, \tag{2.25}$$

$$\sigma^A_{13,1} = \frac{\mu\Omega}{2\pi}\oint_C \frac{X_2}{X_1^2+X_2^2}dx'_2 = -\frac{\mu\Omega}{2\pi}\oint_C \frac{X_1}{X_1^2+X_2^2}dx'_1, \tag{2.26}$$

and these are just the integrals we evaluated earlier. Since the equations of mechanical equilibrium (1.3) hold, we also have

$$\sigma^A_{13,1} = -\sigma^A_{23,2},$$

and so, from (2.18, 2.20) and (2.25, 2.26), we conclude that, if the region A is the interior of an ellipse of semi-major axis a and semi-minor axis b, the 23-component of the stress field *inside* A is

$$\sigma^A_{23} = \mu\Omega\frac{b}{a+b}x_1,$$

the arbitrary constant of integration being found to vanish upon evaluation of (2.23) at the origin. Similarly, one finds

$$\sigma^A_{13} = \mu\Omega\frac{b}{a+b}x_2.$$

If the slip planes of the screw dislocations are taken to be those planes parallel to the x_1x_3-plane, then the condition for equilibrium is that the total 23-component of stress inside the ellipse must be zero. Therefore, as Head et al. (1987) discovered, an applied stress

$$\sigma^{ext}_{23} = -\mu\Omega\frac{b}{a+b}x_1$$

must be imposed to ensure equilibrium of an elliptical patch of α_{33} screw dislocations of constant density. It should also be noted that, as is shown in Section 2.6, it is *necessary* to take Ω to be constant in order to ensure that equilibrium is possible.

2.5.2 A Patch of Edges

A similar result may be derived for a two-dimensional distribution consisting of edge dislocations of the b_1m_2 family. In this case, the stress components are given

by

$$\sigma_{11}^A = -\frac{\mu\Omega}{2\pi(1-\nu)}\iint_A \frac{X_2(3X_1^2+X_2^2)}{(X_1^2+X_2^2)^2}dx_1'dx_2', \tag{2.27}$$

$$\sigma_{22}^A = \frac{\mu\Omega}{2\pi(1-\nu)}\iint_A \frac{X_2(X_1^2-X_2^2)}{(X_1^2+X_2^2)^2}dx_1'dx_2', \tag{2.28}$$

$$\sigma_{12}^A = \sigma_{21}^A = \frac{\mu\Omega}{2\pi(1-\nu)}\iint_A \frac{X_1(X_1^2-X_2^2)}{(X_1^2+X_2^2)^2}dx_1'dx_2'. \tag{2.29}$$

The force exerted on the dislocations is (as given by (1.13)) proportional to the 12-component of the total stress. We follow the same procedure as before (using Green's theorem in the plane) and calculate

$$\sigma_{12,1}^A = \frac{\mu\Omega}{2\pi(1-\nu)}\oint_C \frac{X_1(X_1^2-X_2^2)}{(X_1^2+X_2^2)^2}dx_2',$$

for the case of an elliptical curve C. As shown in Appendix A.5, one finds that inside the ellipse

$$\sigma_{12,1}^A = -\frac{\mu\Omega}{(1-\nu)}\frac{ab}{(a+b)^2}. \tag{2.30}$$

Similarly, since we can write

$$\sigma_{11,1}^A = -\frac{\mu\Omega}{2\pi(1-\nu)}\oint_C \frac{2X_1^2X_2}{(X_1^2+X_2^2)^2} + \frac{X_2}{X_1^2+X_2^2}dx_2',$$

we find that inside the ellipse

$$\sigma_{11,1}^A = 0. \tag{2.31}$$

The equilibrium equations (1.3) tell us in this case that

$$\sigma_{11,1}^A + \sigma_{12,2}^A = 0,$$

and thus from (2.30) and (2.31) we conclude that inside the ellipse C

$$\sigma_{12}^A = -\frac{\mu\Omega}{1-\nu}\frac{ab}{(a+b)^2}x_1,$$

the arbitrary constant being seen to vanish upon evaluation of (2.29) at the origin. Thus we have deduced directly from the Peach-Koehler formula for the stress (1.55) the result of Head et al. (1987), that a two-dimensional distribution of edge

dislocations of constant density Ω occupying an elliptical region is in equilibrium under a linear applied stress

$$\sigma_{12}^{ext} = \frac{\mu\Omega}{(1-\nu)} \frac{ab}{(a+b)^2} x_1.$$

2.6 Dislocation Density of Equilibrium Distributions

We have seen in this chapter how the stress fields of various dislocation distributions may be calculated by using the Peach-Koehler equation (1.55) for the stress field of an arbitrary curved dislocation, and by following an averaging procedure to account for the effect of a large number of discrete dislocations. In particular it has been asserted (Sections 2.3.1, 2.3.3) that planar dislocation sheets exert no force on themselves. On the other hand we have just shown that a two-dimensional, elliptical patch of screw (or edge) dislocations produces a spatially linear stress field, and so an equal and opposite applied linear stress is required to establish equilibrium.

Now the applied stress is not arbitrary but is governed by the usual rules of linear elasticity. For example, when screw dislocations of only one type are present, a state of anti-plane strain exists. Since the applied stress must therefore also correspond to such a state, the hydrostatic stress σ_{kk} must be zero, and, recalling equations (1.1) and (1.6), we have

$$\nabla^2 u_i = 0,$$

which, from (1.1) and (1.4), gives

$$\nabla^2 \sigma_{ij}^{ext} = 0.$$

Next, integrating (2.4) by parts, we may rewrite it as

$$\sigma_{ij} = \frac{\mu}{4\pi} \int \left\{ (\varepsilon_{jmn}\alpha_{in,l'l'm'})^S + \frac{2(\lambda+\mu)}{\lambda+\mu} (\varepsilon_{kmn}\alpha_{kn,i'j'm'} - \varepsilon_{kmn}\alpha_{kn,l'l'm'}\delta_{ij}) \right\} R dV'. \tag{2.32}$$

Returning to the patch (of any shape) of pure screw dislocations, considered in the previous section, for which α_{33} is the only nonzero component of $\boldsymbol{\alpha}$, the condition

for equilibrium is

$$\sigma_{23} + \sigma_{23}^{ext} = 0$$

wherever there are dislocations. In this case the 23-component of (2.32) reduces to

$$\begin{aligned} \sigma_{23} &= -\frac{\mu}{4\pi}\int \frac{1}{2}\alpha_{33,1'k'k'} R dV' \\ &= -\frac{\mu}{8\pi}\int \alpha_{33,1'} R_{,kk} dV', \end{aligned}$$

and so

$$\nabla^2 \sigma_{23} = \mu \alpha_{33,1} = 0,$$

wherever there are dislocations. Thus, we have the result of Head et al. (1987) that, for two-dimensional screw dislocation distributions, the density in the slip plane is constant. Note that, alternatively, this could have been established directly from (2.6) by setting the hydrostatic stress $\sigma_{kk} = 0$.

In general, as we saw in Section 1.2 (equation 1.8), the applied stress will be biharmonic. Head et al. also considered a patch of edge dislocations parallel to the x_3-axis, with Burgers vector in the x_1 direction. Then the slip planes are parallel to the x_1x_3-plane, and there is equilibrium when

$$\sigma_{12} + \sigma_{12}^{ext} = 0.$$

The 12-component of (2.32) reduces, in this case, to

$$\sigma_{12} = -\frac{\mu(\lambda+\mu)}{2\pi(\lambda+2\mu)}\int \alpha_{31,1'2'2'} R dV'.$$

This is not a state of anti-plane strain and so (1.8) holds. Consequently, where there are dislocations

$$\alpha_{31,122} = 0,$$

so that any two-dimensional edge dislocation distribution of the type described above, for which equilibrium is possible under an applied stress, has density of the general form

$$\alpha_{31} = x_2 f_1(x_1) + f_2(x_1) + f_3(x_2),$$

for some functions f_1, f_2, f_3.

Taking ∇^4 of equation (2.32) gives

$$\nabla^4\sigma_{ij} = -2\mu\left[(\varepsilon_{jmn}\alpha_{in,llm})^S + \frac{2(\lambda+\mu)}{\lambda+2\mu}(\varepsilon_{kmn}\alpha_{kn,ijm} - \varepsilon_{kmn}\alpha_{kn,llm}\delta_{ij})\right],$$

and so, in general, a family with Burgers vector $\{b_i\}$, whose slip planes have normal $\{m_j\}$, will be in equilibrium under an applied stress provided that the term on the right above is zero wherever there are dislocations. This retrieval, from the equations of Kröner, of the results of Head et al. for the form of the dislocation density of equilibrium distributions has been given by Head (private communication) and is presented here for completeness.

2.7 Analogy with Electromagnetism

Recall the sheet of screw dislocations described in Section 2.3.1. It is analogous to the vortex sheet in fluid dynamics in that there is a jump in the component of stress on crossing the dislocation sheet, corresponding to a jump in the velocity field as the vortex sheet is crossed. There is in fact a similar analogy with current distributions in electromagnetism[1]: the magnetic field jumps between constant values as a sheet of current is crossed. Also, the Peach-Koehler formula (1.55) for the stress can be thought of as the dislocation equivalent of the Biot-Savart law in electromagnetism (Peach & Koehler 1950).

In pursuing these analogies further, it is useful to examine vortex and current distributions confined to the surface of a cylinder. If the cylinder is made up of vortex loops so that the vorticity is everywhere tangent to the cylinder and at right angles to the generators, it is found that the velocity field has different but constant values inside and outside the cylinder (see Batchelor 1967). The same is true of a current distribution which flows around a cylinder at right angles to the generators (commonly known as a *solenoid*). The cylinder in either of these cases may be of arbitrary cross-section. Clearly, therefore, the corresponding situation in dislocation theory is not going to involve a cylindrical sheet of dislocation loops as described above. The breakdown in the analogy can be seen to be because

[1]See de Wit (1960) for a table of correspondences between vector quantities in magnetostatics and tensors in dislocation theory.

the vorticity of the vortex sheet, and the current of the current distribution are, respectively, always tangential to the vortex and current lines which comprise the cylinder, whereas the Burgers vector of the dislocation loops is a constant. Only if it were possible to have a cylinder sheet of dislocation loops whose Burgers vectors were tangential to the loops, would we expect to find a result comparable to those already mentioned for current and vortex distributions.

So far, we have always taken the Burgers vector to be a constant vector, but in our cut-and-weld definition of the dislocation (Section 1.3.1*(ii)*) it was pointed out that, for the stress components to be continuous away from the cut surface, the displacement needed to be either a translation *or* a rigid body rotation. If we make the latter displacement before welding the body back together again, then we arrive at what is known as a *rotation dislocation*, whose Burgers vector is (in the special case of a circular loop), as required, tangential to the dislocation loop.

It should be noted that the analogy is not such that the stress components are expected to be uniform inside the cylinder and zero outside. Indeed, a stress field of this type can easily be seen to violate the conditions of mechanical equilibrium (1.3). We can see how a circular cylindrical dislocation sheet is analogous to a similarly shaped solenoid by comparing the expressions for the force on each. The force on a current $\boldsymbol{J}$ in a magnetic field $\boldsymbol{B}$ is $\boldsymbol{J} \wedge \boldsymbol{B}$ (see Clemmow 1973, for example) and so is proportional to

$$\boldsymbol{B} \wedge \boldsymbol{\tau},$$

where $\boldsymbol{\tau}$ is tangent to the current lines making up the solenoid. As we have seen (equation (1.12)), the force on a dislocation sheet with unit Burgers vector $\boldsymbol{b}$ in a stress field $\boldsymbol{\sigma}$ is proportional to

$$(\boldsymbol{b}.\boldsymbol{\sigma}) \wedge \boldsymbol{\tau},$$

$\boldsymbol{\tau}$ here being the tangent to the dislocation lines. The correspondence is thus seen to be not between the magnetic field and the stress tensor, but between the magnetic field and the product $\boldsymbol{b}.\boldsymbol{\sigma}$, and we can show that the jump in $\boldsymbol{b}.\boldsymbol{\sigma}$, across the dislocation sheet comprised of rotation dislocations, is a constant.

If the constituent loop dislocations each lie in planes parallel to the x_1x_2-plane, as in Fig. 2.6, then they have Burgers vectors $\hat{b}(b_1, b_2, 0)$ and are such that $b_1 = \tau_1$,

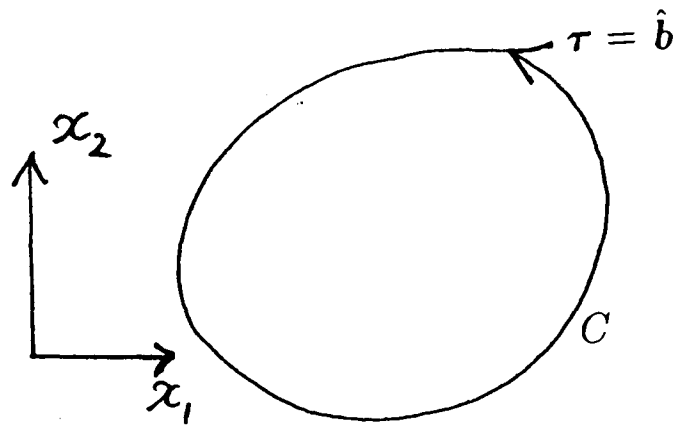

Figure 2.6: A Circular Rotation Dislocation C.

$b_2 = \tau_2$. The stress components of the dislocation sheet are calculated from the Peach-Koehler formula (1.55) to be

$$\sigma_{13}^{rot} = \frac{\mu\Omega}{4\pi}\oint_C \left\{-\frac{X_2}{X_1^2+X_2^2}b_1 dx_1' + \frac{X_1}{X_1^2+X_2^2}b_2 dx_1'\right\},$$

$$\sigma_{23}^{rot} = \frac{\mu\Omega}{4\pi}\oint_C \left\{-\frac{X_2}{X_1^2+X_2^2}b_1 dx_2' + \frac{X_1}{X_1^2+X_2^2}b_2 dx_2'\right\},$$

where Ω is the number density of dislocations in the sheet. These can be written

$$\sigma_{13}^{rot} = \frac{\mu\Omega}{4\pi}\oint_C b_1 \frac{\partial}{\partial n}\log R\, ds, \tag{2.33}$$

$$\sigma_{23}^{rot} = \frac{\mu\Omega}{4\pi}\oint_C b_2 \frac{\partial}{\partial n}\log R\, ds, \tag{2.34}$$

where $\partial/\partial n = \boldsymbol{n}.\boldsymbol{\nabla}$ and $\boldsymbol{n}$ is the unit outward normal to C. In turn (2.33, 2.34) may be written as contour integrals in the complex plane, namely

$$\sigma_{13}^{rot} = \frac{\mu\Omega}{4\pi}\mathcal{I}\oint_C \frac{b_1}{z+w}dw,$$

$$\sigma_{23}^{rot} = \frac{\mu\Omega}{4\pi}\mathcal{I}\oint_C \frac{b_2}{z+w}dw,$$

where $\mathcal{I}$ denotes the imaginary part. From Cauchy's residue theorem it can be seen that as z crosses the curve C there are jumps in the values of σ_{13}^{rot} and σ_{23}^{rot} equal to

$$[\sigma_{13}^{rot}] = \frac{\mu\Omega}{2}b_1, \tag{2.35}$$

$$[\sigma_{23}^{rot}] = \frac{\mu\Omega}{2}b_2, \tag{2.36}$$

where the square bracket indicates the jump in value of the term as the curve C is crossed from the inside.

Consequently

$$[\boldsymbol{b}.\boldsymbol{\sigma}^{rot}] = [b_1\sigma_{13}^{rot} + b_2\sigma_{23}^{rot}] = \frac{\mu\Omega}{2}(b_1^2 + b_2^2) = \frac{\mu\Omega}{2},$$

and the analogy is seen to hold. In general the analogy is not quite so simple. Here, we are aided by the fact that the only nonzero stress components are the off-diagonal elements of the stress tensor. Hence the hydrostatic stress (the trace of the stress tensor) is zero, and Hooke's law (1.4) involves only one of the Lamé constants. The relationship between the stress and strain is in this case exactly analogous to that between the magnetic field density $\boldsymbol{B}$ and the magnetic field intensity $\boldsymbol{H}$, namely that $\boldsymbol{B} = \mu\boldsymbol{H}$ where μ is the "permeability" (see Clemmow 1973, for example).

Chapter 3

ZSE Distributions

We have seen in the previous chapter how simple continuous distributions of dislocations can be built from screws and edges. However, as mentioned in the Introduction, dislocations are often observed not to be arranged in simple sheets, but in three-dimensional configurations with regions of both high and low density. This inhomogeneity is one of the few facts universally acknowledged in respect of dislocations in deformed metals, and with this in mind the aim will be to examine distributions which are confined to a finite region (*finite* or *spatially bounded* distributions).

These inhomogeneous distributions are created by the process depicted schematically in Fig. 1.1. The diagram can be interpreted as follows. Suppose that at the origin O we have a perfect metal crystal; that is, one free from dislocations. The specimen will behave as described in Section 1.1, the crystal remaining perfect as long as the stress does not exceed the yield stress. Beyond the point P_2 the metal will yield, dislocations will be created and will move through the crystal giving plastic strain. Many of the dislocations will move right through the crystal and 'disappear' through the edges, but some will remain when the specimen is unloaded, so that at Q_1 the material will no longer be perfect, although it is unstressed. As this process is repeated, the material will accumulate more and more dislocations. The presence of increasing numbers of dislocations obstructs the motion of those created during deformation and so explains the increase in the proportional limit and yield stress which occur upon loading, unloading and reloading. This process is known as 'work-hardening'.

It should be noted that the yield stress is very much greater than the stress

required to move a single dislocation as described in Section 1.3.2. This may seem to lead to a contradiction, since the movement of a single dislocation certainly corresponds to plastic shear, and so the yield stress might be thought to be the stress required to set in motion a single dislocation in an otherwise perfect crystal. The paradox is resolved when one considers that in practice a large number of dislocations, each exerting stresses on the others, is present. Hence the yield stress must compensate for these stresses, and it is the *resultant* stress on the dislocations at the yield point which is small.

We will begin by considering configurations which are in equilibrium under zero applied stress - that is, we are thinking of a metal described by a point such as Q_1 on the strain axis in Fig. 1.1. As is evident from equation (1.13), for a single family of dislocations equilibrium is achieved if just one component of stress is zero where there are dislocations. That component may be nonzero away from the dislocated region, and certainly the five other independent stress components need not be zero anywhere (although they must of course be biharmonic wherever the strains are compatible, in accordance with equation (1.8)). Given this, it may, therefore, seem unsatisfactory to consider only those distributions which actually produce no stress field at all - that is, in which all components of stress are everywhere zero. However, as we shall soon see, the condition for equilibrium of dislocations actually ensures that, for a large class of finite distributions, the only possible 'self-equilibrium' configuration is one of zero stress everywhere (ZSE) type.

Before proceeding it should be recalled (Section 1.3.2) that a simple cubic lattice is assumed, so that possible slip planes are those planes parallel to the coordinate planes.

3.1 Self-Equilibrium

A continuous distribution of dislocations is the source of a stress field which acts throughout the material concerned, and thus on the distribution itself. The distribution is in equilibrium if the component of the Peach-Koehler force (equation 1.13) in the slip plane, and normal to the dislocation, is zero; in other words if

$$\boldsymbol{F}.\boldsymbol{n} = \sigma_{ij} b_i m_j = 0. \tag{3.1}$$

If this equilibrium is achieved in the absence of externally applied stresses then the distribution is said to be in 'self-equilibrium'.

The condition (3.1) for equilibrium is at first sight a weak condition. If the distribution in question is composed solely of dislocations of one family, then (3.1) indicates (as mentioned above) that only one component of the stress need vanish, and that only where there are dislocations.

A ZSE clearly satisfies equation (3.1) and is thus in equilibrium. It would seem surprising, however, if there were not other distributions which produced some stresses but which nevertheless fulfilled the less restrictive conditions imposed by (3.1). However, the following theorem can be proved.

Theorem 1 Any smooth distribution for which $\boldsymbol{\alpha} \neq \mathbf{0}$ everywhere in a finite simply-connected volume V, and which is in self-equilibrium, must be a ZSE.

Proof We begin by defining the elastic strain energy W as

$$W = \frac{1}{2} \int \sigma_{ij} e_{ij} dV, \tag{3.2}$$

where the integral is over the whole space. Replacing $\boldsymbol{\sigma}$ by its expression in terms of the stress function $\boldsymbol{\psi}$ (equation (1.47)) and integrating twice by parts, the surface terms vanishing at infinity, gives

$$W = \frac{1}{2} \int \psi_{ln} \varepsilon_{ikl} \varepsilon_{jmn} e_{ij,km} dV,$$

where the term in $\boldsymbol{e}$ is minus the incompatibility (equation (1.17)), so that

$$W = -\frac{1}{2} \int \psi_{ln} \eta_{ln} dV. \tag{3.3}$$

Substituting the expression (2.7) for $\boldsymbol{\eta}$ in terms of $\boldsymbol{\alpha}$ we get, since $\boldsymbol{\psi}$ is symmetric,

$$W = \frac{1}{2} \int \psi_{ln} \varepsilon_{nmj} \alpha_{lj,m} dV.$$

Integrating once more by parts, we have

$$W = -\frac{1}{2} \int \phi_{jl} \alpha_{lj} dV, \tag{3.4}$$

where

$$\phi_{jl} = \varepsilon_{jmn} \psi_{nl,m},$$

and

$$\sigma_{ij} = \varepsilon_{ikl}\phi_{jl,k}, \tag{3.5}$$

so that $\boldsymbol{\phi}$ is unique up to the addition of a gradient.

As an example, let us take the situation where the volume V is filled with dislocations of the b_2m_3 family, so that the condition for equlibrium is that $\sigma_{23} = \sigma_{32} = 0$ in V, and the only nonzero components of $\boldsymbol{\alpha}$ are α_{12} and α_{22}. Then (3.4) becomes

$$W = -\frac{1}{2}\int_V \phi_{21}\alpha_{12} + \phi_{22}\alpha_{22}dV.$$

Since $\sigma_{32} = 0$ in V we have $\phi_{21,2} - \phi_{22,1} = 0$ and so can write $\phi_{21} = \partial\zeta/\partial x_1$, $\phi_{22} = \partial\zeta/\partial x_2$, where ζ is continuous and single-valued in V, since V is assumed to be simply-connected. The condition (equation (2.2)) that dislocations do not end, is in this case

$$\alpha_{12,1} + \alpha_{22,2} = 0.$$

Hence

$$W = -\frac{1}{2}\int_V \frac{\partial(\zeta\alpha_{12})}{\partial x_1} + \frac{\partial(\zeta\alpha_{22})}{\partial x_2}dV,$$

or

$$\begin{aligned} W &= -\frac{1}{2}\int_V \boldsymbol{\nabla}.(\zeta\alpha_{12}, \zeta\alpha_{22}, 0)dV \\ &= -\frac{1}{2}\int_{S=\partial V} (\zeta\alpha_{12}, \zeta\alpha_{22}, 0).\boldsymbol{n}dS, \end{aligned}$$

by the divergence theorem, where $\boldsymbol{n}$, being normal to S, is also normal to the dislocations on the boundary of V.

Thus the elastic energy is zero, and since

$$\sigma_{ij}e_{ij} = (\lambda e_{kk}\delta_{ij} + 2\mu e_{ij})e_{ij} \geq 0,$$

(at least for materials whose Poisson ratio $\lambda/2(\lambda+\mu)$ is nonnegative), all the strain components, and therefore the stress components, are zero. A similar method deals with all other possible families of dislocations.

This proof is similar to that used by Kirchhoff to establish uniqueness of solution for problems in elasticity in which either tractions or displacements are given on the boundary of the region in question. Following Kirchhoff, we have used the elastic energy, which, being a convex function, has a unique minimum. Here, however,

we have the added constraint that (1.13) must be satisfied where $\boldsymbol{\alpha} \neq \mathbf{0}$, which is in effect the minimisation of the variation of the elastic energy with respect to dislocation displacement ϵ, so that (1.13) could be written $F_N = \partial W/\partial\epsilon$.

This theorem, though leaving open the possibility that there are non-ZSE equilibrium distributions occupying multiply-connected regions, does reveal that imposing the condition for self-equilibrium greatly restricts the range of valid distributions, and indicates that in metals free from applied stresses ZSEs will play a major role.

Some examples of ZSEs will now be given, and in Section 3.3 the equivalency of ZSEs and dislocation distributions whose incompatibility vanishes everywhere (ZIEs) will be discussed.

3.2 ZSE Distributions

We begin by considering two fundamental ZSE distributions which, though not finite, will nevertheless be useful later in discussing finite distributions. An important finite ZSE will also be discussed, as will an example based on the cylindrical sheet of the previous chapter.

(i) In Section 2.3.1 we saw that a sheet of screw dislocations lying in the $x_1 = 0$ plane, with tangent $\boldsymbol{\tau} = (0,0,1)$, unit Burgers vector $\boldsymbol{b} = (0,0,1)$ and slip plane normal to $\boldsymbol{m} = (0,1,0)$ has a stress field whose only nonzero component is

$$\sigma_{23} = \begin{cases} \mu\Omega/2 & x_1 > 0 \\ -\mu\Omega/2 & x_1 < 0, \end{cases}$$

and for which the only nonzero component of $\boldsymbol{\alpha}$ is

$$\alpha_{33} = \Omega\delta(x_1).$$

Consider next the 'orthogonal family' of screw dislocations with $\boldsymbol{b} = (0,1,0)$, $\boldsymbol{\tau} = (0,-1,0)$, which also covers the plane $x_1 = 0$ with uniform density Ω. This has only one nonzero component of stress, namely

$$\sigma'_{23} = -\sigma_{23},$$

and one nonzero density component,

$$\alpha_{22} = \Omega\delta(x_1),$$

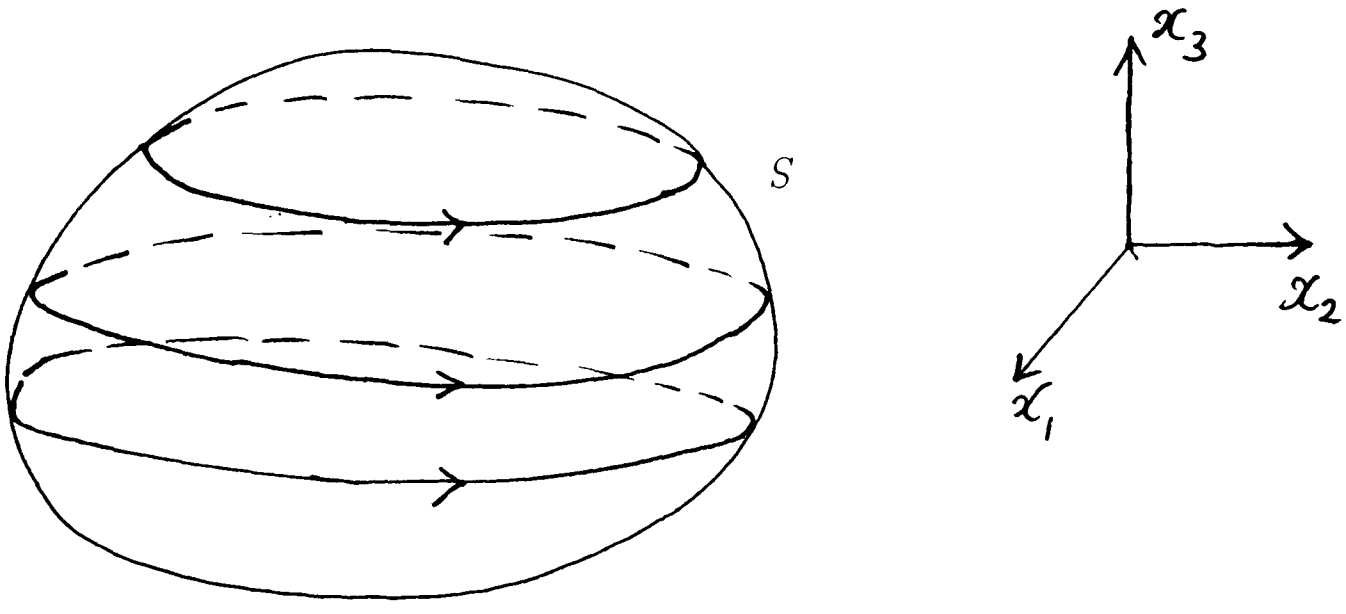

Figure 3.1: Dislocations of the b_2m_3 family lying in a surface S. The arrows denote the tangent $\boldsymbol{\tau}$ to the family.

and so the superposition of these two families has a nonzero density tensor, but zero stress everywhere. In metallurgical terms it is a twist boundary; here it will be termed a *cross-grid of screws.*

It should be noted that it was not necessary here to specify the slip planes, as $\boldsymbol{b}$ and $\boldsymbol{\tau}$ are parallel for pure screw dislocations. However, consideration of how the dislocations could join up if they were (large) loops shows that the α_{33} family lies in x_1x_3-planes, and the α_{22} in x_1x_2-planes. (See also the ZSE box, example *(iii)*).

(ii) The sheet of edges has already been examined in Section 2.3.3, where it was seen that a distribution with nonzero component of $\boldsymbol{\alpha}$

$$\alpha_{31} = \Omega\delta(x_1),$$

is a ZSE. This corresponds to a tilt boundary.

(iii) A simple example of a finite ZSE was found by Head (private communication) by using the expression (2.32) for $\boldsymbol{\sigma}$ in terms of $\boldsymbol{\alpha}$. Consider the family of dislocations of the b_2m_3 slip system, illustrated in Fig. 3.1, which lie in the surface S. For this family (2.2) becomes

$$\alpha_{12,1} + \alpha_{22,2} = 0,$$

and so, for some function $\kappa(x_1, x_2, x_3)$, one may write

$$\alpha_{12} = \frac{\partial\kappa}{\partial x_2}, \qquad \alpha_{22} = -\frac{\partial\kappa}{\partial x_1},$$

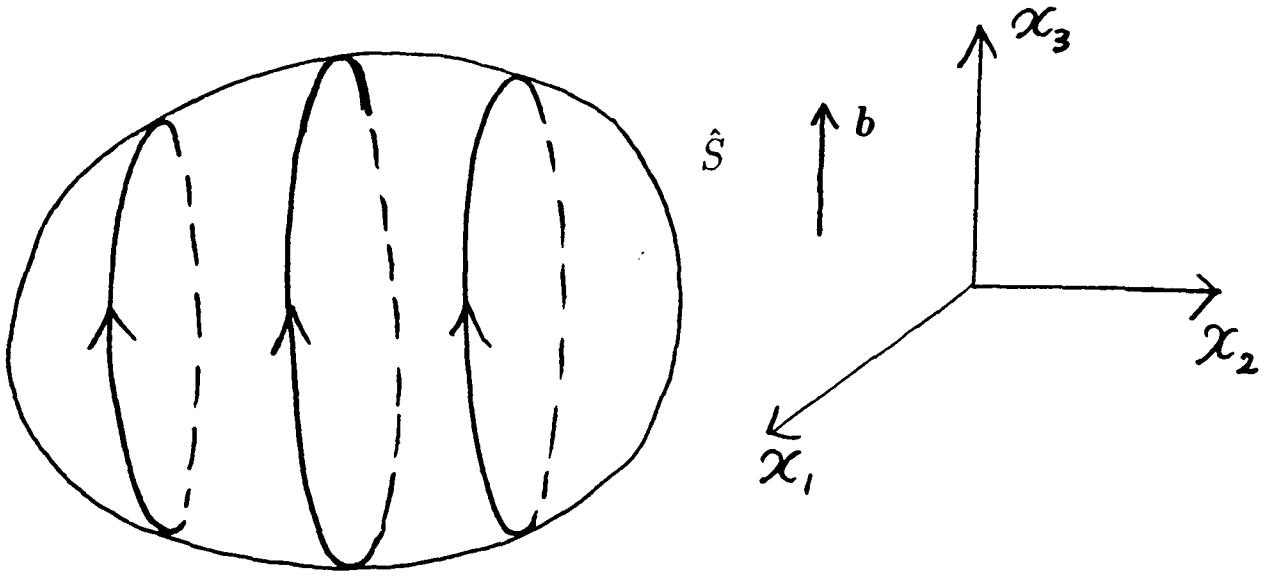

Figure 3.2: Dislocations of the b_3m_2 system, lying in a surface $\hat{S}$.

where, for example, κ could be constant inside the surface and zero outside. The interpretation of functions such as this will be given in Chapter 4. Substituting these expressions for α_{12}, α_{22} into (2.32) gives the σ_{23} component of stress (the component which would move the dislocations) as

$$\sigma_{23} = \sigma_{32} = \frac{\mu}{4\pi}\left[-\frac{1}{2}\nabla^2\frac{\partial^2}{\partial x_1^2} + \frac{2(\lambda+\mu)}{\lambda+2\mu}\left(-\frac{\partial^4}{\partial x_2^2\partial x_3^2} + \frac{\partial^4}{\partial x_1\partial x_2^2\partial x_3}\right)\right]\int \kappa R dV',$$

where we have used the property of R that

$$\frac{\partial R}{\partial x_i} = -\frac{\partial R}{\partial x_i'}.$$

Consider next the 'orthogonal family' of the b_3m_2 system which is shown in Fig. 3.2. In this case (2.2) becomes

$$\hat{\alpha}_{13,1} + \hat{\alpha}_{33,3} = 0,$$

and so one may write

$$\hat{\alpha}_{13} = \frac{\partial\hat{\kappa}}{\partial x_3}, \qquad \hat{\alpha}_{33} = -\frac{\partial\hat{\kappa}}{\partial x_1},$$

for some function $\hat{\kappa}(x_1, x_2, x_3)$. One finds the $\hat{\sigma}_{23}$ component of stress to be

$$\hat{\sigma}_{23} = \hat{\sigma}_{32} = -\frac{\mu}{4\pi}\left[-\frac{1}{2}\nabla^2\frac{\partial^2}{\partial x_1^2} + \frac{2(\lambda+\mu)}{\lambda+2\mu}\left(-\frac{\partial^4}{\partial x_2^2\partial x_3^2} + \frac{\partial^4}{\partial x_1\partial x_2^2\partial x_3}\right)\right]\int \hat{\kappa} R dV'.$$

It is clear, therefore, that if $\hat{\kappa} = \kappa$ then the 23-component of the stress of the combined families will be zero. However, examination of the other stress components

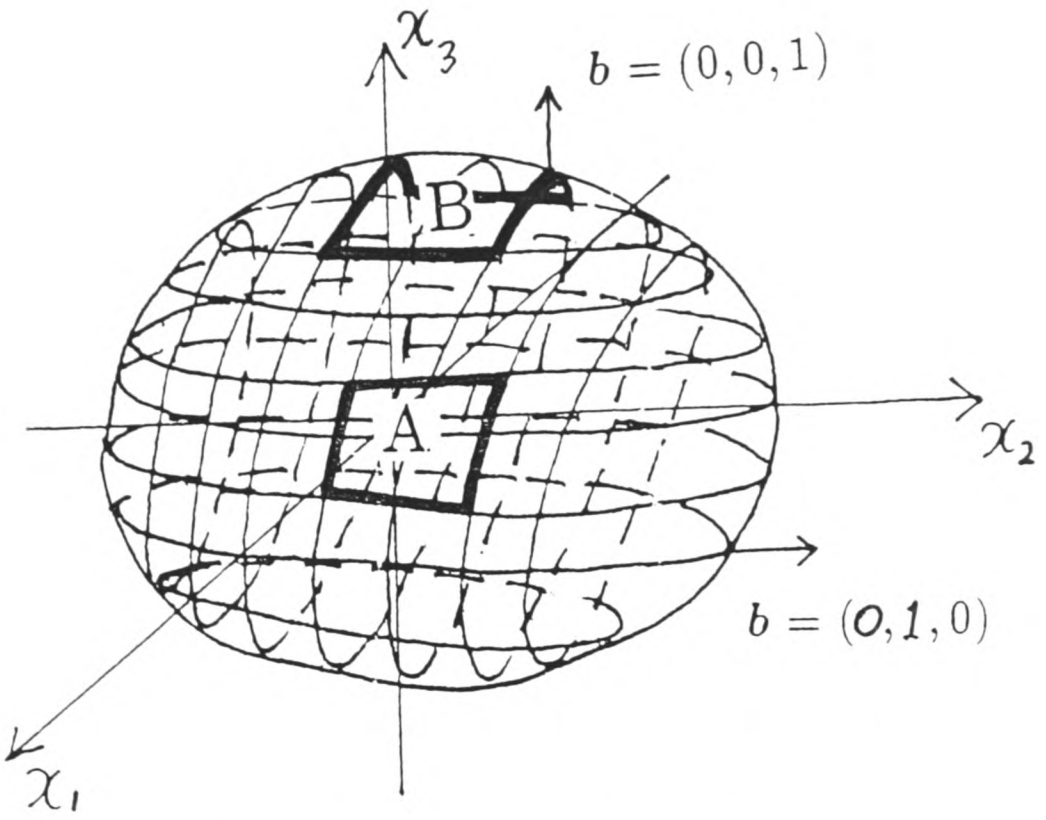

Figure 3.3: A ZSE surface - at A the ZSE looks like a cross-grid of screws, and at B like a sheet of edges.

reveals that they too are identically zero and we have a ZSE. Since $\kappa = \hat{\kappa}$, it is also true that $\alpha_{22} = \hat{\alpha}_{33}$; in other words, the two families lie on the same surface, and locally the superposition is a combination of a cross-grid of screws and a sheet of edges (Fig. 3.3).

A special case of this rather general surface ZSE is that of the cube depicted in Fig. 3.4. Two faces of the cube are cross-grids of screws, while the remaining four are sheets of edges. This ZSE - the "ZSE box" - will be referred to repeatedly in the next chapter where its physical interpretation is given.

(iv) The cylindrical sheet of the previous chapter was composed of dislocations of the b_2m_3 family with nonzero density components α_{12} and α_{22}. It was also described how a cylinder covered by screw dislocations parallel to the x_3-axis would produce an identical stress field if the density was given by

$$\hat{\alpha}_{33} = -\Omega \cos\theta,$$

where θ is the angle between the x_2-axis and the tangent to the cross-section of the cylinder. Thus, if we take the distribution described by

$$\hat{\alpha}_{33} = \Omega \cos\theta,$$

and superimpose this on the cylindrical sheet of the b_2m_3 family (Fig. 3.5), we will obtain a ZSE. The screw component of the b_2m_3 family is

$$\alpha_{22} = \Omega \cos\theta = \hat{\alpha}_{33},$$

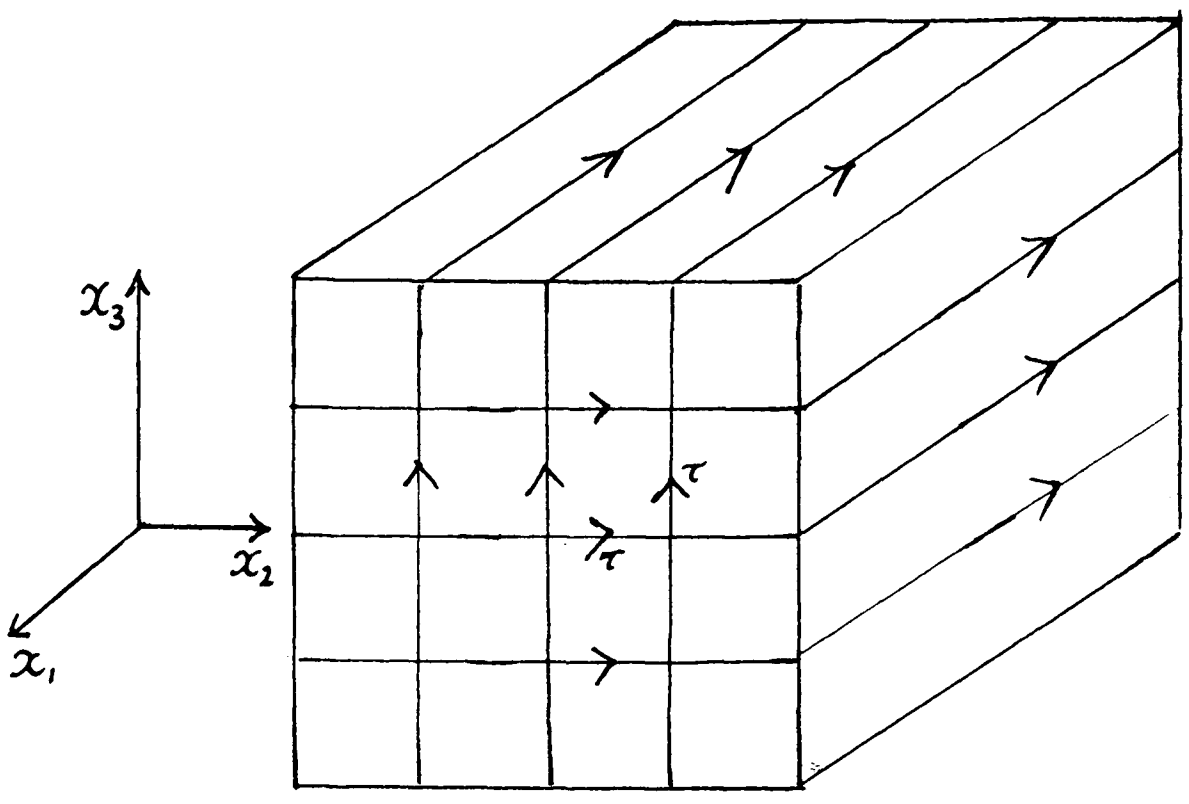

Figure 3.4: The ZSE box: note how the faces are either cross-grids of screws or sheets of edges.

because θ is also the angle between the unit Burgers vector $\boldsymbol{b} = (0, 1, 0)$ and the tangent to the $b_2 m_3$ dislocations. Hence, in common with the cross-grid of screws and the ZSE box, the screw components of the cylinder ZSE are equal, and we can say that, locally, the cylinder ZSE is a combination of a cross-grid of screws and a sheet of edges, and hence another special case of Fig. 3.3.

(v) In plastically deformed metals it is usually the case that dislocations occur in walls which, though considerably thinner than the undislocated regions, are nevertheless comprised of more than a single grid or sheet of dislocations (see Fig. 3.6). The ZSE box is one example taken from a large class of distributions which can be generated from (3.12). A "volume" ZSE can be produced by setting, for example,

$$\begin{aligned} \xi_1 &= \Omega\left[(a_2 - r)H(a_2 - r) - (a_1 - r)H(a_1 - r)\right], \quad \text{where } r^2 = x_1^2 + x_2^2 + x_3^2, \\ \xi_2 &= \xi_3 = 0. \end{aligned}$$

This represents a ZSE distribution occupying an annulus between two spheres with

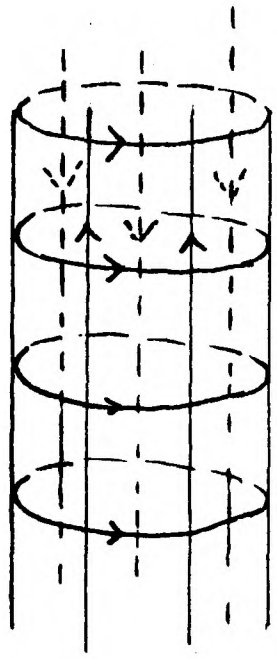

Figure 3.5: Cylindrical ZSE composed of a combination of loops and pure screws.

Figure 3.6: An electron micrograph of work-hardened aluminium. Young et al. (1986).

nonzero density components

$$\alpha_{12} = -\Omega\frac{x_2}{r}[H(a_2 - r) - H(a_1 - r)], \tag{3.6}$$

$$\alpha_{22} = \Omega\frac{x_1}{r}[H(a_2 - r) - H(a_1 - r)], \tag{3.7}$$

$$\alpha_{13} = -\Omega\frac{x_3}{r}[H(a_2 - r) - H(a_1 - r)], \tag{3.8}$$

$$\alpha_{33} = \Omega\frac{x_1}{r}[H(a_2 - r) - H(a_1 - r)]. \tag{3.9}$$

Volume ZSE distributions are just continous distributions of surface ZSEs and can be interpreted correspondingly, as will shortly be seen. There is also experimental evidence, cited in Chapter 4, which supports the contention that the dislocation configurations present in work-hardened metals are similar in nature to volume ZSEs.

3.3 Zero Stress and Zero Incompatibility

It is clear from (1.46) that if $\boldsymbol{\sigma} = \mathbf{0}$ the incompatibility must also be identically zero. That is, every ZSE produces zero incompatibility everywhere (ZIE), and so it is natural to ask whether or not zero incompatibility ensures zero stress. We can in fact prove the following:

For a finite distribution of dislocations zero stress everywhere (ZSE) and zero incompatibility everywhere (ZIE) are equivalent.

As stated above ZSE⇒ZIE by (1.46). To show that ZIE⇒ZSE, we recall that for finite distributions (1.51) holds, and since $\boldsymbol{\eta} = \mathbf{0}$, $\boldsymbol{\chi} = \mathbf{0}$. Then, from (1.54), $\boldsymbol{\sigma} = \mathbf{0}$.

The restriction to finite distributions is important here. Recalling the slab of screw dislocations (Section 2.2.2) it is easy to see that if we add more and more dislocations to the slab, increasing its size (that is, allowing $c \to \infty$) then the whole space will be filled with a dislocation distribution of density $\alpha_{33} = \Omega$, a constant, whose incompatibility is thus zero, but which has nonzero stress component $\sigma_{23} = \sigma_{32} = \mu\Omega x_1$.

Sheets of edges and cross-grids of screws are infinite distributions, but if we think of them as being the appropriate faces of a large ZSE box then they fall within the context of this result.

The importance of this result lies in the fact that, if one wishes to discuss ZSEs, one can restrict consideration to those distributions whose incompatibility is zero. Indeed, we are now in a position to derive the general form of the dislocation density tensor $\boldsymbol{\alpha}$ for finite ZSE distributions. We need to solve (see (2.7) and (2.2))

$$-(\varepsilon_{jmn}\alpha_{in,m})^S = 0, \tag{3.10}$$

and

$$\alpha_{in,i} = 0, \tag{3.11}$$

which constitute nine equations for the nine components of $\boldsymbol{\alpha}$. By using the first six equations (3.10) to write three of the α_{in} in terms of arbitrary functions, and then substituting in the remaining three equations (3.11) for the dislocation densities, one arrives at the result

$$\alpha_{in} = \xi_{i,n} - \xi_{p,p}\delta_{in}, \tag{3.12}$$

where the ξ_i are each arbitrary functions of x_1, x_2, and x_3. For example, the cross-grid of screws can be generated by setting

$$\xi_1 = -\Omega H(x_1), \quad \xi_2 = \xi_3 = 0. \tag{3.13}$$

where H is the Heaviside function. The sheet of edges corresponds to setting

$$\xi_3 = \Omega H(x_1), \quad \xi_1 = \xi_2 = 0. \tag{3.14}$$

The ZSE box can also be seen to be the result of choosing

$$\xi_1 = \kappa = \hat{\kappa}, \quad \xi_2 = \xi_3 = 0, \tag{3.15}$$

with

$$\kappa = \Omega H(a - |x_1|)H(a - |x_2|)H(a - |x_3|),$$

$2a$ being the length of the edges of the box. It is hoped to shed light on the physical interpretation of functions such as $\boldsymbol{\xi}$ in Chapter 4.

3.4 Further Comments

In Section 1.5, the work of a number of authors was cited who had considered distributions of dislocations which produced no "long-range stresses", or rather distributions whose stress field decays exponentially with distance, in contrast to single dislocations, for example, whose stress components decay algebraically. It was also mentioned that if such a discrete array is "smeared out" into a continuous distribution of infinitesimal dislocations, the stress field which results vanishes, as in the case of the cross-grid of screws (Section 3.1), for example, or the sheet of edges (Section 2.3.3). Short-range stress distributions of dislocations predate ZSEs, whose expression in the present context was first given by Head (private communication - see the ZSE surface of Section 3.2) and Mura (1989) (who used the term "impotent" to describe the surface ZSE). However, the origin of ZSEs can be traced back to von Mises (1928) who gave the criterion that a minimum of five *independent* slip systems are necessary if a crystal is to be capable of undergoing general plastic deformation (see Hirth & Lothe 1982, p.297). As detailed in Hirth & Lothe, this means that in a face-centred cubic crystal, for example, in which there are twelve available slip systems (four slip planes, in each of which there are three possible Burgers vectors), the five slip planes necessary for plastic deformation can be chosen from the 12 available in a total of 792 ways. Of these, 144 correspond to leaving the crystal precisely as it was, 264 to a rigid body rotation of one part of the crystal with respect to another, and the remaining 384 to a deformation other than a rigid body rotation. It is the second category that concerns us here - those plastic deformations which result in a rotation of the crystal lattice but no overall change in shape. These ideas will be expanded and clarified in the next chapter.

The approach followed in this chapter to introduce ZSE distributions has not explicitly involved any mention of plastic deformation but has used exclusively the properties of dislocations as sources of stress and incompatibility. Similarly Nye (1953), in introducing the dislocation density tensor, was not concerned *per se* with plastic deformation. The same may be said of Frank (1955) and Bilby et al. (1958). There are thus two alternative approaches to the conceptualisation of ZSEs: *(i)* (as the name ZSE suggests) as distributions of dislocations which produce no stress; and *(ii)* (as will be seen more clearly in Chapter 4) distributions of dislocations

which rotate the lattice lines by means of plastic deformation but which preserve the shape of the material.

3.5 Prismatic Dislocations

Although, as mentioned earlier, we are mainly concerned with glide dislocations, there is one observation which may be made regarding prismatic loops which has implications for the nature of the dislocations in a ZSE. The observation is this: if a ZSE were comprised solely of prismatic dislocations then there would be no screw component. In other words the elements of the trace of $\boldsymbol{\alpha}$ would all be zero. This means, in turn, that, from (3.12)

$$\xi_{1,1} = \xi_{2,2} = \xi_{3,3} = 0,$$

and, consequently, that the dislocation distribution cannot be spatially bounded. Thus, it is concluded that *a finite ZSE cannot be comprised solely of prismatic dislocations.* In the light of Theorem 1, one is therefore led to the conclusion that no finite distribution of purely prismatic dislocations can exist in self-equilibrium, and this further justifies the restriction to glide dislocations imposed here.

Chapter 4

Plastic Distortion - Interpretation of ZSEs

So far, it has been seen how continuous distributions of dislocations may be built up by averaging arrays of discrete dislocations; a set of equations for the stress, incompatibility and dislocation density has been derived, and the model has been closed by giving the condition for equilibrium of a distribution. With the original motivation (a dislocation description of Fig. 1.1) in mind, the role of ZSEs has been highlighted as being obvious candidates for self-equilibrium distributions, and support for the emphasis placed on ZSEs has been supplied by showing that in certain cases these are the only possible self-equilibrium distributions.

In this chapter, our examples of specific ZSEs will be reconsidered in terms of what Kröner (1955) has called "plastic distortion". This will enable us to give a geometrical characterisation of ZSEs and to prove, in a slightly different manner, Theorem 1 of the previous chapter. Having introduced the plastic distortion, and what will be called "total displacement", these quantities will first be given explicitly for the screw and edge dislocations, before the relevant expressions are derived for an arbitrary curved dislocation.

Plastic distortion can be interpreted in a variety of different ways - the "stress-free transformation strain" of Eshelby's (1957) well-known ellipsoidal inclusion problem can be thought of as plastic distortion of the ellipsoid, while Kroupa (1962) interpreted plastic distortion as a continuous distribution of infinitesimal dislocation loops. More will be said about each of these approaches later.

4.1 The Distortion Tensor β

In creating a dislocation loop by cutting over a surface bounded by the line of the proposed dislocation, and displacing the two faces of the cut, holes appear which need filling and some interpenetration will occur for which compensation must be made. If this is indeed the case, then it is extremely difficult to envisage how a displacement may be defined near to the cut. The problem does not arise, however, if one takes the cut surface to be in the plane of the loop, as then the process does not generate any holes or interpenetration except near the line itself, and the displacement is simply defined as the displacement of the material from the reference configuration. Clearly, this displacement is not defined actually on the cut surface itself but only in the limit as the surface is approached from either side.

One way in which to calculate the strain field of a dislocation is to ignore the jump in displacement $\boldsymbol{u}$, differentiate $\boldsymbol{u}$ away from the cut according to (1.1), and note that the result is continuous across the cut. If, however, one wishes to retain information about the cut surface, then the jump in the displacement must not be ignored, and one is led to consider what will be known as the "total displacement" $\boldsymbol{u}^T$, which differs from $\boldsymbol{u}$ solely in the respect that the derivatives of $\boldsymbol{u}^T$ are interpreted as distributions, so that, as shown below, there is an additional term involving a delta function. The gradient of $\boldsymbol{u}^T$ will be written as

$$\beta_{ij}^T = \frac{\partial u_j^T}{\partial x_i}, \tag{4.1}$$

and will be termed "total distortion".

It will be simplest first to give an example. For the screw dislocation (1.29, 1.30)

$$\boldsymbol{u}^T = (0, 0, \theta/2\pi) \qquad -\pi < \theta \leq \pi,$$

where θ is the cylindrical polar coordinate. When the derivatives in (4.1) are interpreted as distributions (see Appendix A.6) one finds

$$\begin{aligned} \beta_{13}^T &= \frac{-\hat{b}x_2}{x_1^2 + x_2^2}, \\ \beta_{23}^T &= \frac{\hat{b}x_1}{x_1^2 + x_2^2} + \hat{b}H(-x_1)\delta(x_2), \end{aligned} \tag{4.2}$$

where H is the Heaviside function. For edge dislocations, where

$$\boldsymbol{u}^T = \left(\arctan\frac{x_2}{x_1} - \frac{x_1x_2}{2(1-\nu)(x_1^2+x_2^2)^2}, \frac{2\nu-1}{4(1-\nu)}\log(x_1^2+x_2^2) + \frac{x_2^2-x_1^2}{4(1-\nu)(x_1^2+x_2^2)}, 0\right),$$

$\boldsymbol{\beta}^T$ has nonzero components

$$\begin{aligned}
\beta_{11}^T &= \frac{\hat{b}}{2\pi}\left[-\frac{x_1}{x_1^2+x_2^2} + \frac{1}{2(1-\nu)}\frac{x_2(x_1^2-x_2^2)}{(x_1^2+x_2^2)^2}\right], \\
\beta_{21}^T &= \frac{\hat{b}}{2\pi}\left[\frac{x_2}{x_1^2+x_2^2} - \frac{1}{2(1-\nu)}\frac{x_1(x_1^2-x_2^2)}{(x_1^2+x_2^2)^2}\right] + \hat{b}H(-x_1)\delta(x_2), \qquad (4.3) \\
\beta_{12}^T &= -\frac{\hat{b}}{2\pi}\left[\frac{1-2\nu}{2(1-\nu)}\frac{x_1}{x_1^2+x_2^2} + \frac{1}{1-\nu}\frac{x_1x_2^2}{(x_1^2+x_2^2)^2}\right], \\
\beta_{22}^T &= -\frac{\hat{b}}{2\pi}\left[\frac{1-2\nu}{2(1-\nu)}\frac{x_2}{x_1^2+x_2^2} - \frac{1}{1-\nu}\frac{x_1^2x_2}{(x_1^2+x_2^2)^2}\right].
\end{aligned}$$

In either situation the respective $\boldsymbol{\beta}$ can be averaged, as were the stress components in Chapter 2, and it is seen that the distortion tensor $\boldsymbol{\beta}^T$ will inevitably have two components. One component (the last terms in each of (4.2) and (4.3)) is the plastic component, subsequently to be called $\boldsymbol{\beta}^P$, in which is encoded the cut-and-weld instructions; it is merely the generalised derivative of the relative displacements through $\boldsymbol{B}$ that have occurred across all the cuts. The other component (the first two terms in (4.2) and (4.3)), subsequently to be called $\boldsymbol{\beta}^E$, is the elastic component resulting from the elastic response to the weld process. We thus write

$$\boldsymbol{\beta}^T = \boldsymbol{\beta}^E + \boldsymbol{\beta}^P,$$

and note that none of these tensors is necessarily symmetric. In the continuum limit both components of $\boldsymbol{\beta}^T$ will be piecewise smooth functions wherever cuts have been made. For example, for the sheet of screws (Section 2.3.1) the only nonzero component of $\boldsymbol{\beta}^P$ is

$$\beta_{23}^P = \Omega H(-x_1),$$

and for the sheet of edges (Section 2.3.3)

$$\beta_{21}^P = \Omega H(-x_1).$$

From these examples it is expected that $\boldsymbol{\beta}^P$ will have support over the cut surface, and indeed it can be shown that this is the case for the arbitrary curved dislocation. In order to derive this result, we first develop the expression for $\boldsymbol{u}^T$ for a curved dislocation.

4.2 Total Displacement of an Arbitrary Curved Dislocation

In Chapter 1 Navier's equations (1.6) for the displacements in a strained elastic body were derived. Clearly, when a dislocation is present in the body, these equations hold only away from the cut surface. Similarly, the total displacement $\boldsymbol{u}^T$ will satisfy Navier's equations away from the cut, but there will be a nonzero right-hand side corresponding to the distributional derivatives. Thus we may write

$$(\lambda + \mu)u^T_{j,ji} + \mu\nabla^2 u^T_i = -g_i, \tag{4.4}$$

where g_i exists only on the cut surface. To solve this equation it is useful to introduce Green's tensor function G_{ij}, the tensor analogue of the usual Green's function which is often used to solve differential equations. Whereas the Green's function $G(\boldsymbol{x})$ represents the response of a system at a point $\boldsymbol{x}$ to a unit impulse applied at the origin, the Green's tensor function here represents the displacement $u^T_i(\boldsymbol{x})$ due to a point force at the origin in the direction x_j. Seeger (1955) has shown that the equation for G_{ij} is

$$(\lambda + \mu)G_{jm,ji}(\boldsymbol{x}) + \mu\nabla^2 G_{im}(\boldsymbol{x}) + \delta_{im}\delta(\boldsymbol{x}) = 0, \tag{4.5}$$

along with the boundary condition that G_{ij} vanishes at infinity. Here, $\delta(\boldsymbol{x})$ is the three dimensional version of the Dirac delta function (Section 1.6.2). The solution of (4.4) is then

$$u^T_k(\boldsymbol{x}) = \int G_{km}(\boldsymbol{x} - \boldsymbol{x}')g_m(\boldsymbol{x}')dV', \tag{4.6}$$

where the integral is over the whole space. Substituting (4.6) in (4.4) and using (4.5) confirms that this is indeed the solution. However, (4.6) is not a very useful expression for $\boldsymbol{u}^T$, and so we begin with the equivalent expression

$$u^T_m = \int_{V/S}\{(\lambda + \mu)G_{im,ik} + \mu\nabla^2 G_{km}\}u^T_k dV', \tag{4.7}$$

where the integral is over the whole space, *apart from the cut surface S*. Evaluating this using the divergence theorem, and denoting the positive side of S by S_+ and the negative side by S_-, we have

$$u_m^T = \int_{S_+,S_-} \{\lambda \delta_{ik} G_{lm,l} + \mu(G_{km,i} + G_{im,k})\} u_k^T n_i dS'. \tag{4.8}$$

The surface terms at infinity vanish since G_{ij} vanishes there. As the displacement u_k^T jumps by the amount B_k, the Burgers vector, on crossing S, (4.8) gives

$$u_m^T(\boldsymbol{x}) = \int_S B_k \{\lambda \delta_{ik} G_{lm,l}(\boldsymbol{R}) + \mu(G_{km,i}(\boldsymbol{R}) + G_{im,k}(\boldsymbol{R}))\} n_i dS', \tag{4.9}$$

where we have written $\boldsymbol{R} = \boldsymbol{x} - \boldsymbol{x}'$.

All that now remains is to evaluate G_{ij} by solving in (4.5). This we can do by using Fourier transforms (Leibfried 1953, see de Wit 1960). Defining the Fourier transform of G_{km} as

$$\bar{G}_{km}(\boldsymbol{k}) = \int G_{km}(\boldsymbol{x}) e^{i\boldsymbol{k}.\boldsymbol{x}} dV_x,$$

the integration being over the whole space, then the inverse transform is

$$G_{km}(\boldsymbol{x}) = \frac{1}{(2\pi)^3} \int \bar{G}_{km}(\boldsymbol{k}) e^{-i\boldsymbol{k}.\boldsymbol{x}} dV_k. \tag{4.10}$$

Taking Fourier transforms of (4.5) gives us

$$(\lambda + \mu) k_j k_i \bar{G}_{jm} + \mu k^2 \bar{G}_{im} = \delta_{im}.$$

Multiplying by k_i and summing over i this becomes

$$(\lambda + \mu) k^2 k_j \bar{G}_{jm} + \mu k^2 k_i \bar{G}_{im} = k_m,$$

and so

$$\bar{G}_{lm}(\boldsymbol{k}) = \frac{1}{\mu}\left[\frac{\delta_{lm}}{k^2} - \frac{\lambda + \mu}{\lambda + 2\mu}\frac{k_l k_m}{k^4}\right],$$

which we can invert using (4.10) to give

$$G_{lm}(\boldsymbol{x}) = \frac{1}{8\pi\mu}\left[\delta_{lm}|\boldsymbol{x}|_{,pp} - \frac{\lambda + \mu}{\lambda + 2\mu}|\boldsymbol{x}|_{,lm}\right]. \tag{4.11}$$

Substituting in (4.9) for G_{km}, we obtain the expression for the displacement as

$$\begin{aligned} u_m^T(\boldsymbol{x}) &= \frac{1}{8\pi}\int_S \left\{ \frac{\lambda}{\lambda+2\mu} B_i R_{,mpp} + \left(B_m R_{,ipp} + B_k \delta_{im} R_{,kpp} - 2\frac{\lambda+\mu}{\lambda+2\mu} R_{,ikm} \right) \right\} n_i dS' \\ &= -\frac{1}{8\pi}\int_S B_i R_{,mpp} dS_i' \\ &\quad + \frac{1}{8\pi}\int_S \{ B_m R_{,ipp} dS_i' + B_k R_{,kpp} dS_m' \} \\ &\quad + \frac{1}{4\pi}\frac{\lambda+\mu}{\lambda+2\mu}\int_S \{ B_i R_{,mpp} - B_k R_{,ikm} \} dS_i' \\ &= \frac{1}{8\pi}\int_S B_m R_{,ipp} dS_i' \\ &\quad + \frac{1}{8\pi}\int_S \{ B_k R_{,kpp} dS_m' - B_i R_{,mpp} dS_i' \} \qquad (4.12) \\ &\quad + \frac{1}{4\pi}\frac{\lambda+\mu}{\lambda+2\mu}\int_S \{ B_i R_{,mpp} - B_k R_{,ikm} \} dS_i'. \end{aligned}$$

The last two terms here can be turned into line integrals around the boundary of the cut surface, that is, along the dislocation line C. Stokes' theorem is, in suffix notation,

$$\int_S \varepsilon_{ijk} A_{k,j} dS_i = \oint_C A_k dx_k,$$

for any open surface S bounded by the curve C. The second term in (4.12) may be written (bearing in mind that $R_{,i} = -R_{,i'}$) as

$$\begin{aligned} \frac{1}{8\pi}\int_S \{ B_k R_{,kpp} dS_m' - B_i R_{,mpp} dS_i' \} &= \frac{1}{8\pi}\int_S B_l \varepsilon_{ijk}\varepsilon_{klm} R_{,ppj} dS_i' \\ &= \frac{1}{8\pi}\oint_C B_l \varepsilon_{klm} R_{,pp} dx_k'. \end{aligned}$$

Applying Stokes' theorem in a similar fashion to the third term in (4.12) we obtain

$$\begin{aligned} u_m^T = \frac{1}{8\pi}\int_S B_m R_{,ppi} dS_i' &+ \frac{1}{8\pi}\oint_C \varepsilon_{klm} B_l R_{,pp} dx_k' \\ &+ \frac{1}{4\pi}\frac{\lambda+\mu}{\lambda+2\mu}\oint_C \varepsilon_{kin} B_n R_{,mi} dx_k', \end{aligned}$$

which we may alternatively write as

$$u_m^T = -\frac{B_m \Omega}{4\pi} - \frac{1}{4\pi}\oint_C \frac{\varepsilon_{mlk} B_l}{R} dx_k' - \frac{1}{4\pi}\frac{\lambda+\mu}{\lambda+2\mu}\left(\oint_C \frac{\varepsilon_{kni} B_n X_i}{R} dx_k' \right)_{,m}, \qquad (4.13)$$

where

$$\Omega = \int_S \frac{X_i}{R^3} dS_i' = -\frac{1}{2} \int_S R_{,ppi} dS_i'$$

is the solid angle subtended at $\boldsymbol{x}$ by the surface S. This is essentially the form given by Burgers (1939) (see de Wit 1960), the minus sign being the consequence of an opposite definition of the Burgers vector. The solid angle is not a single valued function - it changes by an amount 4π on linking the curve C. However, the last two terms in (4.13) are single-valued. The second term can be seen to be so because in vector notation it can be written

$$-\frac{1}{4\pi} \oint_C \frac{\boldsymbol{B} \wedge d\boldsymbol{x}'}{R},$$

which is proportional to the vector potential of a line current in magnetostatics. The third term is the gradient of a single-valued function, and so, when integrated around a closed curve, it gives zero.

De Wit (from whose review article much of the above is taken) obtains the expression (4.13) for the displacement by assuming that the material contains body forces, so that Navier's equations (1.6) have a nonzero right-hand side, and hence that a nontrivial solution may be derived. He then sets the body forces to zero to deduce the formula (4.9). Whilst this gives the correct answer, it is a little misleading, since there are in fact no body forces at all. However, the g_i in (4.4) may be interpreted as being a layer of body forces confined to the cut surface.

Now that we have arrived at an expression for the total displacement of an arbitrary curved dislocation we recall our original motivation, which was to find the associated total plastic distortion. This we do by taking the gradient of the total displacement.

4.3 Total Plastic Distortion of an Arbitrary Curved Dislocation

In deriving their formula (1.55) for the stress tensor of a dislocation as a line integral over the dislocation curve, Peach & Koehler (1950) expressed the solid angle as a line integral and differentiated under the integral sign. It is easier, however, firstly to take the gradient of the solid angle and express that as a line integral.

Again we follow de Wit (1960) and note that

$$\begin{aligned}\frac{1}{2}\oint_C \varepsilon_{jkl} R_{,ppl} dx'_k &= \frac{1}{2}\int_S \{R_{,llpp} dS'_j - R_{,jlpp} dS'_j\} \\ &= \frac{1}{2}\int_S R_{,llpp} dS'_j + \Omega_{,j}.\end{aligned}$$

Using the relation $R_{,llpp} = -8\pi\delta(\boldsymbol{R})$, our expression for the total plastic distortion is

$$\begin{aligned}\beta^T_{ji} = u^T_{i,j} &= \beta^P_{ji} + \beta^E_{ji} \\ &= -B_i \int_S \delta(\boldsymbol{R}) dS'_j \\ &\quad -\frac{B_i}{8\pi}\oint_C \varepsilon_{jkl} R_{,lpp} dx'_k \\ &\quad +\frac{B_l}{8\pi}\oint_C \varepsilon_{ikl} R_{,jpp} dx'_k \\ &\quad +\frac{B_n}{8\pi}\frac{\lambda+\mu}{\lambda+2\mu}\oint_C \varepsilon_{kmn} R_{,ijm} dx'_k. \qquad (4.14)\end{aligned}$$

In common with our earlier examples we have a plastic component (the first term) which has value B_i on the cut surface and is zero elsewhere, and an elastic component comprised of the other three terms.

An immediate consequence of (4.14) is that the elastic distortion gives the components of the strain through the equation

$$e_{ij} = \frac{1}{2}(\beta^E_{ij} + \beta^E_{ji}), \qquad (4.15)$$

and thus the stress components (1.55) through Hooke's law (1.4). Indeed, by neglecting the plastic distortion, this was how Peach & Koehler (1950) derived the expression for the stress tensor.

At the beginning of this chapter it was stated that, in order to give physical meaning to the total displacement, we would always take the cut surface to be in the plane of the dislocation. It should be noted, however, that in the derivation leading to (4.13) the cut surface could be any surface whose boundary is the dislocation line. We will say more about this shortly.

4.4 Distortion and the Density Tensor

Since the plastic distortion $\boldsymbol{\beta}^P$ effectively records the cut-and-weld procedure, it is not surprising that the dislocation density tensor $\boldsymbol{\alpha}$ may be written in terms of $\boldsymbol{\beta}^P$. The appropriate relation was first written down by Kröner (1955); three observations will help us to identify the nature of this relation. The first is to note that (2.2) expresses the fact that the divergence of $\boldsymbol{\alpha}$ is zero. This means that $\boldsymbol{\alpha}$ may be written as the "curl" of a function which is unique up to the addition of a gradient. Secondly, from (1.17), (2.3) and (4.15), we have that

$$\varepsilon_{jmn}\alpha_{in,m} + \varepsilon_{imn}\alpha_{jn,m} = \varepsilon_{ikl}\varepsilon_{jmn}(\beta^E_{ln} + \beta^E_{nl})_{,km}.$$

This suggests that the dislocation density is the "curl" of the elastic distortion $\boldsymbol{\beta}^E$. To relate $\boldsymbol{\alpha}$ to the plastic distortion we make our final observation. The equation

$$\boldsymbol{\nabla} \wedge \boldsymbol{\beta}^T = \boldsymbol{\nabla} \wedge (\boldsymbol{\beta}^E + \boldsymbol{\beta}^P) = \mathbf{0}, \tag{4.16}$$

would be automatically satisfied in the classical sense if $\boldsymbol{u}^T$ were differentiable, since $\boldsymbol{\beta}^T$ is the gradient of $\boldsymbol{u}^T$, but it is always satisfied in the sense of distributions. Thus we are led to suggest that $\boldsymbol{\alpha}$ is minus the curl of $\boldsymbol{\beta}^P$, a suggestion which we can show to be true by re-examining (4.14). From (4.14) we have

$$\beta^P_{ln} = -B_n \int_S \delta(\boldsymbol{R}) dS'_l, \tag{4.17}$$

whose curl is

$$\begin{aligned} \varepsilon_{ikl}\beta^P_{ln,k} &= B_n \int_S \varepsilon_{ikl}\delta(\boldsymbol{R})_{,k'} dS'_l \\ &= -B_n \int_S \{\boldsymbol{m} \wedge \boldsymbol{\nabla}\delta(\boldsymbol{R})\}_i dS', \end{aligned}$$

where $\boldsymbol{m}$ is the outward normal to S and the subscript 'i' here denotes the i'th component rather than the derivative with respect to x_i. Therefore (using the formula $\oint_C \phi d\boldsymbol{x} = \int_S \boldsymbol{n} \wedge \boldsymbol{\nabla}\phi dS$ from vector analysis)

$$\begin{aligned} -\varepsilon_{ikl}\beta^P_{ln,k} &= B_n \oint_C \delta(\boldsymbol{R}) dx'_i \\ &= B_n \tau_i \oint_C \delta(\boldsymbol{R}) dl', \end{aligned}$$

$\boldsymbol{\tau}$ being the unit tangent vector to the dislocation line, and dl' a line element. The right-hand side here is clearly the 'in'-component of the dislocation density, since the integral is a delta function along the dislocation line, and so we have

$$\alpha_{in} = -\varepsilon_{ikl}\beta^P_{ln,k}. \tag{4.18}$$

It follows immediately from (4.16) that

$$\alpha_{in} = \varepsilon_{ikl}\beta^E_{ln,k}. \tag{4.19}$$

From the expressions for $\boldsymbol{\beta}^E$ and $\boldsymbol{\beta}^P$ in (4.14) it is seen that $\boldsymbol{\beta}^P$ is not unique, due to the arbitrariness of the cut surface spanning the dislocation line. Thus, if $\boldsymbol{\beta}^P$ were defined by (4.18), the appropriate surface would have to be given to ensure uniqueness. On the other hand $\boldsymbol{\beta}^E$, being an integral around the dislocation line, is unique. If $\boldsymbol{\beta}^E$ were to be defined through (4.19) we would therefore require a "gauge" condition. This is supplied by substituting (4.15) into the equilibrium equations (1.3) giving

$$(\lambda\beta^E_{kk}\delta_{ij} + 2\mu(\beta^E_{ij})^S)_{,i} = 0, \tag{4.20}$$

and, indeed, this condition can be shown to ensure uniqueness of $\boldsymbol{\beta}^E$ (see Mura (1963) and Willis (1967)[1] where the explicit Green's function representation $\beta^E_{mn}(\boldsymbol{x}) = \int C_{ijkl}G_{nk,l}(\boldsymbol{x}-\boldsymbol{x}')\varepsilon_{rmj}\alpha_{ri}(\boldsymbol{x}')dx'$ is displayed, C_{ijkl} being the elastic constants for the anisotropic case).

4.5 Choice of the Cut Surface

It has already been stated that the emphasis here is on glide dislocations, and it has been assumed that the available slip planes are parallel to the coordinate planes. For a dislocation which fulfils these criteria it is natural to choose the surface in which to make the cut to be the slip plane. In this case it can be seen from (4.17) that only one off-diagonal component of $\boldsymbol{\beta}^P$ is nonzero.[2] For example,

[1]This situation is also reminiscent of electromagnetism where the gauge condition div $\boldsymbol{A} = 0$ ensures the uniqueness of the vector potential whose curl is the magnetic field (in fact $\boldsymbol{A} = \int \boldsymbol{j}dv/|\boldsymbol{r}|$, where $\boldsymbol{j}$ is the current).

[2]It is important for later purposes to observe that the restriction to glide dislocations implies that the diagonal components of $\boldsymbol{\beta}^P$ are each zero.

if the dislocation were given by

$$\alpha_{12} = \sin\theta\delta(1-r)\delta(z), \tag{4.21}$$

$$\alpha_{22} = -\cos\theta\delta(1-r)\delta(z), \tag{4.22}$$

where (r,θ) are polar coordinates in the x_1x_2-plane, then we would have $\beta^P_{32} = H(1-r)\delta(z)$ with all other components being zero. In later sections it will always be assumed that the cut is chosen in this way, but it is illuminating to consider other examples. The cut may be made over any open surface whose boundary is the dislocation loop, so that $\boldsymbol{\beta}^P$, which spans the surface, will have a different form depending upon the chosen cut. If, for instance, in the above example the spanning surface were the semi-infinite cylinder $r = 1, z \geq 0$, the nonzero components of $\boldsymbol{\beta}^P$ would be

$$\beta^P_{22} = \sin\theta\delta(1-r)H(z),$$

$$\beta^P_{12} = \cos\theta\delta(1-r)H(z).$$

Any other spanning surface would have a combination of $\beta^P_{32}, \beta^P_{22}$, and β^P_{12}, as can be observed from (4.17).

A slight variation on this example is if the dislocation loop, while still a glide dislocation, is such that its slip plane is not parallel to one of the coordinate planes. If the cut is, nevertheless, chosen to be in the slip plane, then the diagonal elements of $\boldsymbol{\beta}^P$ are nonzero (Fig. 4.1), but since the Burgers vector is normal to the slip plane normal, it can be deduced from (4.17) that the trace of $\boldsymbol{\beta}^P$ is zero.

In summary, for glide dislocations there are two cases: if the slip planes are all parallel to coordinate planes and the cuts have been made in the slip planes, then the diagonal elements of $\boldsymbol{\beta}^P$ are each zero; in the case in which the slip planes are not parallel to the coordinate planes, but the cuts are made in the slip planes, one can say that $\beta^P_{kk} = 0$. The breaking of either of these conditions implies the presence of prismatic dislocations.

4.6 Construction of ZSEs

Now that the concept of plastic distortion has been introduced and the implications of the choice of cut surface have been explored, we will return to the theme of the

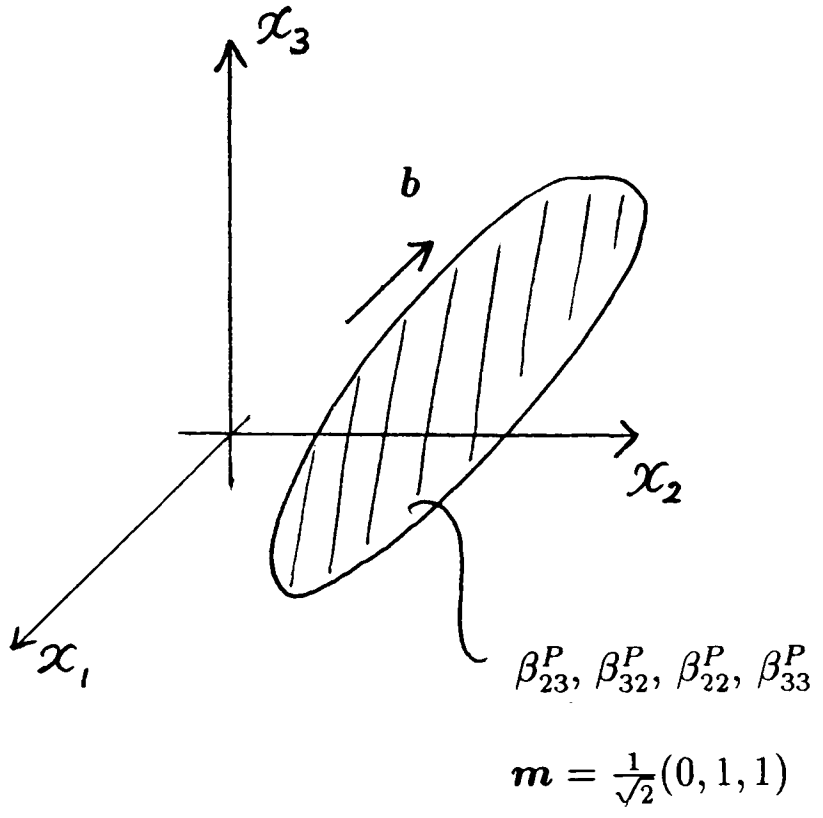

Figure 4.1: A dislocation loop whose slip plane is not parallel to one of the coordinate planes, and therefore which has nonzero diagonal elements of $\boldsymbol{\beta}^P$.

previous chapter, and discuss how an understanding of plastic distortion can enable us to create ZSEs following the idea of Mura (1989) and Head et al. (1992). It will be assumed that we are concerned with glide dislocations, that all slip planes are parallel to coordinate planes, and that the cuts needed to create the dislocations are made in the slip planes. Let us begin by making an observation. Substituting (4.18) into (2.3) gives

$$\eta_{ij} = \varepsilon_{ikl}\varepsilon_{jmn}(\beta^P_{ln})^S_{,km}; \tag{4.23}$$

hence the skew-symmetry of $\boldsymbol{\beta}^P$ ensures the vanishing of $\boldsymbol{\eta}$, and in turn $\boldsymbol{\sigma}$ (see Section 3.3). Thus, supposing we are given a family of dislocations, we can ask whether it is possible to "cancel" the stress field of this family by superposing a second family in such a way as to ensure a skew-symmetric $\boldsymbol{\beta}^P$. The feasibility of this construction can be seen, for example, when we have a given distribution of b_2m_3 dislocations, giving nonzero α_{12}, α_{22}. Here, from (4.17), the only nonzero component of $\boldsymbol{\beta}^P$ is β^P_{32}. Now superpose a new distribution whose only nonzero component is

$$\beta'^P_{23} = -\beta^P_{32}.$$

It will only have $b_3 m_2$ dislocations (with α_{13}, α_{33} the only nonzero dislocation densities), each of which will be orthogonal to the original family. However, $\boldsymbol{\beta}^P + \boldsymbol{\beta}'^P$ is skew-symmetric and so there is zero stress and zero incompatibility everywhere. This procedure can evidently be extended to more general families, as will be illustrated shortly.

The cross-grid of screws (Section 3.2*(i)*) can be generated by a skew-symmetric plastic distortion with nonzero components

$$\beta^P_{23} = \Omega H(-x_1) = -\beta^P_{32}. \tag{4.24}$$

Incidentally, (4.24) also indicates that the slip planes have been chosen to be those parallel to the x_1x_3 and x_1x_2-planes for the α_{33} and α_{22} dislocations respectively.

The ZSE box is composed of dislocations of the b_2m_3 and b_3m_2 families for which cuts were made inside the box parallel to the x_1x_2 and x_1x_3-planes respectively. The relevant nonzero components of $\boldsymbol{\beta}^P$ are consequently

$$\beta^P_{23} = -\beta^P_{32} = \Omega H(a - |x_1|)H(a - |x_2|)H(a - |x_3|). \tag{4.25}$$

On the other hand, the sheet of edges is not produced by a skew-symmetric $\boldsymbol{\beta}^P$, but by a single nonzero component

$$\beta^P_{21} = \Omega H(-x_1), \tag{4.26}$$

if the cuts are made in the negative x_1-plane.

The expressions (4.24, 4.26, 4.25) for the plastic distortion resemble closely those for the vector $\boldsymbol{\xi}$ (3.13, 3.14, 3.15). This is not a coincidence, and it will be seen later in what sense $\boldsymbol{\beta}^P$ and $\boldsymbol{\xi}$ are related in ZSEs.

4.7 Distortion in ZSEs

As stated above, the skew-symmetry of $\boldsymbol{\beta}^P$ ensures that $\boldsymbol{\eta}$ and $\boldsymbol{\sigma}$ vanish, and if we were to compare the expression for $\boldsymbol{\alpha}$ in terms of $\boldsymbol{\xi}$ as given in (3.12) with that for $\boldsymbol{\alpha}$ in terms of $\boldsymbol{\beta}^P$ as given in (4.18), we would be encouraged to ask whether $\boldsymbol{\beta}^P$ is always skew-symmetric in a ZSE. In fact we can show that this is indeed the

case when we impose the restriction that there are no prismatic dislocations. The proof is given in Appendix A.7. From (4.14) we then obtain

$$\frac{1}{2}(u^T_{i,j} + u^T_{j,i}) = (\beta^P_{ij})^S + (\beta^E_{ji})^S = 0. \tag{4.27}$$

This means that, up to rigid body rotations and translations of the entire body, $\boldsymbol{u}^T = \mathbf{0}$, and consequently (see (4.14)) that $\boldsymbol{\beta}^E + \boldsymbol{\beta}^P = \mathbf{0}$.

Since the incompatibility is zero everywhere, both $\boldsymbol{\beta}^E$ and $\boldsymbol{\beta}^P$ satisfy the compatibility equations and so it will be possible to define both a single-valued elastic displacement $\boldsymbol{u}^E$ and a single-valued "plastic displacement" $\boldsymbol{u}^P$, although neither $\boldsymbol{u}^E$ nor $\boldsymbol{u}^P$ need be continuous. In regions where $\boldsymbol{\alpha} = \mathbf{0}$, $\boldsymbol{u}^E$ and $\boldsymbol{u}^P$ will be classical continuous displacements, and so will correspond to rigid body rotations and translations. Now, from (4.14), $\boldsymbol{u}^T = \boldsymbol{u}^E + \boldsymbol{u}^P$ and since $\boldsymbol{u}^T = \mathbf{0}$ we have $\boldsymbol{u}^P = -\boldsymbol{u}^E$. That is, in a ZSE, *the elastic displacement is exactly cancelled by an equal and opposite "plastic displacement"* $\boldsymbol{u}^P$.

As an example, let us consider a ZSE situation where the dislocations are confined to a closed surface surrounded by material which has not been subjected to any "cuts" during the cut-and-weld procedure. Hence outside the surface $\boldsymbol{u}^P = \boldsymbol{u}^E = 0$, and inside the surface we have

$$\boldsymbol{u}^P = \boldsymbol{\omega} \wedge \boldsymbol{r} + \boldsymbol{c}, \qquad \boldsymbol{u}^E = -\boldsymbol{\omega} \wedge \boldsymbol{r} - \boldsymbol{c}, \tag{4.28}$$

for suitable constants $\boldsymbol{\omega}$ and $\boldsymbol{c}$. This corresponds to removing the interior, cutting along one family of slip planes (illustrated in Fig. 4.2 for the simple cubic case) and displacing along those planes to strain the interior, and then cutting and displacing along the second family to "cancel" this strain (thereby creating $\boldsymbol{u}^P$) and finally rigid-body-rotating back (through $\boldsymbol{u}^E$) to enable the interior to be reinstated. In this case the support of $\boldsymbol{\beta}^P$ is the surface and its interior, and the support of $\boldsymbol{\alpha}$ is the surface itself. Note that if we did not rotate between the second cut and reinsertion, stresses would be necessary for the interior to be reinstated, which would then leave a non-ZSE configuration. Fig. 4.2 is also an example of what was mentioned in Chapter 3 in the context of the von Mises criterion for the general plastic deformation of a crystal. The crystal can be seen to have suffered a plastic deformation which *retains the shape* of the material.

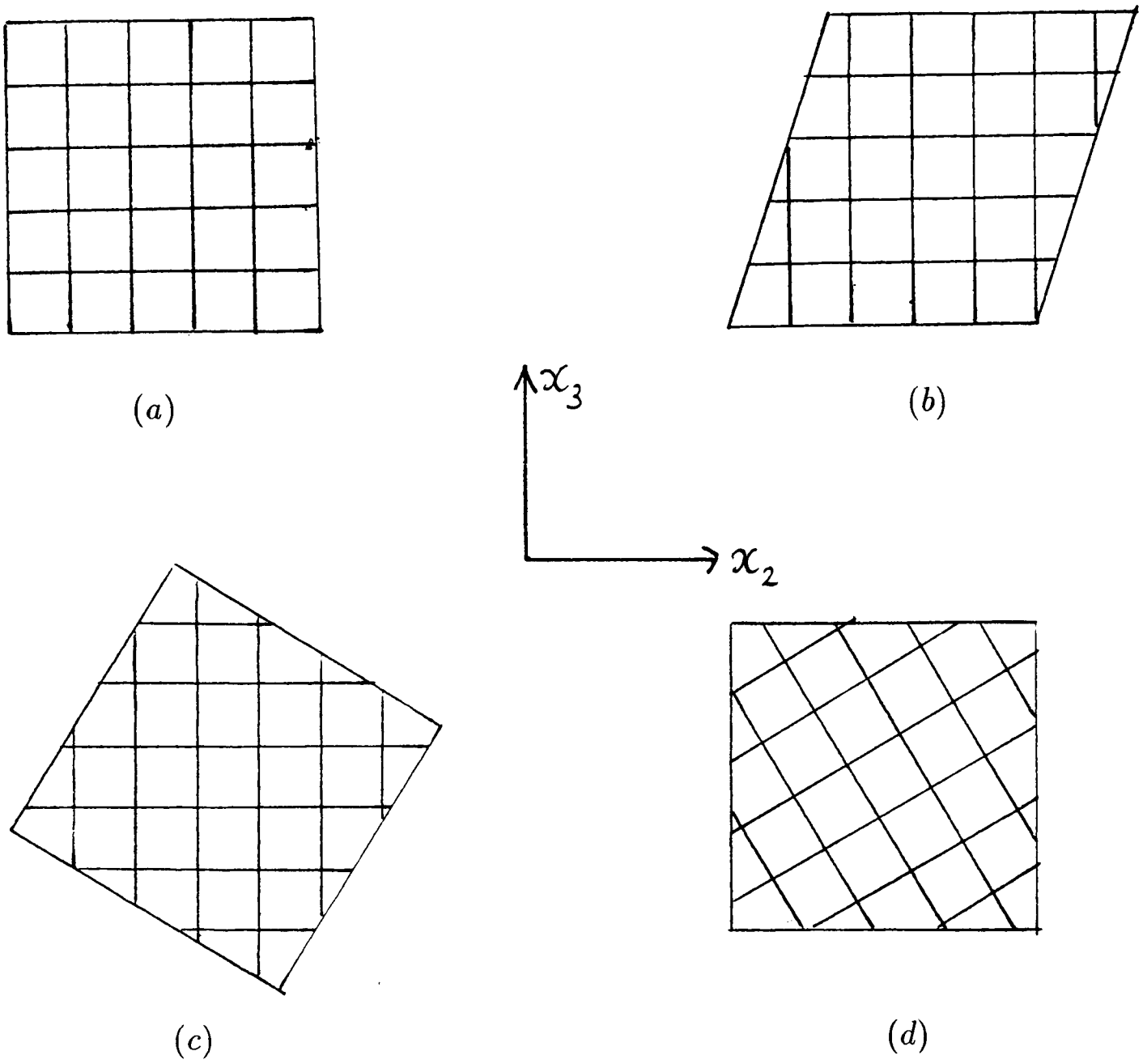

(a) (b) (c) (d)

Figure 4.2: (a) The interior of the cube; (b) Plastic distortion β^P_{32}; (c) Plastic distortion $\beta^P_{23} = -\beta^P_{32}$; (d) Rigid body rotation.

The ZSE box (Section 3.2*(iii)*) could be produced by just such a process. It can be followed explicitly (illustrated in Fig. 4.2): take the first set of cuts to be along planes parallel to the x_1x_2-plane and displace in the x_2 direction. Then cut along planes parallel to the x_1x_3-plane and displace in the minus x_3 direction. If the displacements are uniformly distributed throughout the cube V, then the elements β^P_{32} and β^P_{23} of $\boldsymbol{\beta}^P$ will be constant throughout V, and will vanish in the region exterior to V. Then

$$u^P_{2,3} = \beta^P_{32} = \begin{cases} c & \text{inside } \partial V \\ 0 & \text{outside } \partial V, \end{cases}$$

$$u^P_{3,2} = \beta^P_{23} = -\beta^P_{32},$$

and

$$u^P_{i,j} = 0 \qquad \forall\, i,j \neq 2,3,$$

everywhere. Hence

$$u^P_2 = \begin{cases} cx_3 & \text{inside } \partial V \\ 0 & \text{outside } \partial V, \end{cases}$$

$$u^P_3 = \begin{cases} -cx_2 & \text{inside } \partial V \\ 0 & \text{outside } \partial V. \end{cases}$$

and

$$u^E_2 = -u^P_2, \qquad u^E_3 = -u^P_3.$$

This thought experiment, which involves removing a piece of material, plastically deforming it and applying the appropriate elastic deformation (a simple rotation in the case above) to return the piece to its original shape, is similar to that of Kröner (1958) when introducing the concept of incompatibility. Kröner imagines the material to be cut into a large number of volume elements, which are then plastically strained. The original state of the material is described as 'connected', to indicate the absence of holes. After the elements have been strained, however, they no longer (in general) fit together, and the body is thus no longer connected. Incompatibility is, physically, the result of plastic distortions which destroy the connectedness of the body. In reality, plastic deformation does not, of course, occur through such a mechanism. To achieve the final state described above, dislocations would have to either "move in" from infinity, or "out" from

sources inside the surface. Plastic and elastic deformation would then occur simultaneously. Nevertheless, the thought experiment is an aid to understanding the resultant state and the complementary effects of elastic and plastic distortion.

In terms of our formulation, connectedness corresponds to

$$\oint_C du_i^T = \oint_C u_{i,j}^T dx_j = 0 \tag{4.29}$$

for any closed curve C in the body. If the derivatives of $\boldsymbol{u}^T$ are interpreted in a distributional sense, (4.29) will hold unless there are holes in the material.

4.7.1 Note on Surface Dislocations

Surface distributions have been represented here by a dislocation density tensor which has a delta function over the surface. For example, the sheet of screws (Section 2.2.1) has nonzero density tensor component

$$\alpha_{33} = \Omega\delta(x_1),$$

and this is interpreted as meaning that a screw dislocation family of strength Ω occupies the plane $x_1 = 0$. There is an alternative approach to the concept of the surface dislocation distribution, first given by Bilby (1955). If $\boldsymbol{\beta}^P$ is uniformly distributed throughout a region V, then there is a dislocation distribution confined to the surface of V, and the strength of the distribution can be written

$$-\varepsilon_{ikl}[\beta_{ln}^P]n_k,$$

where $\boldsymbol{n}$ is the unit outward normal to the surface, and $[\boldsymbol{\beta}^P] = \boldsymbol{\beta}_+^P - \boldsymbol{\beta}_-^P$, where $\boldsymbol{\beta}_+^P$ denotes the value of $\boldsymbol{\beta}^P$ just outside the surface and $\boldsymbol{\beta}_-^P$ is the value of $\boldsymbol{\beta}^P$ just inside the surface.

Surface currents in electromagnetism, and surface vorticity in fluid dynamics can be defined in a similar manner as the jumps in the tangential component of the magnetic field or the velocity field respectively.

4.8 More ZSEs

Armed with the ideas enunciated above, we can now construct some ZSEs of a more elementary composition. Recall the dislocation C (Section 4.5) whose only

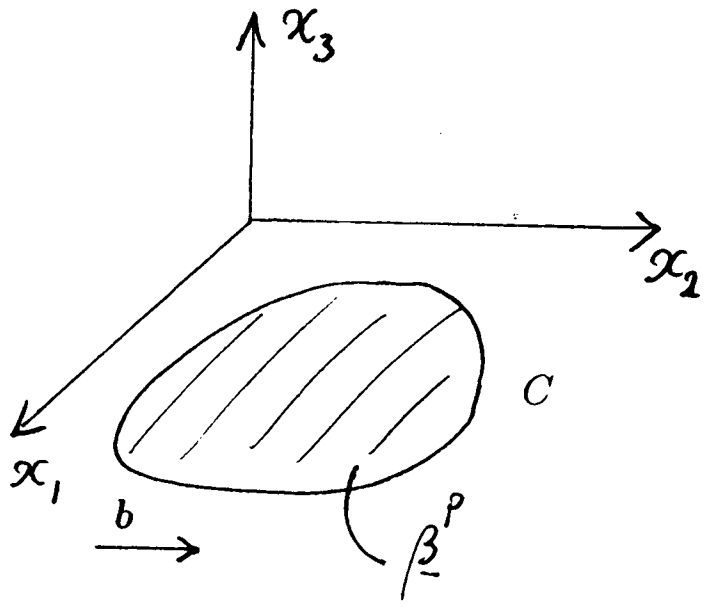

Figure 4.3: Dislocation line C with β^P_{32} spanning the interior.

nonzero component of $\boldsymbol{\beta}^P$ is $\beta^P_{32} = H(1-r)\delta(x_3)$, if the cut is taken inside the loop. The cancelling dislocation family thus has

$$\beta'^P_{32} = -H(1-r)\delta(x_3).$$

The relevant dislocation densities are

$$\begin{aligned} \alpha_{12} &= -\sin\theta\delta(1-r)\delta(x_3), \\ \alpha_{22} &= \cos\theta\delta(1-r)\delta(x_3), \end{aligned}$$

and

$$\begin{aligned} \alpha'_{13} &= -H(1-r)\delta'(x_3), \\ \alpha'_{33} &= \cos\theta\delta(1-r)\delta(x_3). \end{aligned}$$

Hence the cancelling family represents a uniform distribution of edge dislocation dipoles "enclosing" S as in Fig. 4.4.

ZSEs such as that in Fig. 4.4 can now be superimposed to generate a surface ZSE such as that discussed in Section 3.2*(iii)*. In order that the dipoles cancel in the interior of the surface the superposition must be of dipoles of equal strength. The surface dislocation can, alternatively, be viewed as a superposition of more basic dislocation arrangements involving dipoles; the logical conclusion of this decomposition of dislocation distributions into their most fundamental elements is a description in terms of infinitesimal dislocation loops, first given by Kroupa (1962), and which will be examined in more detail later in this chapter.

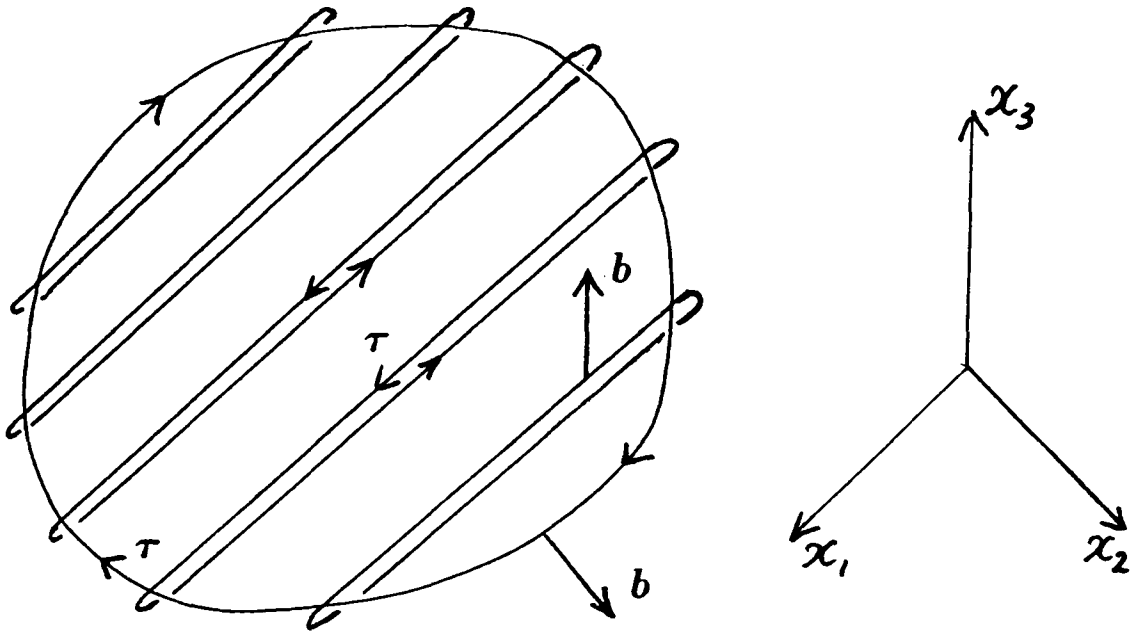

Figure 4.4: Dislocation loop and cancelling family of dipoles.

4.9 Theorem 1 Revisited

Using the ideas presented concerning plastic distortion, we can now prove again the theorem of the previous chapter and extend it to cover the case of distributions confined to simply-connected surfaces. Again consider the elastic energy W (equation (3.2)). From (4.14) and (4.15) we may write

$$e_{ij} = \frac{1}{2}(u^T_{i,j} + u^T_{j,i}) - \frac{1}{2}(\beta^P_{ij} + \beta^P_{ji}).$$

Substituting this into (3.2), we have (using the symmetry of σ_{ij} and (1.3))

$$\begin{aligned} W &= \frac{1}{2}\int(\sigma_{ij}u^T_{i,j} - \sigma_{ij}\beta^P_{ij})dV \\ &= \frac{1}{2}\int((\sigma_{ij}u^T_i)_{,j} - \sigma_{ij}\beta^P_{ij})dV. \end{aligned}$$

Integrating the first term by means of the divergence theorem, and taking the tractions $\sigma_{ij}n_j$ to be zero at infinity, leaves us with

$$W = -\frac{1}{2}\int \sigma_{ij}\beta^P_{ij}dV. \tag{4.30}$$

Assuming $\boldsymbol{\beta}^P$ to have support in the plane of the each dislocation loop, then if the dislocated region contains loops of the b_2m_3 family, for example, the only nonzero component of $\boldsymbol{\beta}^P$ will be β^P_{32}. Since $\boldsymbol{\beta}^P$ can be nonzero even if $\boldsymbol{\alpha} = \mathbf{0}$ (as in the case of a dislocation loop or surface dislocation distribution, for example), the

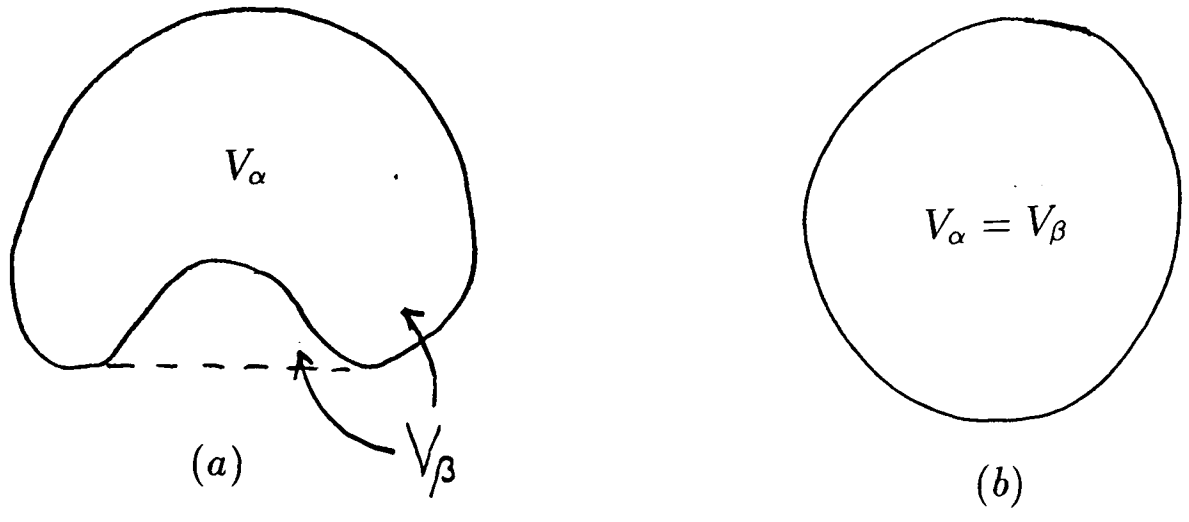

Figure 4.5: (a) Non convex region, $V_\alpha \subseteq V_\beta$; (b) Convex region, $V_\alpha = V_\beta$.

dislocated region V_α will be contained within the plastically distorted region V_β, as depicted in Fig. 4.5. It is not difficult to see that if the region V_α is convex, then $V_\alpha = V_\beta$, whereas otherwise $V_\alpha \neq V_\beta$.

Hence (4.30) reduces to

$$W = -\frac{1}{2}\int_{V_\beta} \sigma_{ij}\beta^P_{ij} dV, \tag{4.31}$$

and since only $\beta^P_{32} \neq 0$ we have

$$W = -\frac{1}{2}\int_{V_\beta} \sigma_{23}\beta^P_{32} dV.$$

The condition for equilibrium (equation (3.1)) is, in this case, that $\sigma_{23} = 0$ in V_α, so, for a simply-connected *convex* region V_α, we have $W = 0$, and as before this implies $\boldsymbol{\sigma} = \mathbf{0}$.

If the region is not convex, then (4.31) reduces to

$$W = -\frac{1}{2}\int_{V_\beta/V_\alpha} \sigma_{23}\beta^P_{32} dV,$$

since $\sigma_{23} = 0$ only in V_α. In order to show that this equation vanishes, it is necessary to express $\boldsymbol{\sigma}$ as the curl of a tensor potential function $\boldsymbol{\phi}$ as in (3.5) and to integrate by parts to arrive once again at the expression (3.4) for W in terms of $\boldsymbol{\phi}$ and $\boldsymbol{\alpha}$. This method therefore simplifies the proof of the theorem only in the case of a simply-connected *convex* dislocated region.

In order to extend Theorem 1 to the case of surface dislocations, we take up the proof at expression (4.31) for the elastic energy. Substituting for σ_{ij} from (3.5)

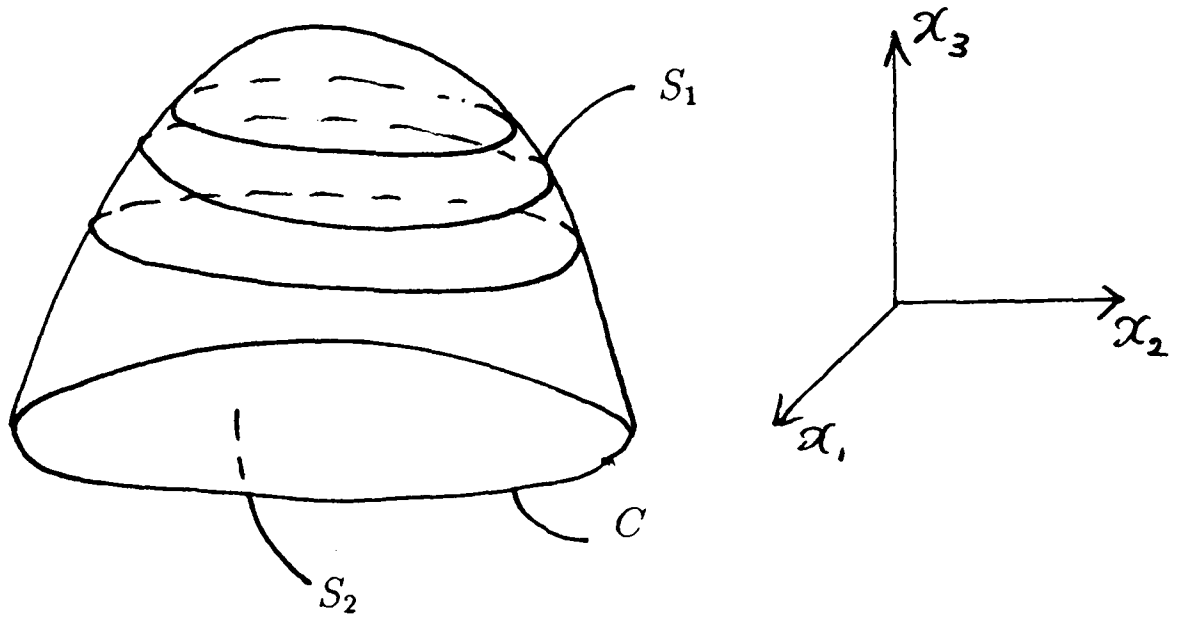

Figure 4.6: Dislocations of the b_2m_3 family covering the surface S_1. S_2 is parallel to the x_1x_2-plane and is free of dislocations. C is the bounding curve of S_1.

gives us

$$W = -\frac{1}{2}\int_{V_\beta} \varepsilon_{ikl}\phi_{jl,k}\beta^P_{ij}dV,$$

which can be integrated by parts to give

$$W = -\frac{1}{2}\int_{\partial V_\beta} \varepsilon_{ikl}\phi_{jl}\beta^P_{ij}n_k dS - \frac{1}{2}\int_{V_\beta} \phi_{jl}\alpha_{lj}dV, \tag{4.32}$$

where ∂V_β is the boundary of V_β and thus is the surface containing the dislocations. There are no dislocations inside the surface and so the second term involving $\boldsymbol{\alpha}$ is zero. Next, let us suppose that we have only one family of dislocations, as we did previously. If the family is the b_2m_3 family then the only nonzero component of $\boldsymbol{\beta}^P$ is β^P_{32}, and so (4.32) is reduced to

$$W = -\frac{1}{2}\int_{\partial V_\beta} \beta^P_{32}(\phi_{22}n_1 - \phi_{21}n_2)dS. \tag{4.33}$$

The situation is as depicted in Fig. 4.6, for example, where the dislocations are supposed to cover a 'cap' S_1. The boundary ∂V_β consists of S_1, in which the dislocations lie, and S_2, which is dislocation-free. Since S_2 is parallel to the x_1x_2-plane, $n_1 = n_2 = 0$ there, and (4.33) can be written

$$W = -\frac{1}{2}\int_{S_1} \beta^P_{32}(\phi_{22}n_1 - \phi_{21}n_2)dS. \tag{4.34}$$

Now, in equilibrium $\sigma_{23} = 0$ on S_1, and since S_1 is simply-connected we may write, once again, $\phi_{22} = \partial\zeta/\partial x_2$, $\phi_{21} = \partial\zeta/\partial x_1$, where ζ is single-valued. Also,

since $\boldsymbol{\alpha} = \mathbf{0}$ in V, $\beta_{32}^P = \beta_{32}^P(x_3)$, and so, decomposing S_1 into a set of curves (in fact corresponding to the dislocation lines) lying in the planes parallel to the x_1x_2-plane, (4.34) is a sum of integrals of the form

$$\oint_C (\zeta_{,2}n_1 - \zeta_{,1}n_2)dl = \oint_C \nabla\zeta.d\boldsymbol{x},$$

which vanish because ζ is single-valued, and the proof is complete.

It should be noted that this proof is valid for any number of dislocation families so long as they fulfil the requirements that they are comprised entirely of glide dislocations and occupy a simply-connected region.

If the dislocations were not confined to a finite region, but were such that each family of dislocations had a nonzero density (decaying at infinity) at every point of space, then it is possible to prove the same result as above: namely that any self-equilibrium distribution must be a ZSE. This can be done by noting that, in such a case, one component of stress would be zero throughout the whole space for each family of dislocations. A tedious manipulation, involving cross-differentiation of the equations (2.6) and an appeal to uniqueness of solution for linear partial differential equations whose dependent variables vanish at infinity, establishes the result.

4.9.1 Multiply-Connected Regions of Dislocations

The proof of Theorem 1 fails when the dislocated region concerned is multiply-connected, since the function ζ is then no longer necessarily single valued, leading to the possibility that the elastic strain energy does not vanish. However, in the absence of counter examples, it is conjectured that the theorem holds even in the non-simply-connected case and the following argument is presented in support.

An example of a doubly-connected surface distribution is that illustrated in Fig. 4.8(a) where a family of b_2m_3 dislocations covers four sides of a cube. Let us consider the cut-and-weld operations necessary to create such a distribution. Firstly, a cube of material is removed from the body as in Fig. 4.7(a). The cube is then cut into 'slices' and the slices displaced in the x_1-direction before being welded back together (Fig. 4.7(b)). Applying tractions to the sheared cube in Fig. 4.7(b) returns it to its original shape (Fig. 4.7(c)) whence it can be

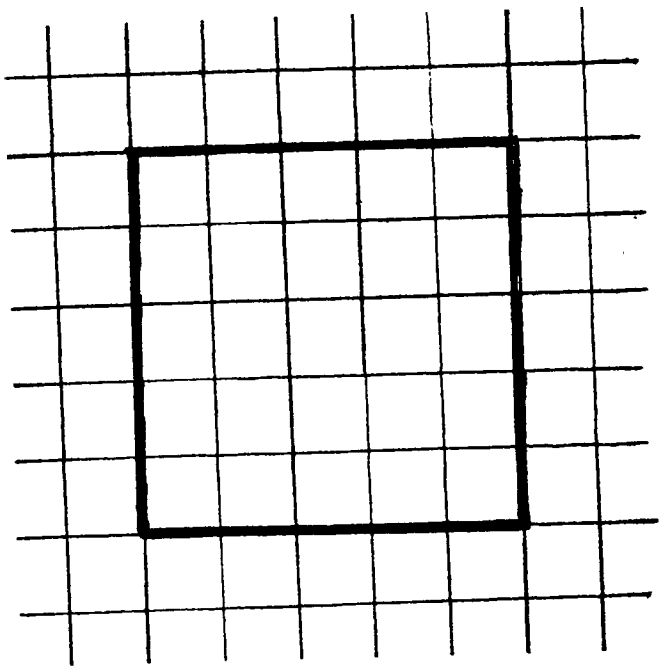

(a)

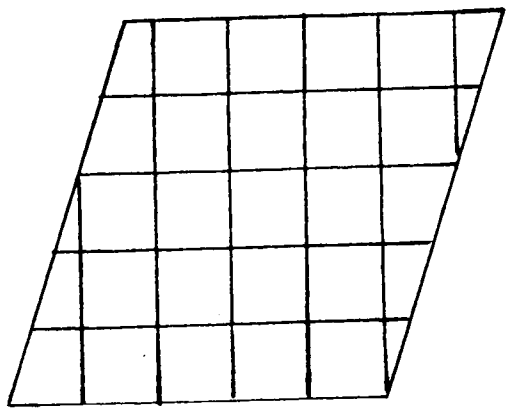

(b)

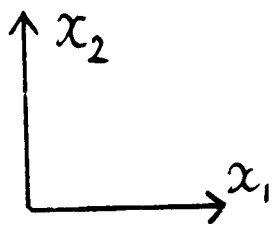

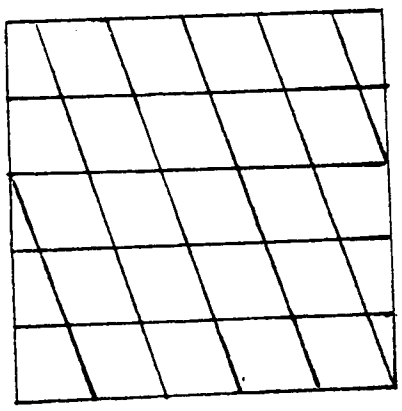

(c)

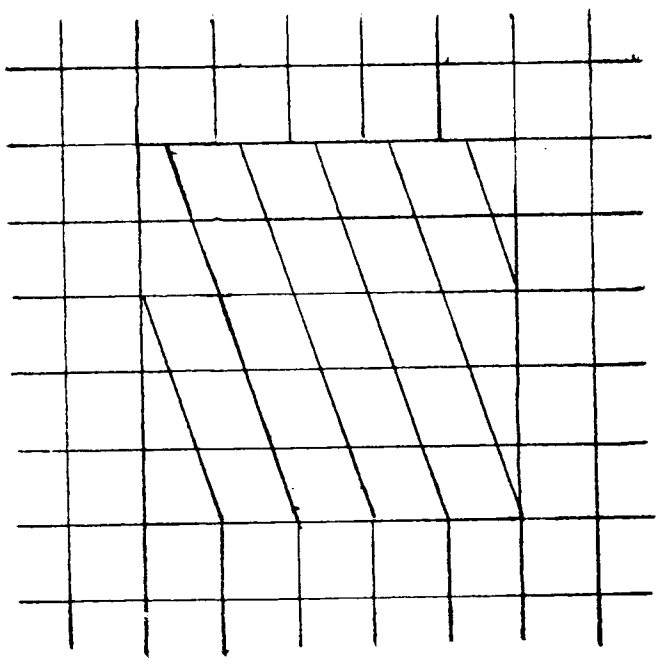

(d)

Figure 4.7: Creation of a doubly-connected surface distribution of dislocations. (a) The original specimen with the surface over which the cut is to be made marked in bold. (b) The cube is plastically sheared in the x_1-direction. (c) The shape of the cube is regained by applying tractions. (d) The cube is replaced in the 'matrix'.

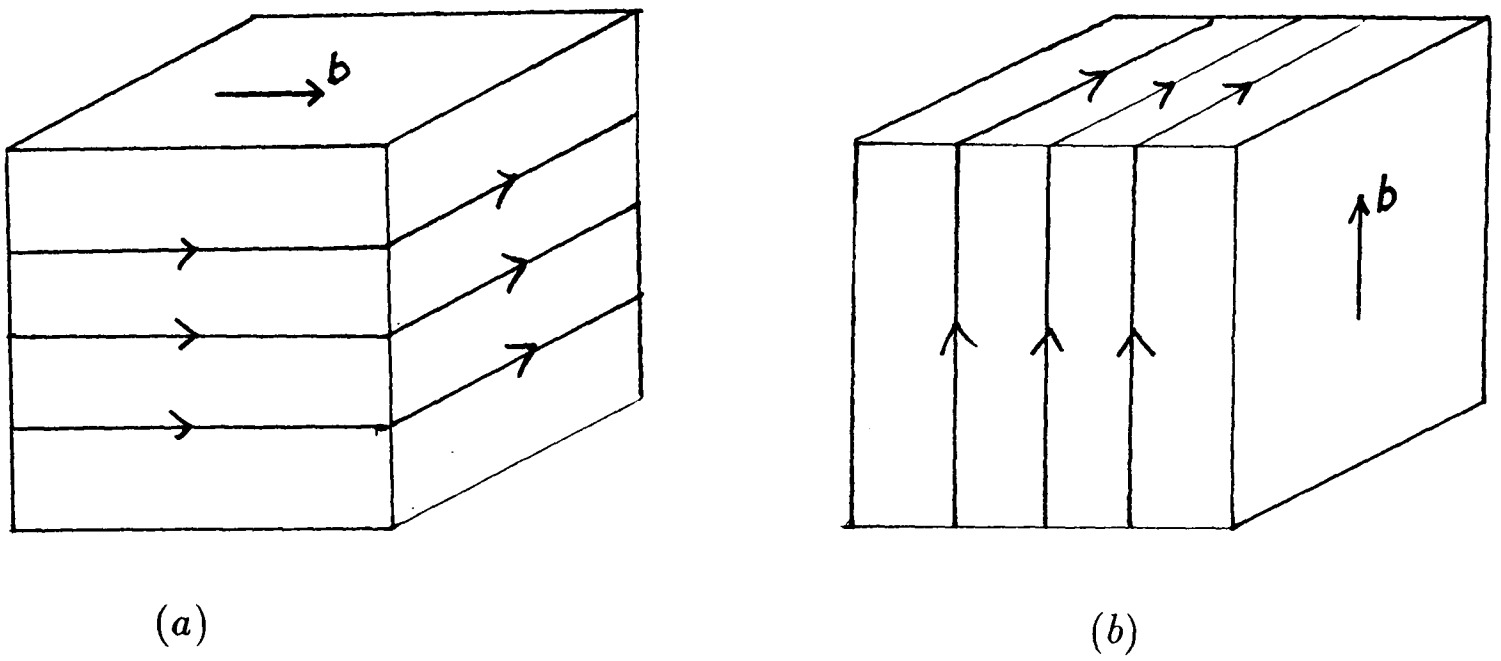

(a) (b)

Figure 4.8: The component families of the ZSE cube.

replaced in the body from which it was cut (Fig. 4.7(d)). Dislocations now occupy the surface as depicted in Fig. 4.8(a). If the surface dislocation were in self-equilibrium, the dislocations would not move when the applied tractions were released. It is intuitively apparent, though, that when the tractions are removed the dislocations will experience a force and will either shrink or expand to infinity. In the specific case of the cube this intuitive response can be verified explicitly from the mathematical model by means of a simple observation.

Assume that the given b_2m_3 distribution is in self-equilibrium. If S_1 denotes the four faces of the cube covered by this family then the condition for equilibrium is that $\sigma_{23} = 0$ on S_1. Next, observe that if the b_2m_3 family is rotated clockwise through 90° about the x_1-axis, one arrives at the situation illustrated in Fig. 4.8(b). That is, the b_3m_2 family is just the b_2m_3 family rotated and so must also be in equilibrium. If S_2 denotes the four faces of the cube occupied by the b_3m_2 family then the 23-component of the stress field of this family must vanish on S_2. Now, the stress due to the b_2m_3 family is minus that due to the b_3m_2 family, because together they constitute a ZSE, and so one concludes that $\sigma_{23} = 0$ on S_2 also. The surface of the cube is a simply-connected surface and hence one may invoke Theorem 1 to show that the distribution must be a ZSE. On the other hand, the dislocations comprising the surface distribution are slip dislocations created

through the imposition of a plastic distortion β^P_{23}. $\boldsymbol{\beta}^P$ is not, therefore, skew-symmetric and so the distribution cannot be a ZSE, giving us a contradiction which implies that the assumption of self-equilibrium is incorrect.

The simplest multiply-connected dislocation distribution is, of course, the single discrete loop dislocation. It is well-known (see Gavazza & Barnett 1976, Titchener 1988) that a dislocation loop exerts a self-force. In the context of this model the dislocation would, therefore, either shrink in on itself or expand to infinity, but could not be in self-equilibrium.

4.9.2 Non-ZSE Equilibria

Given the above, it may be thought that the only distributions in self-equilibrium are ZSEs. This is not the case, however, and it is worth noting at this point some of the counterexamples. A single screw or edge dislocation will remain in equilibrium in the absence of applied stresses and provides the simplest counterexample, though also the most degenerate. Similarly, a sheet of screw dislocations lying in the x_2x_3-plane with Burgers vector $\boldsymbol{b} = (0, 0, 1)$ and whose slip planes are normal to $\boldsymbol{m} = (0, 1, 0)$ is in self-equilibrium. The force on the sheet is, by the Peach-Koehler formula, proportional to σ_{23}. This component of the stress is, however, zero on the sheet.

Many other examples of non-ZSE equilibrium distributions exist involving discrete edge dislocations, as detailed in Chen et al. (1964) where dislocation multipoles are considered. Two examples are given in Fig. 4.9. The quadrupole in Fig. 4.9(a) consists of two pairs of dislocations where the line segments connecting each pair bisects the other. In Fig. 4.9(b) a multipole consisting of seven edge dislocations is shown. Each dislocation in the lower row sits half way (in the x_1 direction) between neighbouring dislocations in the upper row. This multipole may be extended to include more dislocations provided only that one dislocation remains unpaired.

4.10 Elastic and Plastic Rotation

Having seen how in a ZSE, though there is no elastic strain, the material has undergone a rotation caused by the movement of dislocations, we should be able

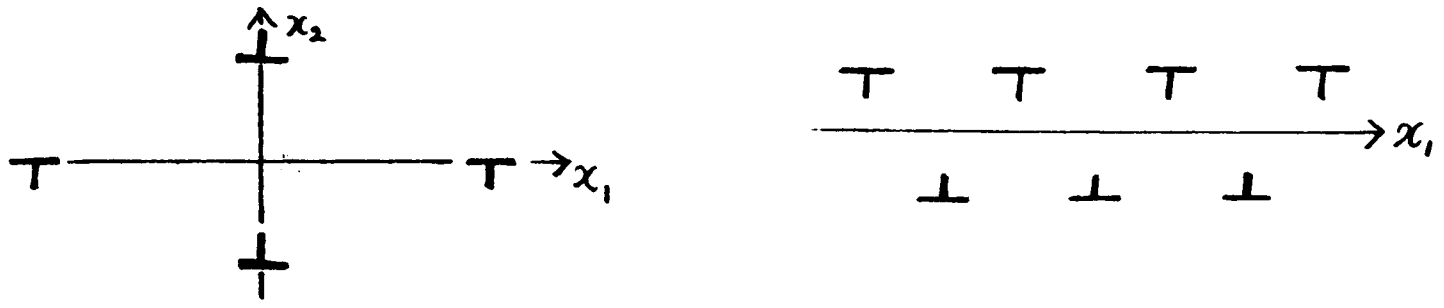

(a) (b)

Figure 4.9: Examples of non-ZSE equilibrium distributions of edge dislocations.

to write down a relation between the dislocation density tensor and the rotation. By analogy with linear elasticity we define the *total* rotation (using 4.14) as

$$\frac{1}{2}(u^T_{i,j} - u^T_{j,i}) = \frac{1}{2}(\beta^E_{ji} - \beta^E_{ij}) + \frac{1}{2}(\beta^P_{ji} - \beta^P_{ij}) = \omega^E_{ij} + \omega^P_{ij}, \tag{4.35}$$

where ω^E_{ij} is the elastic rotation and ω^P_{ij} is, correspondingly, the plastic rotation. In the absence of dislocations ω^P_{ij} would be zero, and ω^E_{ij} would be the usual elastic rotation given by

$$\omega^E_{ij} = \frac{1}{2}(u_{i,j} - u_{j,i}).$$

Elastic strain is defined by (4.15), plastic strain (analogously) by

$$e^P_{ij} = \frac{1}{2}(\beta^P_{ij} + \beta^P_{ji}), \tag{4.36}$$

and total strain is the sum of the two terms. Since the rotation tensors ω^E_{ij} and ω^P_{ij} are skew-symmetric, we may write them in terms of vectors, so that

$$\begin{aligned} \omega^E_{ij} &= -\varepsilon_{ijk}\omega^E_k, \\ \omega^P_{ij} &= -\varepsilon_{ijk}\omega^P_k. \end{aligned}$$

Then we have

$$e_{ij} = \beta^E_{ij} + \varepsilon_{ijk}\omega^E_k, \tag{4.37}$$

and a similar equation for $\boldsymbol{e}^P$. Taking the curl of (4.37) gives

$$\begin{aligned} \varepsilon_{pqi}e_{ij,q} &= \varepsilon_{pqi}\beta^E_{ij,q} + \varepsilon_{ipq}\varepsilon_{ijk}\omega^E_{k,q} \\ &= -\alpha_{pj} + \delta_{pj}\omega^E_{q,q} - \omega^E_{p,j}, \end{aligned}$$

from (4.19). The divergence of ω_k^E may be written in terms of $\boldsymbol{\alpha}$ as follows:

$$\begin{aligned}
\omega_{k,k}^E &= -\frac{1}{2}\varepsilon_{kij}\omega_{ij,k}^E \\
&= -\frac{1}{2}\varepsilon_{kij}(\beta_{ji,k}^E - \beta_{ij,k}^E) \\
&= \varepsilon_{kij}\beta_{ij,k}^E \\
&= \alpha_{kk}.
\end{aligned}$$

Thus we obtain

$$\omega_{p,j}^E = -\alpha_{pj} + \frac{1}{2}\delta_{pj}\alpha_{qq} - \varepsilon_{pqi}e_{ij,q}. \tag{4.38}$$

Similarly

$$\omega_{p,j}^P = \alpha_{pj} - \frac{1}{2}\delta_{pj}\alpha_{qq} - \varepsilon_{pqi}e_{ij,q}^P, \tag{4.39}$$

with $\omega_{k,k}^P = -\alpha_{kk}$.

Equation (4.38) can be solved as follows to give the elastic rotation in terms of $\boldsymbol{\alpha}$ alone. Differentiating (4.38) with respect to x_j and summing over j yields

$$\nabla^2\omega_p^E = -\alpha_{pj,j} + \frac{1}{2}\alpha_{qq,p} - \varepsilon_{pqi}e_{ij,qj}. \tag{4.40}$$

Substituting Hooke's law (1.4) into the equation of mechanical equilibrium (1.3) one finds that

$$2\mu e_{ij,j} + \lambda e_{kk,j} = 0,$$

and thus we have

$$\varepsilon_{pqi}e_{ij,qj} = -\frac{\lambda}{2\mu}\varepsilon_{pqi}e_{kk,iq} = 0.$$

Consequently we may write the solution of (4.40) which vanishes at infinity as the integral over the whole space

$$\omega_p^E = -\frac{1}{4\pi}\int \frac{-\alpha_{pj,j} + (1/2)\alpha_{qq,p}}{R}dV. \tag{4.41}$$

In the absence of a result for the plastic strain $\boldsymbol{e}^P$ corresponding to Hooke's law for $\boldsymbol{e}$, one cannot in general find a similar expression for the plastic rotation ω_p^P.

Equation (4.38) was first written down by Nye (1953) for $\boldsymbol{e} = \mathbf{0}$, that is, in the ZSE case. Kröner (1955) obtained the full expression (4.38), but assumed that

the strain could be divided into compatible and incompatible parts, and that $\boldsymbol{e}$ in (4.38) is the incompatible element, so that when $\boldsymbol{\alpha} = \mathbf{0}$, so are $\boldsymbol{e}$ and ω_p^E. In the Nye (ZSE) case

$$\omega_{p,j}^E = -\omega_{p,j}^P,$$

which, we can see, ties in (through (4.35)) with the earlier statement (Section 4.7) that $\boldsymbol{u}^T = \mathbf{0}$ in a ZSE. The example given in Section 4.7 of a surface ZSE can easily be interpreted using (4.38). Both within and outside the surface, $\boldsymbol{\alpha} = \mathbf{0}$, and so the vector $\boldsymbol{\omega}^E$ is constant inside and outside the surface and suffers a jump across the surface.

With $\boldsymbol{e} = \mathbf{0}$, we may rewrite (4.38) and (4.39) as expressions for $\boldsymbol{\alpha}$ in terms of the appropriate rotation. We get

$$\begin{aligned} \alpha_{pj} &= -\omega_{p,j}^E + \delta_{pj}\omega_{k,k}^E \\ &= \omega_{p,j}^P - \delta_{pj}\omega_{k,k}^P. \end{aligned} \tag{4.42}$$

This last expression is identical in form to (3.12), which was derived by solving the equations $\boldsymbol{\eta} = \mathbf{0}$ and $\boldsymbol{\nabla}.\boldsymbol{\alpha} = \mathbf{0}$, but which gave no insight into the physical interpretation of $\boldsymbol{\xi}$. We can now identify $\boldsymbol{\xi}$ as a rotation vector.

Similarly, in a ZSE, $\boldsymbol{\beta}^P$ is skew symmetric and so, by examining (4.18) and (3.12), we may make the comparison

$$\begin{aligned} \xi_1 &= \beta_{23}^P = -\beta_{32}^P, \\ \xi_2 &= \beta_{31}^P = -\beta_{13}^P, \\ \xi_3 &= \beta_{12}^P = -\beta_{21}^P. \end{aligned}$$

4.10.1 Rotation in Volume ZSEs

The effect of a ZSE surface dislocation upon the orientation of the two parts of the material which it separates was described in Section 4.7, and now we proceed by means of example to discuss the properties of dislocations distributed throughout a volume.

(i) Firstly we consider a slab of cross-grids of screws. The relevant dislocation densities are (see Section 2.3.2)

$$\alpha_{22} = \alpha_{33} = \Omega(H(c - x_1) - H(-c - x_1)),$$

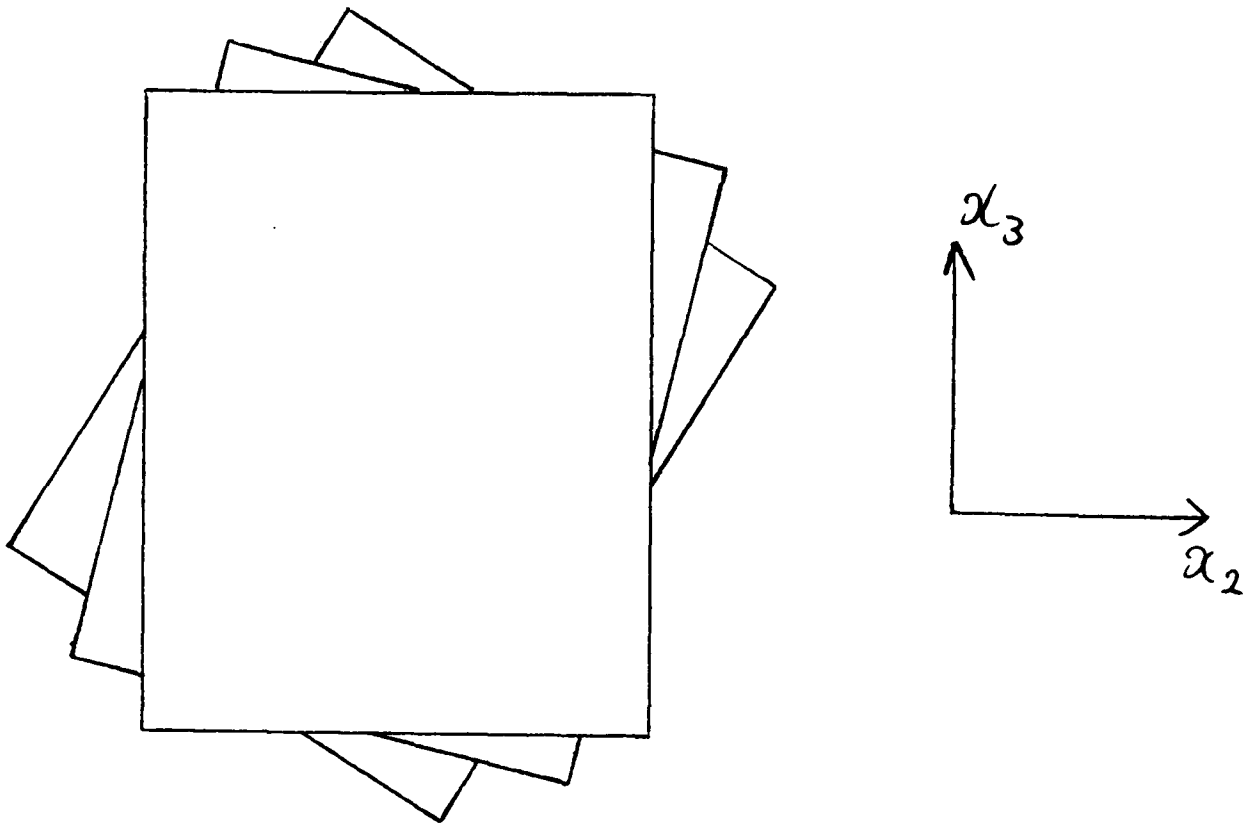

Figure 4.10: Schematic diagram showing rotation of slip planes in a slab of cross-grids of screws.

and from (4.42) we find that the rotation is

$$\omega_1^E = \begin{cases} -c\Omega & x_1 \leq -c \\ \Omega x_1 & -c \leq x_1 \leq c \\ c\Omega & x_1 \geq c, \end{cases}$$

$$\omega_2^E = \omega_3^E = 0.$$

Thus the slab of cross-grids imposes a continuous rotation about the x_1-axis upon the slip planes parallel to the x_2x_3-plane (Fig. 4.10).

(ii) As a further example, we recall the volume ZSE considered in Section 3.2*(v)*. The screw components of the distribution, α_{11} and α_{22}, are equal (equations 3.6-3.9) as expected, and locally it has the character of a slab of cross-grids of self-cancelling screws or a stress free slab of edge dislocations (Section 2.3). The effect of this ZSE is described by

$$\omega_1^E = \begin{cases} -\Omega(a_2 - a_1) & r \leq a_1 \\ -\Omega(a_2 - r) & a_1 \leq r \leq a_2 \\ 0 & r \geq a_2, \end{cases}$$

$$\omega_2^E = \omega_3^E = 0.$$

This is a rotation of concentric spheres about the x_1-axis, the magnitude of the rotation increasing continuously from 0 to $\Omega(a_2 - a_1)$ as the radius is traversed inwards from the boundary of the dislocated region to the inner sphere $r = a_1$

There is experimental evidence to support the notion that dislocation configurations such as this are commonly found in crystalline metals. An X-ray study of both hard (e.g. copper, aluminium) and soft (e.g. lead, tin) work-hardened metals by Gay, Hirsch & Kelly (1954) concludes that the regions of low dislocation density (which they term 'particles') are separated by boundaries consisting of distributions of dislocations which are responsible for "large plastic curvature" and which occupy "volumes of material large compared with those associated with a cross-grid of screw dislocations". It is also stated that the curvature is continuous across the boundaries between particles.

4.10.2 Incompatibility of Rotation[3]

In a ZSE stress, strain and incompatibility are zero, as if the body containing the ZSE were a perfect metal crystal free from externally applied forces. We have seen in this chapter that the factor distinguishing a perfect crystal from a crystal possessing ZSEs is the matter of the rotation of the slip planes. A material with ZSEs may thus be described as a body with compatible elastic strains ($\boldsymbol{\eta} = \mathbf{0}$) but with "incompatible rotations", and a *tensor of rotational incompatibility* may be introduced to complement $\boldsymbol{\eta}$.

The expression for $\boldsymbol{\alpha}$ in terms of elastic distortion (4.18) may be written

$$\alpha_{in} = \frac{1}{2}(\varepsilon_{ikl}(\beta^E_{ln} + \beta^E_{nl})_{,k} + (\varepsilon_{ikl}(\beta^E_{ln} - \beta^E_{nl})_{,k}).$$

Taking the curl of $\boldsymbol{\alpha}$ yields

$$\begin{aligned} -\varepsilon_{jmn}\alpha_{in,m} &= -\left(\varepsilon_{ikl}\varepsilon_{jmn}e_{ln,km} + \varepsilon_{ikl}\varepsilon_{jmn}e^P_{ln,km}\right) \\ &= \eta_{ij} + \nu_{ij}, \end{aligned}$$

where $\boldsymbol{\eta}$ is the elastic incompatibility and $\boldsymbol{\nu}$ is the rotational incompatibility. Like $\boldsymbol{\eta}$, $\boldsymbol{\nu}$ is symmetric and divergence-free, so that

$$\nu_{ij,j} = 0.$$

[3] I am grateful to J.B. Titchener for helpful correspondence concerning this topic.

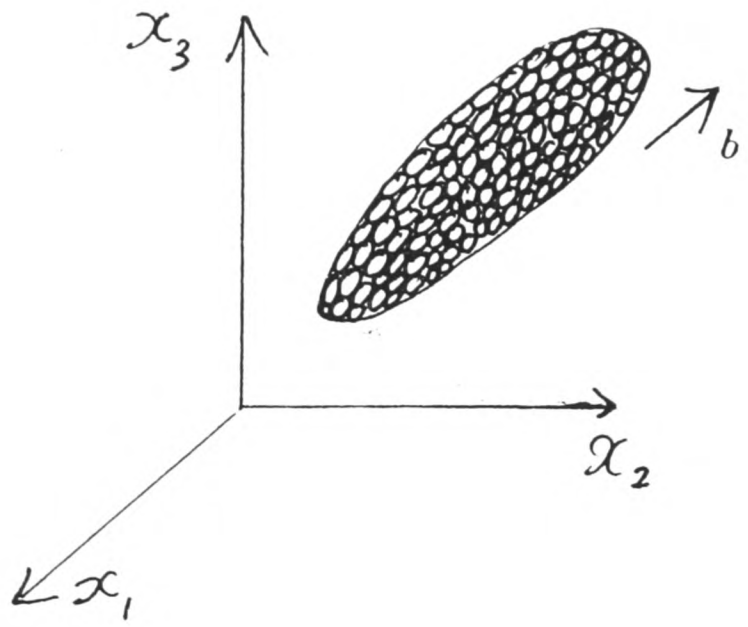

Figure 4.11: The loop shown contributes to the γ_{22}, γ_{23}, γ_{32}, and γ_{33}, components of the dislocation loop density.

The value of $\boldsymbol{\nu}$ is that it allows us to construct a correspondence between the properties of dislocations as sources of stress and strain on the one hand, and, equally, of rotation on the other, as in the table below.

$\boldsymbol{\eta}$	$\boldsymbol{\nu}$
$\boldsymbol{e}$, $\boldsymbol{\sigma}$	$\boldsymbol{\omega}^E$
$\boldsymbol{e}^P = (\boldsymbol{\beta}^P)^S$	$\boldsymbol{\omega}^P$

In a ZSE the quantities on the left-hand side of the the table are all zero, but those on the right-hand side are not. Thus, if we wish to fully describe a dislocated material, we must have information concerning not only the prevailing state of stress and strain but also of the rotation.

4.11 Kroupa Loops

The interpretation of plastic distortion as a continuous distribution of infinitesimal dislocation loops, as given by Kroupa (1962), has already been mentioned a number of times. Kroupa denotes the density of infinitesimal loops by the tensor γ_{ij} which is defined as the j-th component of the sum of the Burgers vectors of all the loops which enclose the unit vector in the i-th direction (see Fig. 4.11).

By inspection it can be seen that the diagonal components of $\boldsymbol{\gamma}$ describe the

loops whose Burgers vectors are perpendicular to the plane of the loop. Thus the diagonal components represent the prismatic element of a distribution of loops, and similarly the off-diagonal components describe the glide element.

If a region A in the x_1x_2-plane is filled with identical loops each of which possesses Burgers vector $\boldsymbol{b} = (0,1,0)$ and normal $\boldsymbol{n} = (0,0,1)$ then the resultant effect is that the positive side of A is displaced by an amount equal to $\boldsymbol{b}$ relative to the negative side. Thus the boundary of the loop is a dislocation line, and the infinitesimal loops amount to a plastic distortion corresponding to β^P_{32} with support over the interior of A. Expansion of the dislocation is effected by the creation of more loops to fill the area swept out by the dislocation, and likewise shrinkage of the dislocation requires removal of loops.

Kroupa (1962) also gave the expression for the total displacement $\boldsymbol{u}^T$ due to a continuous distribution of infinitesimal loops. He arrived at this formula by integrating the displacement due to a single infinitesimal loop. The same may be obtained by using the plastic distortion formulation developed here.

From (4.14) and (4.15) we have

$$e_{ij} = \frac{1}{2}(u^T_{i,j} + u^T_{j,i}) - \frac{1}{2}(\beta^P_{ij} + \beta^P_{ji}). \tag{4.43}$$

Using Hooke's law (1.4) and substituting in (1.3) gives

$$(\lambda + \mu)u^T_{j,ji} + \mu\nabla^2 u^T_i + \lambda\beta^P_{kk,i} + \mu(\beta^P_{ij,j} + \beta^P_{ji,j}) = 0.$$

Noting that this is just (4.4) with

$$g_i = \lambda\beta^P_{kk,i} + \mu(\beta^P_{ij,j} + \beta^P_{ji,j}),$$

the solution is (4.6) for which we have already calculated the Green's function (4.11). After some manipulation and integrations by parts one arrives at

$$u^T_k = \frac{1}{8\pi}\frac{1}{1-\nu}\int \frac{1}{R^2}\left\{\frac{1-2\nu}{R}(2(\beta^P_{ki})^S X_i - \beta^P_{ll}) + 3(\beta^P_{pi})^S\frac{X_kX_pX_i}{R^3}\right\}dV', \tag{4.44}$$

where ν is Poisson's ratio and the integral is over the region of nonzero $\boldsymbol{\beta}^P$.

The expression (4.44) serves to highlight a number of points. Firstly, one notices that $\boldsymbol{u}^T$ is solely dependent on the *symmetric part* of $\boldsymbol{\beta}^P$. If, as in a ZSE (comprised

of slip dislocations), $\boldsymbol{\beta}^P$ is skew-symmetric, the total displacement vanishes, as was discovered earlier (Section 4.7). Furthermore, (4.43) and Hooke's law (1.4) show explicitly that $\boldsymbol{\sigma}$ also depends only on $(\boldsymbol{\beta}^P)^S$, confirming what we have seen in the study of ZSEs - that the stress field of any dislocation family can be cancelled by choosing a distribution of plastic distortion which renders $\boldsymbol{\beta}^P$ skew-symmetric.

4.12 Elastic Inclusions

Suppose that one carries out a procedure similar to that necessary to create the doubly-connected dislocation distribution illustrated in Fig. 4.8(a) - firstly a region is cut out of an elastic body and undergoes plastic deformation specified by $\boldsymbol{e}^P$, the symmetric part of $\boldsymbol{\beta}^P$. In Eshelby's (1957) terminology this is a "stress-free transformation strain" and according to Furuhashi & Mura (1979) it is known as an "eigenstrain". If tractions are applied to the boundary of the region which serve to restore it to its original shape, and if it is replaced in the body from which it was cut (the 'matrix') before the tractions on the boundary are removed, then the region (the cube in Fig. 4.8 (a)) is called an 'elastic inclusion'[4] and the body is in a state of self-stress. Eshelby deduced the well-known result that if the transformation strain is uniform (that is $(\boldsymbol{\beta}^P)^S$ is constant) throughout an ellipsoidal region then, inside the ellipsoid, the elastic strain and the stress are also uniform. This effectively amounts to showing that if the region of integration in (4.44) is an ellipsoid then $\boldsymbol{u}^T$ is linear in $\boldsymbol{x}$ and thus $\boldsymbol{e}$ is a constant from (4.43).

The elliptical cylindrical sheet of Section 2.4 is an example of an inclusion with eigenstrain

$$e^P_{23} = H(1 - f(x_1, x_2)) \qquad f(x_1, x_2) = \frac{x_1^2}{a^2} + \frac{x_2^2}{b^2}.$$

Since $\boldsymbol{e}^P$ is uniform inside the elliptical cylinder, Eshelby's result predicts that the stress inside the cylinder is also uniform, as was shown directly in Chapter 2.

A ZSE such as the cylindrical ZSE, or the surface ZSE of Section 3.1, is an example of an inclusion which possesses a trivial eigenstrain $\boldsymbol{e}^P = \boldsymbol{0}$, but a nontrivial dislocation density. Furuhashi & Mura (1979) have pointed out that, in general,

[4]The term 'inclusion' is often used to describe a cavity or region within a material possessing elastic constants different from the matrix, but here it will be used only as described above.

the condition that an eigenstrain should not be a source of internal stress is that $\boldsymbol{e}^P$ takes the form

$$e^P_{ij} = \frac{1}{2}(\beta^P_{ij} + \beta^P_{ji}) = \frac{1}{2}(v_{i,j} + v_{j,i}), \tag{4.45}$$

for some functions v_i. This is the general solution of the equation $\boldsymbol{\eta} = \boldsymbol{\nabla} \wedge \boldsymbol{\nabla} \wedge \boldsymbol{e}^P = \mathbf{0}$ (1.17), as one would expect.

As we have seen in Section 4.7, the ZSEs with which we are most concerned are those for which $\boldsymbol{\beta}^P$ is skew-symmetric, and hence which correspond to trivial eigenstrains $\boldsymbol{e}^P = \mathbf{0}$. In this case $\boldsymbol{v}$ corresponds to a rigid body rotation or translation of the material within the inclusion with respect to that outside. However, one may still have a ZSE even if $\boldsymbol{e}^P \neq \mathbf{0}$, since the eigenstrain must simply be of the form given in (4.45). Such ZSEs, having less trivial eigenstrains than those we have been concerned with here, may be expected to have less trivial dislocation densities, for example. Examination of an example given by Furuhashi & Mura (1979) will show that this is not necessarily the case. They discuss a ZSE whose eigenstrain is given by

$$\boldsymbol{e}^P = (\boldsymbol{\beta}^P)^S = \begin{pmatrix} x_1 H(1-r) & \frac{1}{2}x_2 H(1-r) & \frac{1}{2}x_3 H(1-r) \\ \frac{1}{2}x_2 H(1-r) & 0 & 0 \\ \frac{1}{2}x_3 H(1-r) & 0 & 0 \end{pmatrix},$$

which is derived from the function

$$v_1 = \frac{1}{2}(r^2 - 1)H(1-r),$$

so that $(\boldsymbol{\beta}^P)^S$ is distributed throughout a sphere. Since only the symmetric part of $\boldsymbol{\beta}^P$ is presented, the dislocation density which this distortion represents is not uniquely defined by (4.18). For example, $e^P_{12} = \frac{1}{2}(\beta^P_{12} + \beta^P_{21}) = \frac{1}{2}x_2 H(1-r)$. Thus we may choose either $\beta^P_{12} = x_2 H(1-r)$ or $\beta^P_{21} = x_2 H(1-r)$, or an appropriate combination of the two. Hence there are essentially four choices for $\boldsymbol{\beta}^P$ (in the sense that any other choice is a linear combination of these four) and they are detailed below with the corresponding $\boldsymbol{\alpha}$.

A.

$$\boldsymbol{\beta}^P = \begin{pmatrix} x_1 H(1-r) & 0 & x_3 H(1-r) \\ x_2 H(1-r) & 0 & 0 \\ 0 & 0 & 0 \end{pmatrix},$$

$$\boldsymbol{\alpha} = \begin{pmatrix} -(x_2x_3/r)\delta(1-r) & 0 & 0 \\ (x_1x_3/r)\delta(1-r) & 0 & -H(1-r)+(x_3^2/r)\delta(1-r) \\ 0 & 0 & -(x_2x_3/r)\delta(1-r) \end{pmatrix}.$$

B.

$$\boldsymbol{\beta}^P = \begin{pmatrix} x_1H(1-r) & x_2H(1-r) & x_3H(1-r) \\ 0 & 0 & 0 \\ 0 & 0 & 0 \end{pmatrix},$$

$$\boldsymbol{\alpha} = \begin{pmatrix} 0 & 0 & 0 \\ (x_1x_3/r)\delta(1-r) & (x_2x_3/r)\delta(1-r) & -H(1-r)+(x_3^2/r)\delta(1-r) \\ (x_1x_2/r)\delta(1-r) & H(1-r)-(x_2^2/r)\delta(1-r) & (x_2x_3/r)\delta(1-r) \end{pmatrix}.$$

C.

$$\boldsymbol{\beta}^P = \begin{pmatrix} x_1H(1-r) & 0 & 0 \\ x_2H(1-r) & 0 & 0 \\ x_3H(1-r) & 0 & 0 \end{pmatrix},$$

$$\boldsymbol{\alpha} = \begin{pmatrix} 0 & 0 & 0 \\ 0 & 0 & 0 \\ 0 & 0 & 0 \end{pmatrix}.$$

D.

$$\boldsymbol{\beta}^P = \begin{pmatrix} x_1H(1-r) & x_2H(1-r) & 0 \\ 0 & 0 & 0 \\ x_3H(1-r) & 0 & 0 \end{pmatrix},$$

$$\boldsymbol{\alpha} = \begin{pmatrix} (x_2x_3/r)\delta(1-r) & 0 & 0 \\ 0 & (x_2x_3/r)\delta(1-r) & 0 \\ -(x_1x_2/r)\delta(1-r) & H(1-r)-(x_2^2/r)\delta(1-r) & 0 \end{pmatrix}.$$

Possibility A appears to consist of two families of dislocations, one with density components α_{11}, α_{21} (a b_1m_3 family), and one with density components α_{23}, α_{33} (a b_3m_1 family). This would at first sight seem to be a standard example in which the two families are 'orthogonal' with equal screw components. Problems arise, however, when one attempts to interpret the dislocations physically. A cross-section of the b_3m_1 family is shown in Fig. 4.12.

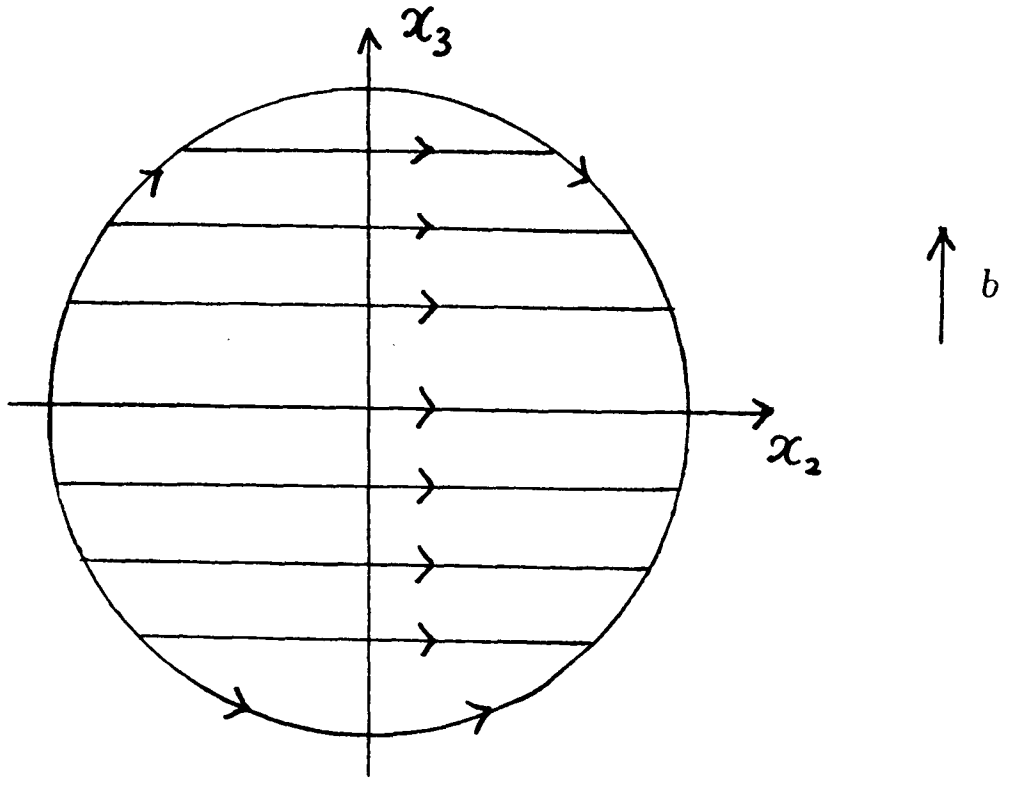

Figure 4.12: A diagram showing the dislocations of the b_3m_1 family corresponding to the plastic distortion given in A. Arrows indicate the tangents to the dislocations. It is seen that the dislocations do not form closed loops, and hence that the plastic distortion chosen is physically unacceptable.

The distribution can be seen to consist of a uniform density of edge dislocations filling the interior of the sphere, combined with a layer of curved dislocations on its surface. The diagram shows that the dislocations do not form closed loops. This seems to contradict our most fundamental assumption about dislocations, since the fact that the divergence of $\boldsymbol{\alpha}$ is zero (2.2) implies that the dislocations *do* form closed loops. This problem arises from a 'bad' choice of $\boldsymbol{\beta}^P$. One may choose any function at all for $\boldsymbol{\beta}^P$ and then, by definition, the divergence of $\boldsymbol{\alpha}$ will vanish. Not all choices of $\boldsymbol{\beta}^P$, though, will lead to *families* of dislocations. The reason why this is so can be elicited from an interpretation of the β^P_{13} component of plastic distortion as a distribution of Kroupa loops. Since this component varies with x_3, the density of Kroupa loops varies in the direction of the Burgers vector, and so the infinitesimal loops do not combine to give a constant jump in displacement across the x_2x_3-plane. Possibility A is thus rejected as an acceptable dislocation arrangement on physical grounds. Possibilities B and D are likewise ruled out and one is left with the trivial case C for which the plastic distortion is a solution of the equation $\boldsymbol{\alpha} = -\boldsymbol{\nabla} \wedge \boldsymbol{\beta}^P = \mathbf{0}$, so that in (4.45) one has chosen

$$\beta^P_{ij} = v_{j,i}.$$

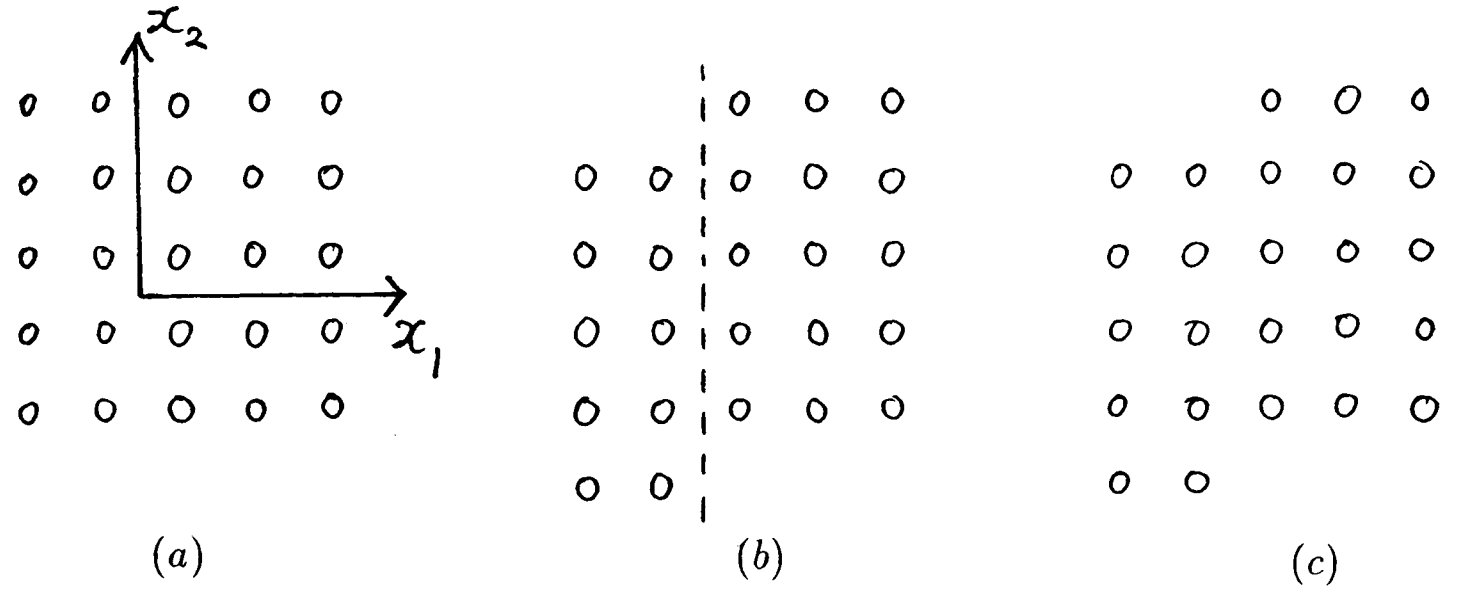

Figure 4.13: Plastic distortion which does not dislocate the material. (a) Perfect crystal. (b) Cut along the x_2x_3-plane and displace in the x_2 direction. (c) Weld to give dislocation-free crystal.

It only remains to answer the question as to what is the nature of a plastic distortion which is not responsible for a dislocation distribution. As an example, consider the simplest case, in which only one of the functions v_i is involved, and which, additionally, is dependent on only one variable. Thus take

$$v_2 = H(x_1), \quad v_1 = v_3 = 0.$$

The only nonzero component of $\boldsymbol{\beta}^P$ is then

$$\beta^P_{12} = \delta(x_1).$$

This has the effect of displacing the two halves of the solid, separated by the x_2x_3-plane, with respect to each other as illustrated in Fig. 4.13.

Since we are dealing with situations in which $(\boldsymbol{\beta}^P)^S \neq 0$, it is not surprising that we will no longer be restricted to glide dislocations, and we should expect to encounter prismatic dislocations. The choice

$$v_1 = H(x_1), \quad v_2 = v_3 = 0,$$

causes a plastic distortion

$$\beta^P_{11} = \delta(x_1),$$

which is a distribution of prismatic loops, and can be thought of as the limiting case as $a \to \infty$ of the circular disc distribution

$$\beta^P_{11} = \delta(x_1)H(a-r) \qquad r^2 = x_2^2 + x_3^2,$$

which is responsible for the prismatic dislocation given by

$$\begin{aligned} \alpha_{21} &= \frac{x_3}{r}\delta(x_1)\delta(a-r), \\ \alpha_{31} &= -\frac{x_2}{r}\delta(x_1)\delta(a-r). \end{aligned}$$

As described earlier (Section 1.3.3), a prismatic dislocation corresponds to the presence of a disc of vacancies in the crystal, and a cross-section of a prismatic loop is shown in Fig. 1.6. As a increases to infinity, it is apparent that the effect of the plastic distortion will be to remove a whole sheet of atoms, thus leaving the crystal perfect as before, and hence dislocation-free.

A less trivial example is shown in Fig. 4.14. Take

$$v_1 = H(a-|x_1|)H(a-|x_2|), \quad v_2 = v_3 = 0,$$

to give

$$\begin{aligned} \beta_{11} &= \bar{+}\,\delta(a-|x_1|)H(a-|x_2|), \\ \beta_{21} &= \bar{+}\,H(a-|x_1|)\delta(a-|x_2|), \end{aligned}$$

the sign depending on whether x_1 (or x_2) is positive or negative respectively. Fig. 4.14 shows that this plastic distortion amounts to a 'shuffling' of the atoms which leaves the crystal undistorted. At $x_1 = a$ the prismatic element of $\boldsymbol{\beta}^P$ introduces vacancies (Fig. 4.14(a)). The shear element β^P_{21} displaces the material inside the square $|x_1|, |x_2| \leq a$ in the x_1 direction (Fig. 4.14(b)), and finally (Fig. 4.14(c)) atoms are introduced by β^P_{11} at $x_1 = -a$ leaving the lattice undistorted and hence dislocation-free. Thus we conclude that, though ZSEs consisting of purely glide dislocations have trivial eigenstrains, they nevertheless have nontrivial dislocation densities. Conversely we have also seen that certain nontrivial eigenstrains actually involve plastic distortions which lead to the trivial result $\boldsymbol{\alpha} = 0$.

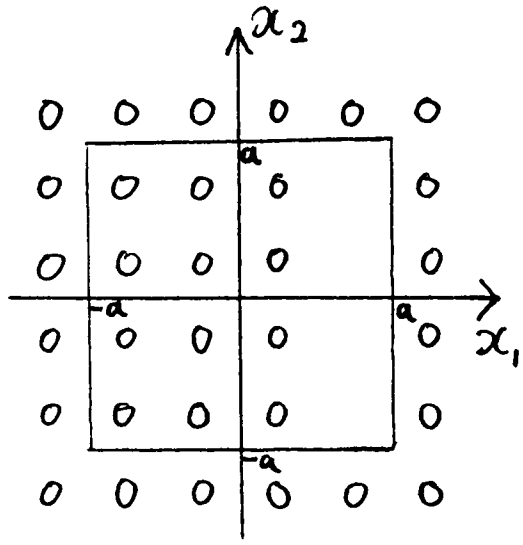

(a)

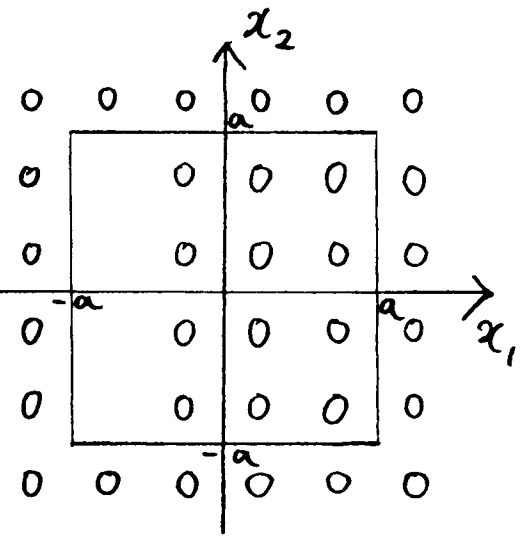

(b)

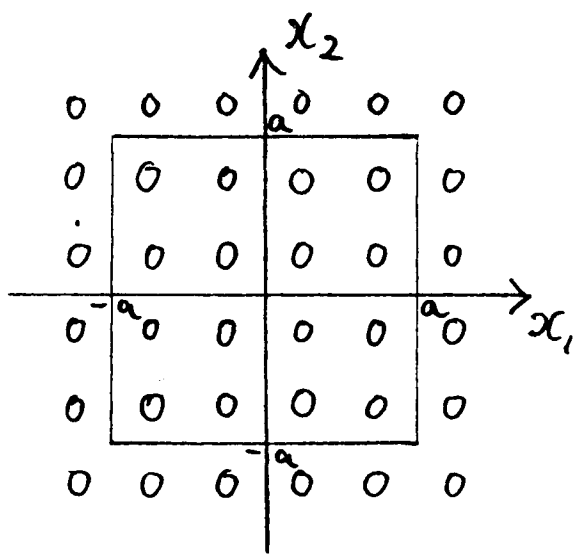

(c)

Figure 4.14: The 'shuffling' of atoms caused by a nontrivial 'impotent' eigenstrain which results in a lattice free of dislocations. (a) Plastic distortion β_{11}^P at $x_1 = a$; (b) Plastic distortion β_{21}^P; (c) Plastic distortion β_{11}^P at $x_1 = -a$.

Chapter 5

Response to Applied Stresses

So far, a framework has been described which enables us to think of general equilibria of dislocation continua under zero applied stress, and of ZSEs in particular. In this chapter, following Head et al. (1992), the possible response to tractions applied at the boundary of the material will be considered. As Fig. 1.1 shows, the stress-strain response is linear almost until the onset of plastic flow. The task is to reconcile this linear behaviour with the presence within the material of large numbers of dislocations, which will respond to stress fields by adopting some equilibrium configuration in which the appropriate stress components vanish. It will be assumed that before any stress is applied, the distributions in the specimen are arranged in a ZSE configuration, and we will consider how this must respond to an increase in the applied stresses. The discussion will be confined to simple cubic crystals for simplicity (although some of our arguments will not apply to other crystal structures).

Motion of dislocations, which has already been touched upon in Section 4.9.1, introduces extra equations into the model. For each family there will be a conservation equation which states that dislocations are neither created nor destroyed during the unsteady motion. These additional equations also introduce (unknown) velocities so that the system is not over-determined. The full model is presented in Appendix A.8.

Firstly, the cross-grid of screws will be considered, followed by the less trivial cross-grid slab of screws, and finally some comments will be made concerning the cylindrical ZSE with circular cross-section, as a first step towards the goal of

understanding the evolution of the ZSE box, in the first instance, and, ultimately, volume ZSEs.

Much experimental evidence exists (see Gay et al. 1954, Bailey 1963, Bailey & Hirsch 1962, Kuhlmann-Wilsdorf & van der Merve 1982, for example) which describes how work-hardened metals commonly possess a 'honeycomb' structure in which a substantial proportion of the material is more-or-less free from dislocations, while the dislocations are arranged in 'walls' interspersed between 'good' patches (or 'particles'). That this scenario is in accord with the mathematical model is suggested by the following argument. Suppose, as is usually the case, that significant numbers of dislocations from all the six possible families of slip dislocations are present, and suppose also that they are distributed throughout the specimen with the respective densities α_{in} being everywhere smooth. Then, in equilibrium, there would be a nonzero density of *each* family at most points, which is perfectly possible for a ZSE; however, when a stress is applied, the three off-diagonal stress components must still vanish where there are dislocations of each of the six families. This might be achieved by a wholesale rearrangement of the dislocation network but not by a continuous response to the applied stress. Thus the possibility that the original ZSE configuration has a smoothly varying density distribution is rejected, and the honeycomb configuration is certainly possible. With this scenario, the function of the 'good' regions is to transmit stress as in conventional elasticity theory, while the response of the walls is that of a polarisation[1] in the sense that the dislocations within them move a short distance so as to accommodate the stress in the neighbouring 'good' patches. If the walls were quite thick, their dislocation density would cause $\boldsymbol{\sigma}$ to vanish in much of the material, and so it is assumed they are thin (as mentioned in Chapter 4, this is confirmed by experimental evidence), with their faces presenting 'naked' dislocations to the 'good' patches in such a way as to match the stress therein. This is consistent with the result (Section 2.3.1) that there is a constant jump in stress across a sheet of screw dislocations. It may be further conjectured that, as the external stresses are increased, so the degree of polarisation increases until the point is reached at which some of the dislocation walls can polarize no further. At

[1]This idea is due to A.K.Head and S.D. Howison.

this stage, which is tentatively identified with the onset of large-scale plastic deformation, the response to yet further stress would be an irreversible change in the dislocation configuration as dislocations move large distances across the interstices of the honeycomb structure; such movement can be interpreted as plastic flow.

5.1 The Cross-grid of Screws

We recall from Sections 2.3.1, 3.2*(i)* that a sheet of screw dislocations with Burgers vector $(0,0,1)$ covering the plane $x_1 = 0$ with uniform density Ω (i.e. $\alpha_{33} = \Omega\delta(x_1)$, $\alpha_{ij} = 0$ otherwise), generates the piecewise constant stress field

$$\sigma_{23} = \sigma_{32} = \begin{cases} \mu\Omega/2 & x_1 > 0 \\ -\mu\Omega/2 & x_1 < 0. \end{cases}$$

By superposing onto this sheet the orthogonal sheet $\alpha_{22} = \Omega\delta(x_1)$ which generates a stress

$$\sigma'_{23} = \sigma'_{32} = \begin{cases} -\mu\Omega/2 & x_1 > 0 \\ \mu\Omega/2 & x_1 < 0, \end{cases}$$

we create the simple cross-grid of screws ZSE.

Consider now the response of a cross-grid of screws to an external stress

$$\sigma_{23}^{ext} = \sigma_{32}^{ext} = \sigma_0 > 0,$$

say. There are three possible equilibrium configurations: the cross-grid may remain in place, its two components may separate and remain a finite distance apart, or they may have to move to infinity. The first occurs when $0 \leq \sigma_0 < \mu\Omega/2$; when $\sigma_0 = \mu\Omega/2$, however, the two sheets can remain in equilibrium separated by any distance. Suppose (without loss of generality) that they are at $x_1 = \pm 1$; the total 23-stress component is $\sigma_{23} + \sigma'_{23} + \sigma_0$, which (since it is assumed that the stress due to each sheet vanishes on the sheet itself) takes the values

$$\sigma_{23} + \sigma'_{23} + \sigma_0 = \begin{cases} \mu\Omega/2 & x_1 < -1 \\ 0 & x_1 = -1 \\ -\mu\Omega/2 & -1 < x_1 < 1 \\ 0 & x_1 = +1 \\ \mu\Omega/2 & x_1 > 1. \end{cases}$$

Thus the α_{33} sheet is in equilibrium at $x_1 = -1$ under the two equal and opposite stresses σ_0 and σ'_{23}, and the α_{22} sheet is in equilibrium at $x_1 = +1$ under the two equal and opposite stresses σ_0 and σ_{23}.

Finally, if $|\sigma_0| > \mu\Omega/2$, no equilibrium is possible with either sheet at a finite value of x_1.

This model presents an extremely crude paradigm for the 'polarisation' described earlier; the value $\sigma_0 = \mu\Omega/2$ is the critical stress at which an irreversible configuration change might occur.

This simple calculation can be backed up by an analysis of a continuous slab of cross-grids, which is now presented.

5.2 The evolution of a cross-grid slab

In this section the unsteady response of a slab of cross-grids is considered. Hitherto little has been mentioned concerning dislocation dynamics, but in this situation, following Head (1972a), a simple mobility law (see Section 1.4.1) will be assumed according to which a screw dislocation in a stress field which would act to disturb its equilibrium (i.e. having the relevant non-zero off-diagonal components) moves in its slip plane with a velocity proportional to the excess stress. The slab of cross-grids, initially in equilibrium under zero applied stress, will be subject to a constant applied stress switched on at $t = 0$.

Consider, then, the distribution of 2 families of screw dislocations for which at $t = 0$ the nonzero density tensor components $\{\alpha_{ij}\}$, $\{\alpha'_{ij}\}$ are

$$\alpha_{33} = \begin{cases} \omega > 0 & |x_1| < L \\ 0 & |x_1| > L, \end{cases} \tag{5.1}$$

$$\alpha'_{22} = \alpha_{33}. \tag{5.2}$$

It is assumed that the slip planes for the unprimed and primed families are respectively x_1x_3 and x_1x_2-planes, so both can move in the x_1-direction. The stress fields of these dislocations have nonzero components

$$\sigma_{32} = \sigma_{23} = \begin{cases} \mu\omega L & x_1 \geq L \\ \mu\omega x_1 & -L \leq x_1 \leq L \\ -\mu\omega L & x_1 \leq -L, \end{cases} \tag{5.3}$$

$$\sigma'_{23} = \sigma'_{32} = -\sigma_{23}. \tag{5.4}$$

Clearly this distribution is a ZSE.

Suppose now that an external stress

$$\sigma_{23}^{ext} = \sigma_{32}^{ext} > 0$$

is switched on. In the subsequent motion the α_{33} dislocations move in the direction of increasing x_1, the α'_{22} ones in the opposite direction; $v(x_1,t)$ and $v'(x_1,t)$ are their velocities, and (see Appendix A.8) conservation of dislocations is represented by the equations

$$\frac{\partial \alpha_{33}}{\partial t} + \frac{\partial}{\partial x_1}(\alpha_{33} v) = 0,$$

$$\frac{\partial \alpha'_{22}}{\partial t} + \frac{\partial}{\partial x_1}(\alpha'_{22} v') = 0.$$

These are two additional equations, and v and v' are additional unknowns. Moreover, the 23-components of the stresses generated by the distributions satisfy

$$\frac{\partial \sigma_{23}}{\partial x_1} = \mu \alpha_{33}, \quad \frac{\partial \sigma'_{23}}{\partial x_1} = -\mu \alpha'_{22}.$$

Lastly, it is assumed that the mobility law has the form

$$v = A(\sigma_{23} + \sigma'_{23} + \sigma_{23}^{ext}), \tag{5.5}$$

$$v' = -A(\sigma_{23} + \sigma'_{23} + \sigma_{23}^{ext}), \tag{5.6}$$

where A is constant and the minus sign in (5.6) incorporates the parity of the primed family.

Substituting for v, v' from (5.5), (5.6), and for α_{33}, α'_{22} from (5.1), (5.2), we obtain two equations which, after integrating with respect to x_1 (the arbitrary function of t that arises vanishes), can be written as the hyperbolic system

$$\frac{\partial \sigma_{23}}{\partial t} + \frac{A}{\mu}(\sigma_{23} + \sigma'_{23} + \sigma_{23}^{ext}) \frac{\partial \sigma_{23}}{\partial x_1} = 0,$$

$$\frac{\partial \sigma'_{23}}{\partial t} - \frac{A}{\mu}(\sigma_{23} + \sigma'_{23} + \sigma_{23}^{ext}) \frac{\partial \sigma'_{23}}{\partial x_1} = 0,$$

with initial conditions (5.3), (5.4).

The Riemann invariants of this system yield

$$\sigma_{23} = \text{ constant on } \frac{dx_1}{dt} = \frac{A}{\mu}(\sigma_{23} + \sigma'_{23} + \sigma_{23}^{ext}),$$

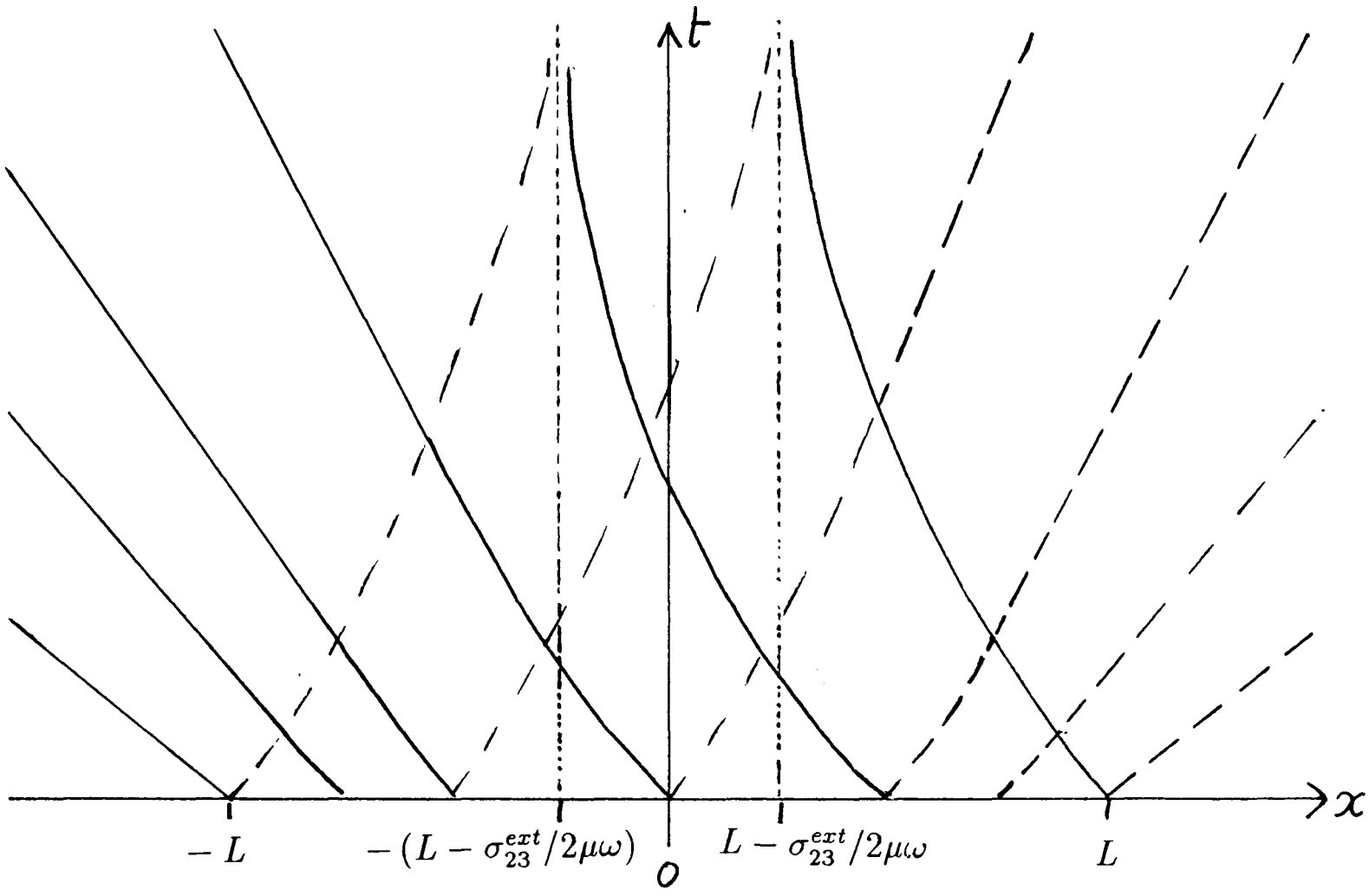

Figure 5.1: Broken lines represent characteristics of α_{33} dislocations, solid lines those of α'_{22} dislocations.

$$\sigma'_{23} = \text{ constant on } \frac{dx_1}{dt} = -\frac{A}{\mu}(\sigma_{23} + \sigma'_{23} + \sigma_{23}^{ext}).$$

A characteristic diagram is shown in Fig. 5.1. The important feature as far as our discussion is concerned is the behaviour of the characteristics through $x_1 = \pm L$, for these trace the evolution of the edges of the slab. The outward-going characteristics are straight lines with slope $\pm A\sigma_{23}^{ext}/\mu$, while the inward-going characteristics have the equations $x_1 = \pm\left\{\sigma_{23}^{ext}(1 - e^{-2A\omega t}) - 2\mu\omega L\right\}/2\mu\omega$. We see that the slab 'sheds' a proportion $\sigma_{23}^{ext}/2\mu\omega L$ of its original dislocations from each side; these dislocations move off to infinity with constant speed, and the proportion $(1 - \sigma_{23}^{ext}/2\mu\omega L)$ that is left forms a thinner slab of thickness $2L - \sigma_{23}^{ext}/\mu\omega$ and density equal to that of the original slab. This new slab is in fact a ZSE, but it is 'shielded' from σ_{23}^{ext} by the dislocations from the original slab that have moved away towards $x_1 = \pm\infty$.

Note that this more detailed model is in fact capable of describing, with some limitations imposed by the high degree of symmetry assumed, the onset of the polarisation mentioned above, and the evolution of two faces of naked dislocations

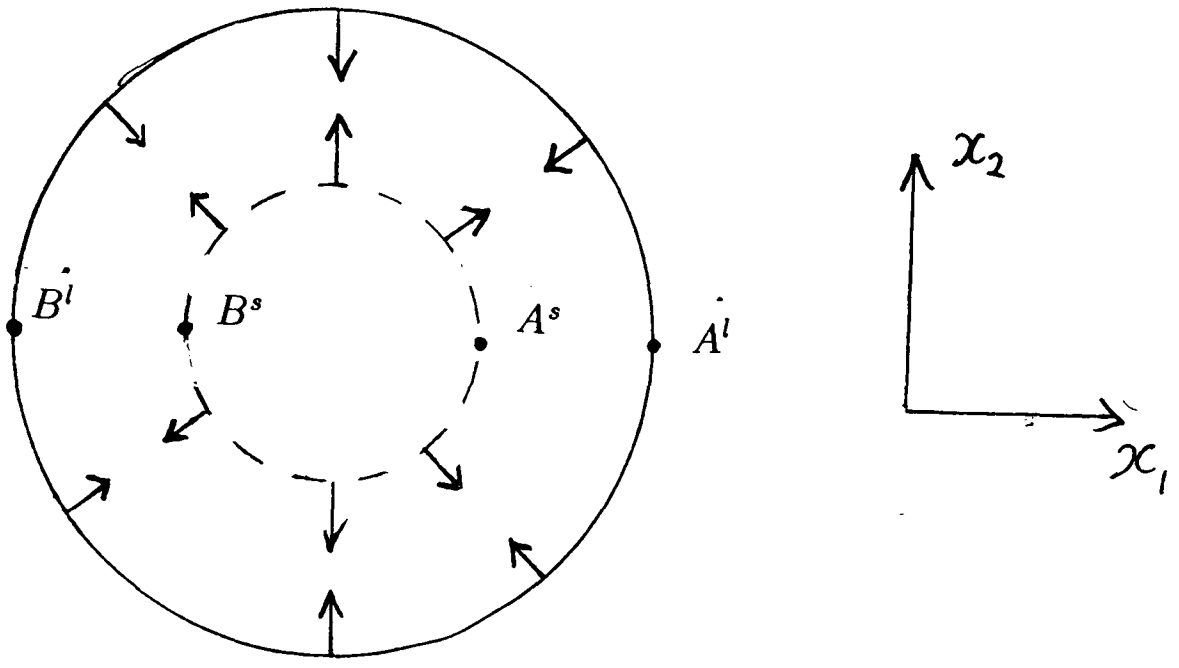

Figure 5.2: Cylindrical ZSE whose families have been separated by a small radial distance. Arrows indicate direction of force.

shielding a ZSE. If, however, the external stress is too large ($\sigma_{23}^{ext} > 2\mu\omega L$), all the original slab separates out into its constituent sheets and moves to infinity, and the slab may be said to have broken down.

5.3 'Unzipping' of the Cylindrical ZSE

In this section some preliminary remarks will be made regarding the cylindrical ZSE described in Section 3.2.*(iv)* as a first step towards understanding the three-dimensional version of the cylindrical ZSE, namely the ZSE box.

Suppose that the cylinder has circular cross-section, and that the ZSE is comprised of screw dislocations of the b_2m_3 system as generators, and loops of the b_3m_2 system. Suppose also that the two families have been separated by a small radial distance as in Fig. 5.2, so that they exert an attractive force upon each other. The 23-component of stress (the component which would move the dislocations) is, for each family (Appendix A.4)

$$-\sigma_{23}^{s} = \begin{cases} 1 & \text{inside } C_s \\ \frac{r_s^2}{r^2}\cos 2\theta & \text{outside } C_s, \end{cases}$$

$$\sigma_{23}^{l} = \begin{cases} 1 & \text{inside } C_l \\ \frac{r_l^2}{r^2}\cos 2\theta & \text{outside } C_l, \end{cases}$$

where θ is the polar angle, r is the polar length and the letters l and s denote loops and screws respectively. The self-stress on the dislocations is half the sum

of the values on either side of the respective curve, as can be established by an examination of the complex variable analysis in Appendix A.4. Thus

$$\begin{aligned} \sigma_{23}^{s}(C_s) &= -\frac{1}{2}[1+\cos 2\theta], \\ \sigma_{23}^{l}(C_l) &= \frac{1}{2}[1+\cos 2\theta]. \end{aligned}$$

The total stess on each family is then

$$\sigma_{23}^{s}(C_s) + \sigma_{23}^{l}(C_s) = \frac{1}{2}[1-\cos 2\theta],$$

on the screws, and

$$\sigma_{23}^{l}(C_l) + \sigma_{23}^{s}(C_l) = \frac{1}{2}\left[1+\frac{r_l^2-2r_s^2}{r_l^2}\cos 2\theta\right],$$

on the loops.

Since the normal component of the force on the dislocations is proportional to this component of stress, it is apparent that the force is directed as shown schematically in Fig. 5.2. The important point to note is that at A^s, A^l, B^s and B^l, the stress vanishes when $r_s = r_l$, and the dislocations experience no mutually attractive force at these points. This suggests that when a stress is applied to a cylindrical ZSE it will begin to 'unzip' such that the points A^l, A^s and B^l, B^s separate first (see Fig. 5.3), and the screw dislocations move across the interior of the cylinder. This mechanism will be reversible until the screw dislocations meet their opposites and annihilate.

In one respect this scenario is counter-intuitive - at the points A^l, A^s and B^l, B^s the ZSE is, locally, a cross-grid of screws, and at C and D the screw component is zero. One would, therefore, have supposed that it would be at the points C and D that the families would not experience a force. On the other hand, it also seems unlikely that the screw dislocations near C and D would 'unzip' since, being confined to slip planes whose normal is in the x_2-direction, they can only move parallel to the x_1-direction.

Clearly, further analysis is required to confirm that the ZSE unzips as conjectured, and also to determine how the shapes of the unzipped segments of the dislocations evolve.

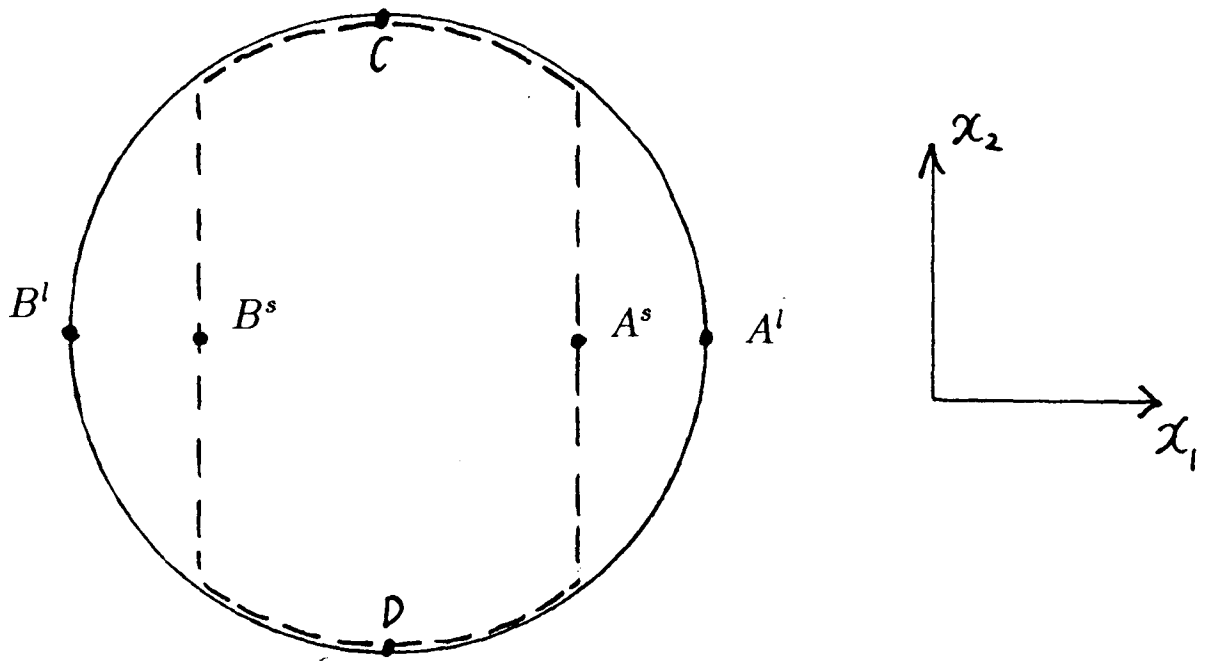

Figure 5.3: Conjectured 'unzipping' of ZSE cylinder under applied stress. The dotted line indicates screws; the solid line loops.

Chapter 6

Conclusions & Further Work

A typical crystalline metal behaves as depicted in Fig. 1.1 upon loading, unloading and reloading. The material is elastic and obeys a linear stress-strain relation for small applied stresses. This relation becomes nonlinear (though the material is still elastic) as the loading is gradually increased, and finally a point is reached (the yield point) where the material deforms irreversibly. Here, this behaviour has been examined from the viewpoint of dislocation theory. It is known that work-hardened metals (that is, metals which have undergone the process just described) possess large numbers of dislocations and that the irreversible (plastic) deformation is enabled by the movement through the material of these dislocations. Since it is not feasible to model vast numbers of dislocations individually, a continuum model, based on a dislocation density tensor, has been developed by smoothing out large numbers of similar dislocations into 'families', and deriving the stress fields of such families by averaging results obtained for discrete dislocations. Having introduced the continuum model, it is then used to derive various results including those for dislocation distributions which occupy an elliptical region - it is known that the ellipse, in two dimensions, and the ellipsoid, in three dimensions, are special (see Eshelby 1957, Head et. al 1987) and a similar conclusion is drawn here.

Returning to the stress-strain curve Fig. 1.1, it is natural to begin the investigation by attempting to determine the character of those dislocation configurations that exist in the unloaded metal. It is intuitively obvious that distributions of dislocations which produce zero stress everywhere (ZSEs) are likely candidates for self-equilibrium arrangements. It is not clear, however, that ZSEs must be the only distributions in equilibrium in the absence of applied stresses. The condition

for equilibrium is that the component of the Peach-Koehler force normal to each dislocation should be zero; this requires only one of the six components of stress to vanish, and then only where there are dislocations. It comes as a surprise, therefore, to discover that the model predicts that any distribution of dislocations which fills a simply-connected volume, or covers a simply-connected surface, must be a ZSE if it is to be in equilibrium. The result adds weight to the experimental evidence (e.g. Gay et al. 1954) that ZSEs figure prominently in real plastically deformed metals, and in fact Kuhlmann-Wilsdorf (1987, 1989) has proposed that most arrangements of dislocations are "low energy dislocation structures" (or LEDS) - a proposal that is in accord with the above result since ZSEs have *zero* energy.

The simplest ZSEs - the sheet of edges and the cross-grid of screws - are formed by smoothing out into a continuum discrete rows of screws and edges. These discrete distributions may be regarded as the forerunners of ZSEs, and they have been known for some time (Taylor (1934) discussed the sheet of edges, and Frank (1948) examined the cross-grid of screws). Indeed, these "short-range stress" dislocation distributions have been used, if not directly studied, by a number of authors (Nye 1953, Bilby et. al 1957). However, if one wishes to trace the origins of the ZSE, then one must return to the work of von Mises' (1928) (see Section 3.4), who gave the criterion for general plastic deformation of a crystal. Von Mises work is also important in that it indicates that the results derived here for ZSEs, based on the model simple cubic lattice, can, in principle, be extended to real crystals, although this may in practice be complicated by the larger number of slip systems (12 in face-centred cubic and body-centred cubic compared to 6 in simple cubic).

The physical interpretation of both volume and surface distributions of dislocations is facilitated by the concept of "plastic distortion" introduced by Kröner (1955) and defined here as the generalised derivative of the discontinuous displacements that result from the creation of dislocations via the cut-and-weld mechanism. Plastic distortion is denoted $\boldsymbol{\beta}^P$, and the displacements, known as "total displacements", are denoted $\boldsymbol{u}^T$. The plastic distortion is shown to be related to the dislocation density tensor through the equation $-\text{curl}\boldsymbol{\beta}^P = \boldsymbol{\alpha}$. For a given dislocation distribution $\boldsymbol{\beta}^P$ is thus unique only up to the addition of a gradient, this being, physically, a consequence of the fact that many different surfaces may be chosen over which to make the cut in the cut-and-weld process.

The classical part of the derivative of total displacement has been called "elastic distortion" (written $\boldsymbol{\beta}^E$) since the symmetric part of $\boldsymbol{\beta}^E$ is the strain $\boldsymbol{e}$. Thus, in a ZSE, $\boldsymbol{e} = (\boldsymbol{\beta}^E)^S = 0$; but it has also been shown that, for a ZSE, $(\boldsymbol{\beta}^P)^S$ is also zero, as is the total displacement $\boldsymbol{u}^T$. These facts (which are valid for ZSEs consisting entirely of slip dislocations) allow the interpretation of ZSEs which is that, in the case of surface distributions, the slip planes within the surface have undergone a rotation with respect to the slip planes outside the surface. In the case of a volume ZSE the rotation is continuous across the dislocated region, as is borne out by experimental observation (Gay et al. 1954).

Plastic distortion has a close relationship to what are known as 'inclusions' - in fact an inclusion is merely a region which has undergone plastic distortion, although this is usually given in terms of its symmetric part (or "eigenstrain"). There is a well-known result due to Eshelby (referred to above) for ellipsoidal inclusions, and the cylindrical sheet of Chapter 2 with elliptical cross-section is shown to be the two-dimensional simplification of this. There is a problem concerning the connection between an inclusion and the dislocation density which it represents: namely, since an eigenstrain involves the symmetric part of the plastic distortion, the dislocation density (which is minus the curl of $\boldsymbol{\beta}^P$) is not uniquely defined. It is important, therefore, to examine the possible dislocation densities to ensure that the chosen plastic distortion is the cause of a 'sensible' dislocation density; that is, it should represent a family or combination of families of dislocations. In the case of an 'impotent' eigenstrain (any nonzero eigenstrain which nonetheless gives a zero stress field), as given by Furuhashi & Mura (1979), it is seen that the only reasonable dislocation density representing the inclusion is the trivial one $\boldsymbol{\alpha} = \mathbf{0}$. It is a point of interest to ask whether all such 'impotent' eigenstrains give the same result and are thus the source of nothing more than a 'shuffling' of atoms which leaves the crystal undeformed.

There is an interpretation, due to Kroupa (1962), of plastic distortion as a continuous distribution of infinitesimal loops, which has a parallel in electromagnetism where a current line can be replaced by a continuous distribution of fictitious infinitesimal current loops. Kroupa loops are helpful in distinguishing slip dislocations from their prismatic counterparts, and also in unravelling the physical meaning of the impotent eigenstrains already mentioned.

Prismatic dislocations have been discussed in a number of places although usually they have been excluded, as most plastic deformation is a consequence of shear stresses rather than the hydrostatic stresses which prismatic dislocations serve to relieve. In addition to this it is shown that a (finite) ZSE cannot be comprised entirely of prismatic dislocations, although whether combinations of prismatic and slip dislocations can be ZSEs remains an open question.

Some headway has been made in describing the evolution of ZSEs. The concept of 'polarisation' has been introduced to cope with the fact that, along the elastic portion of the stress-strain curve, the dislocation distributions have, presumably, not broken down and yet can accommodate applied stresses. With one eye on the eventual goal of understanding the evolution of the ZSE box, some preliminary observations have been made regarding the simplest two-dimensional approximation - the cylindrical ZSE with circular cross-section. It is conjectured that this ZSE will 'unzip', the component families separating gradually as the applied stress is increased, and recombining if the stress is removed before the ZSE collapses.

The electromagnetic analogy was mentioned above in relation to Kroupa loops, and, indeed, this analogy is quite extensive - the similarity between the Peach-Koehler formula for the stress of a dislocation as an integral over the dislocation line, and the Biot-Savart formula for the magnetic field of a current loop, is well-known. Here it has been shown that a cylindrical sheet of dislocations suffers a constant jump in the product $\boldsymbol{\sigma}.\boldsymbol{b}$, as the sheet is crossed, in comparison to the constant jump in magnetic field $\boldsymbol{B}$ which is experienced upon crossing a cylindrical current sheet (or solenoid).

With regard to possible future work, an extension of Theorem 1 to cover multiply-connected dislocated regions would be most welcome. The argument presented in Chapter 4 to rule out the specific case of the single family of b_2m_3 dislocations lying on the surface of a cube may be a helpful indicator as to how to proceed. On the other hand, extending this work to more realistic crystal structures such as *fcc* or *bcc* could widen the possibility of the existence of non-ZSE equilibrium distributions, as then so-called "Lomer-Cottrell locks" may be present. These locks, which rely on the creation of 'partial' dislocations (see Hirth & Lothe 1982) are not possible in the model simple cubic lattice, but may serve

as barriers to the demise of an otherwise unstable dislocation distribution in the crystals in which they occur.

Again with an eye to further work there are the questions which arose above regarding the possibility of ZSEs comprised of combinations of slip and prismatic dislocations, and a determination of whether or not impotent eigenstrains must always leave a crystal undistorted.

The most natural development of this work would be an analysis of the circular cylindrical ZSE. Being a state of anti-plane strain the field equation is just Laplace's equation, rather than the biharmonic equation which will hold in the ZSE box case, and this should simplify matters. An analysis of the evolution of the ZSE box would follow this, and a homogenisation over many boxes would be the final step.

Appendices

A.1 The Incompatibility Tensor

The incompatibility tensor may be written in a more convenient form as follows. (See de Wit 1960).

$$\begin{aligned}
\eta_{ij} &= -\varepsilon_{ikl}\varepsilon_{jmn}e_{ln,km} \\
&= -\varepsilon_{ikl}\varepsilon_{jmn}e_{pq,km}(\varepsilon_{npr}\varepsilon_{rql} + \delta_{pq}\delta_{ln}) \\
&= -(\delta_{jp}\delta_{mr} - \delta_{jr}\delta_{mp})(\delta_{ir}\delta_{kq} - \delta_{iq}\delta_{kr})e_{pq,km} - (\delta_{ij}\delta_{km} - \delta_{im}\delta_{kj})e_{pp,km} \\
&= e_{ij,kk} + e_{kk,ij} - (e_{ik,jk} + e_{jk,ik}) + (e_{kl,kl} - e_{kk,ll})\delta_{ij}.
\end{aligned}$$

A.2 Proof that Equation (1.47) holds.

This proof follows de Wit (1960). Any vector $\boldsymbol{v}$ that vanishes at infinity can be decomposed into a 'gradient' and a 'curl'. That is, we may write

$$v_i = \phi_{,i} + \varepsilon_{ijk}A_{k,j}. \tag{A.1}$$

Consequently, if T_{ij}, α_{lj}, A_{ln} are second rank tensors, and a_i, b_j are vectors, we may write

$$T_{ij} = a_{j,i} + \varepsilon_{ikl}\alpha_{lj,k}, \tag{A.2}$$

and

$$\alpha_{lj} = b_{l,j} + \varepsilon_{jmn}A_{ln,m}, \tag{A.3}$$

so that, substituting (A.3) into (A.2), we get

$$\begin{aligned}
T_{ij} &= a_{j,i} + \varepsilon_{ikl}b_{l,jk} - \varepsilon_{ikl}\varepsilon_{jmn}A_{ln,mk} \\
&= a_{j,i} + c_{i,j} - \varepsilon_{ikl}\varepsilon_{jmn}A_{ln,mk},
\end{aligned}$$

where

$$c_i = \varepsilon_{ikl} b_{l,j}.$$

Putting

$$a_i + c_i = \phi_i,$$

we obtain

$$T^S_{ij} = \frac{1}{2}(\phi_{i,j} + \phi_{j,i}) - \varepsilon_{ikl}\varepsilon_{jmn} A^S_{ln,mk},$$

where 'S' again denotes 'symmetric part of'. Thus, since σ_{ij} is a symmetric tensor, we may write

$$\sigma_{ij} = \frac{1}{2}(\phi_{i,j} + \phi_{j,i}) - \varepsilon_{ikl}\varepsilon_{jmn}\psi_{ln,mk}, \tag{A.4}$$

where ψ_{ln} is also a symmetric tensor. We know that $\sigma_{ij,j} = 0$, and so

$$\phi_{i,ji} + \phi_{j,ii} = 0. \tag{A.5}$$

Differentiating with respect to x_j gives

$$\phi_{i,ijj} + \phi_{j,iij} = 0,$$

which may be written as

$$\nabla^2(\phi_{i,i} + \phi_{j,j}) = 0,$$

and so

$$\nabla^2(\phi_{i,i}) = 0. \tag{A.6}$$

Now ϕ_i vanishes at infinity and so $\phi_{i,i}$ must as well. The solution of (A.6) is

$$\phi_{i,i} = 0,$$

since ϕ_i and therefore $\phi_{i,i}$ vanishes at infinity. Substituting this in (A.5) gives

$$\phi_{j,ii} = \nabla^2\phi_j = 0,$$

and so by the same argument we have

$$\phi_j = 0,$$

and thus conclude from (A.4) that

$$\sigma_{ij} = -\varepsilon_{ikl}\varepsilon_{jmn}\psi_{ln,mk}.$$

A.3 Proof that Equation (1.50) always holds

Again we follow de Wit (1960). Suppose we found a solution χ'_{ij} of (1.49) which does not satisfy (1.50). The function

$$\chi_{ij} = \chi'_{ij} + \frac{1}{2}(\phi_{i,j} + \phi_{i,j}), \tag{A.7}$$

will then give the same value of σ_{ij} in (1.48) as χ'_{ij}, by virtue of the fact that

$$\varepsilon_{ikl}\varepsilon_{jmn}(\phi_{l,n} + \phi_{n,l})_{,km} = 0.$$

Now if (1.50) must hold for χ_{ij}, then

$$\chi'_{ij,j} + \frac{1}{2}(\phi_{i,jj} + \phi_{j,ij}) = 0,$$

or

$$(\phi_{i,jj} + \phi_{j,ij}) = -2\chi'_{ij,j}.$$

A solution of this equation is

$$\phi_i(\boldsymbol{x}) = -\frac{1}{8\pi}\int[\chi'_{kl,l'}(\boldsymbol{x}')R_{,ik} - 2\chi'_{il,l'}(\boldsymbol{x}')R_{,kk}]dV',$$

where $R = (X_iX_i)^{\frac{1}{2}}$ and $X_i = x_i - x'_i$. This solution can be verified using the relation

$$R_{,iijj} = -8\pi\delta(\boldsymbol{R}).$$

Therefore, since χ'_{ij} is known, we can calculate ϕ_i. We can then use (A.7) to find a function χ_{ij} which satisfies (1.50).

A.4 Stress Field of an Elliptical Cylindrical Sheet

Note firstly that

$$\oint_C \frac{X_1}{X_1^2 + X_2^2}dx'_2 = \frac{1}{2}\mathcal{I}\left\{\oint_C \frac{dw - d\bar{w}}{z - w}\right\}, \tag{A.8}$$

$$\oint_C \frac{X_2}{X_1^2 + X_2^2}dx'_2 = \frac{1}{2}\mathcal{R}\left\{\oint_C \frac{dw - d\bar{w}}{z - w}\right\}, \tag{A.9}$$

where $w = x'_1 + ix'_2$, $z = x_1 + ix_2$, $\mathcal{I}$ denotes the 'imaginary part', $\mathcal{R}$ denotes the 'real part', and a bar implies the complex conjugate.

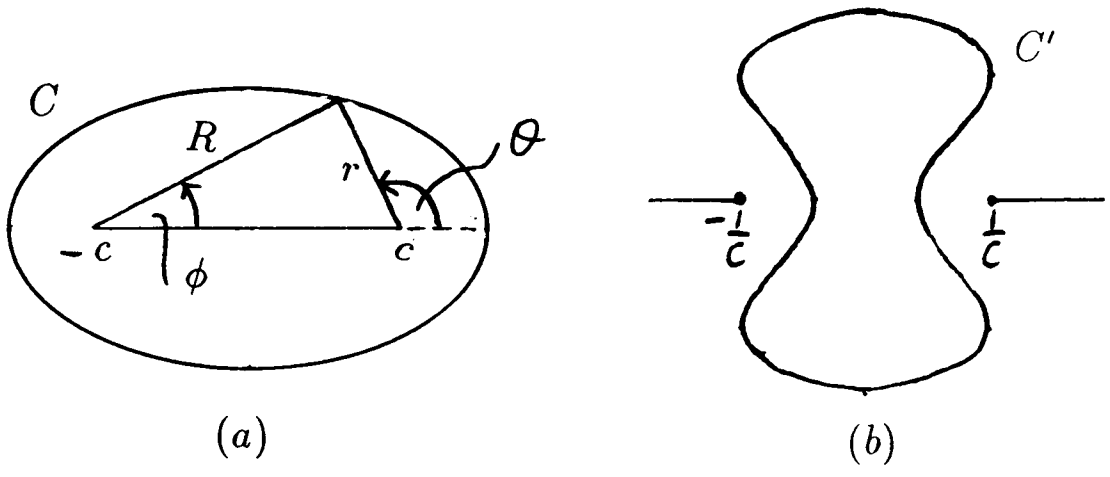

Figure A.1: (a) Ellipse C and branch cut; (b) Curve C' with branch cut.

To calculate the contour integral in (A.8, A.9) we proceed as follows. For the ellipse

$$\frac{x_1'^2}{a^2} + \frac{x_2'^2}{b^2} = 1$$

the equation relating w and $\bar{w}$ is given by

$$\bar{w} = \frac{a^2+b^2}{c^2} w - \frac{2ab}{c^2}(w^2 - c^2)^{\frac{1}{2}} \qquad c^2 = a^2 - b^2. \tag{A.10}$$

The square root is defined by

$$(w^2 - c^2)^{\frac{1}{2}} = (Rr)^{\frac{1}{2}} e^{\frac{1}{2}i(\theta+\phi)},$$

where R and r are as in Fig. A.1(a), and $\theta \in (0, 2\pi)$, $\phi \in (0, 2\pi)$. Hence

$$d\bar{w} = \frac{a^2+b^2}{c^2} dw - \frac{2ab}{c^2} \frac{w}{(w^2-c^2)^{\frac{1}{2}}} dw,$$

and so

$$\oint_C \frac{dw - d\bar{w}}{z-w} = \frac{2b^2}{c^2} \oint_C \frac{dw}{w-z} - \frac{2ab}{c^2} \oint_C \frac{w}{(w-z)(w^2-c^2)^{\frac{1}{2}}} dw.$$

The first term can be calculated by Cauchy's integral theorem. In the second term, the square root factor introduces a branch cut which we take to run from $w = -c$ to $w = c$, as shown in Fig. A.1(a). Next we make the substitution

$$w = \frac{1}{v},$$

so that

$$dw = -\frac{1}{v^2} dv.$$

Then

$$\oint_C \frac{w}{(w-z)(w^2-c^2)^{\frac{1}{2}}}dw = \frac{1}{z}\oint_{C'} \frac{-dv}{v(v-\frac{1}{z})(1-v^2c^2)^{\frac{1}{2}}},$$

where now C' is a curve in the v-plane, such that, if the point z is inside C, the point $1/z$ is outside C' and vice-versa. Also, the branch cut now runs from $w=-\infty$ to $w=-1/c$, and from $w=1/c$ to $w=\infty$, as in Fig. A.1(b). Thus, if z is within C we have a pole at $v=0$ whose residue is $2\pi i$; if z is outside C, we have poles at $v=0$ and $v=1/z$, so that the residue is $2\pi i(1-z/(z^2-c^2)^{1/2})$.

Thus

$$\oint_C \frac{dw-d\bar{w}}{z-w} = \begin{cases} -4\pi ib/(a+b) & z \text{ inside } C \\ (-4\pi iab/c^2)(1-z/(z^2-c^2)^{1/2}) & z \text{ outside } C, \end{cases} \qquad (A.11)$$

and so, from (A.8)

$$\oint_C \frac{X_1}{X_1^2+X_2^2}dx_2' = \begin{cases} -2\pi b/(a+b) & z \text{ inside } C \\ (-2\pi ab/c^2)\mathcal{R}\{1-z/(z^2-c^2)^{1/2}\} & z \text{ outside } C. \end{cases} \qquad (A.12)$$

Also, since

$$\oint_C \frac{X_1}{X_1^2+X_2^2}dx_1' + \oint_C \frac{X_2}{X_1^2+X_2^2}dx_2' = \oint_C \nabla(\log(X_1^2+X_2^2)^{\frac{1}{2}}).\boldsymbol{dx}' = 0, \qquad (A.13)$$

we have

$$\oint_C \frac{X_1}{X_1^2+X_2^2}dx_1' = \begin{cases} 0 & z \text{ inside } C \\ (-2\pi ab/c^2)\mathcal{I}\{1-z/(z^2-c^2)^{1/2}\} & z \text{ outside } C. \end{cases}$$

It is easy to see how the expression (A.11) reduces in the case of a circle for points within the circle. However, for points outside the circle it is not simple to express the real part of the complex function $(1-z/(z^2-c^2)^{1/2})$ in terms of x_1 and x_2, and confocal coordinates, as given by (2.21), collapse to give $z=0$ when $a=b$. However it is straightforward to achieve the desired result by repeating the

calculation above for the case when $c = 0$. One obtains

$$\oint_C \frac{dw - d\bar{w}}{z - w} = \begin{cases} -2\pi i & z \text{ inside } C \\ 2r^2\pi i/z^2 & z \text{ outside } C \end{cases}$$

for a circle of radius r. Consequently, we have

$$\oint_C \frac{X_1}{X_1^2 + X_2^2} dx_2' = \begin{cases} -\pi & (x_1, x_2) \text{ inside } C \\ r^2\pi(x_1^2 - x_2^2)/(x_1^2 + x_2^2)^2 & (x_1, x_2) \text{ outside } C, \end{cases}$$

$$\oint_C \frac{X_1}{X_1^2 + X_2^2} dx_1' = \begin{cases} 0 & (x_1, x_2) \text{ inside } C \\ -2r^2\pi x_1 x_2/(x_1^2 + x_2^2)^2 & (x_1, x_2) \text{ outside } C. \end{cases}$$

A.5 Stress Field of an Elliptical Patch of Edge Dislocations

We have

$$\frac{1}{2}\oint_C \frac{((z-w) + (\bar{z} - \bar{w}))(\bar{z} - \bar{w})^2}{(z-w)^2(\bar{z} - \bar{w})^2}(dw - d\bar{w}) = 2i\oint_C \frac{X_1(X_1^2 - X_2^2)}{(X_1^2 + X_2^2)^2} dx_2' + 4\oint_C \frac{X_1^2 X_2}{(X_1^2 + X_2^2)^2} dx_2'. \quad \text{(A.14)}$$

Thus

$$\frac{2\pi(1-\nu)}{\mu\Omega}\sigma_{12,1}^A = \frac{1}{4}\mathcal{I}\oint_C \left(\frac{1}{z-w} + \frac{\bar{z} - \bar{w}}{(z-w)^2}\right)(dw - d\bar{w}).$$

Substituting for $\bar{w}$ from (A.10), and using

$$\oint_C \frac{w\, dw}{(w-z)^2} = \oint_C \frac{dw}{(w-z)} = 2\pi i \begin{cases} 1 \\ 0 \end{cases} \quad \text{(A.15)}$$

$$\oint_C \frac{w\, dw}{(w-z)(w^2 - c^2)^{\frac{1}{2}}} = 2\pi i \begin{cases} 1 \\ 1 - z/(z^2 - c^2)^{\frac{1}{2}} \end{cases} \quad \text{(A.16)}$$

$$\oint_C \frac{dw - d\bar{w}}{(w-z)^2} = 2\pi i \begin{cases} 0 \\ 2ab/(z^2 - c^2)^{\frac{3}{2}} \end{cases} \quad \text{(A.17)}$$

$$\oint_C \frac{w^2\, dw}{(w-z)^2(w^2 - c^2)^{\frac{1}{2}}} = 2\pi i \begin{cases} 1 \\ 1 - z/(z^2 - c^2)^{\frac{1}{2}} + zc^2/(z^2 - c^2)^{\frac{3}{2}} \end{cases} \quad \text{(A.18)}$$

$$\oint_C \frac{(w^2 - c^2)^{\frac{1}{2}}}{(w-z)^2} dw = 2\pi i \begin{cases} 1 \\ 1 - (z^2 - c^2)^{\frac{1}{2}}/z - c^2/z(z^2 - c^2)^{\frac{1}{2}}, \end{cases} \quad \text{(A.19)}$$

where in each case the upper term is for points inside C and the lower for points outside C. We obtain

$$\oint_C \left(\frac{1}{z-w} + \frac{\bar{z}-\bar{w}}{(z-w)^2} \right) (dw - d\bar{w}) = 2\pi i \begin{cases} -4ab/(a+b)^2 \\ 4f(z), \end{cases}$$

where

$$\begin{aligned} f(z) &= -\frac{ab(a^2+b^2)}{c^4} + \frac{a^3 b}{c^4} \frac{z}{(z^2-c^2)^{\frac{1}{2}}} + \frac{ab^3}{c^4} \frac{(z^2-c^2)^{\frac{1}{2}}}{z} \\ &+ \frac{ab^3}{c^2} \frac{1}{z(z^2-c^2)^{\frac{1}{2}}} + \left(\frac{ab}{2}\bar{z} - \frac{ab(a^2+b^2)}{2c^2} z \right) \frac{1}{(z^2-c^2)^{\frac{3}{2}}}. \end{aligned}$$

Hence finally

$$\sigma^A_{12,1} = \frac{\mu\Omega}{1-\nu} \begin{cases} -ab/(a+b)^2 \\ \mathcal{R}\{f(z)\}. \end{cases}$$

Also

$$-\frac{2\pi(1-\nu)}{\mu\Omega} \sigma^A_{11,1} = \oint_C \frac{2X_1^2 X_2}{(X_1^2+X_2^2)^2} + \frac{X_2}{(X_1^2+X_2^2)} dx_2',$$

which from (A.14) and (2.20) is equal to

$$\begin{cases} 0 & z \text{ inside } C \\ 2\pi\mathcal{I}\left\{ -f(z) - ab/c^2 \left(1 - z/(z^2-c^2)^{1/2}\right) \right\} & z \text{ outside } C. \end{cases}$$

Thus

$$\sigma^A_{11,1} = \frac{\mu\Omega}{1-\nu} \begin{cases} 0 & z \text{ inside } C \\ \mathcal{I}\{g(z)\} & z \text{ outside } C, \end{cases}$$

where

$$\begin{aligned} g(z) &= -\frac{2ab^3}{c^4} + \frac{ab^3}{c^4} \frac{z}{(z^2-c^2)^{\frac{1}{2}}} + \frac{ab^3}{c^4} \frac{(z^2-c^2)^{\frac{1}{2}}}{z} \\ &+ \frac{ab^3}{c^2} \frac{1}{z(z^2-c^2)^{\frac{1}{2}}} + \left(\frac{ab}{2}\bar{z} - \frac{ab(a^2+b^2)}{2c^2} z \right) \frac{1}{(z^2-c^2)^{\frac{3}{2}}}. \end{aligned}$$

A.6 Derivatives of Total Displacement

From the cut-and-weld definition of a screw dislocation (Section 1.3.1*(ii)*) the total displacement is seen to have the form

$$\boldsymbol{u}^T = (0, 0, u_3^T(x_1, x_2)).$$

Since there is a jump of $\hat{b}$ in the value of u_3 on crossing the cut half-plane $(x_1 < 0,\ x_2 = 0)$ we have

$$\lim_{t \to 0_+} \left\{ u_3^T(x_1, t) - u_3^T(x_1, -t) \right\} = \hat{b} H(-x_1).$$

Dividing each side by $2t$, multiplying by a test function $\phi(x_2)$ and integrating, we have

$$\begin{aligned} \int_{-\infty}^{\infty} \lim_{t \to 0} \frac{\{u_3^T(x_1, t) - u_3^T(x_1, -t)\}}{2t} \phi(x_2) dx_2 &= \int_{-\infty}^{\infty} \frac{\partial u_3^T}{\partial x_2} \phi(x_2) dx_2 \\ &= \frac{\hat{b} H(-x_1)}{2} \lim_{t \to 0} \int_{-\infty}^{\infty} \frac{\phi(x_2)}{t} dx_2. \end{aligned}$$

This reduces to

$$\begin{aligned} \int_{-\infty}^{\infty} \frac{\partial u_3^T}{\partial x_2} \phi(x_2) dx_2 &= \frac{\hat{b} H(-x_1)}{2} \lim_{t \to 0} \int_{-t}^{t} \frac{\phi(x_2)}{t} dx_2 \\ &= \frac{\hat{b} H(-x_1)}{2} \lim_{t \to 0} \int_{-t}^{t} \frac{1}{t} (\phi(0) + x_2 \phi'(0) + \ldots) dx_2, \end{aligned}$$

upon expanding $\phi(x_2)$ in a Taylor series about the origin. Hence

$$\int_{-\infty}^{\infty} \frac{\partial u_3^T}{\partial x_2} \phi(x_2) dx_2 = \hat{b} H(-x_1) \phi(0),$$

and we may conclude that

$$\frac{\partial u_3^T}{\partial x_2} = \hat{b} H(-x_1) \delta(x_2) + \frac{\hat{b} x_1}{x_1^2 + x_2^2}.$$

In the case of an edge dislocation, as in Section 1.3.1*(ii)*, the total displacement has the form

$$\boldsymbol{u}^T = (u_1^T(x_1, x_2), u_2^T(x_1, x_2), 0),$$

with a jump in the u_1^T component such that

$$\lim_{t \to 0_+} \left\{ u_1^T(x_1, t) - u_1^T(x_1, -t) \right\} = \hat{b} H(-x_1).$$

Hence there is a contribution to the x_2 derivative of u_1^T equal to

$$\hat{b} H(-x_1) \delta(x_2),$$

and β_{21}^T is as given in (4.3).

A.7 Skew-symmetry of β^P in ZSEs

If we take the support of β^P to be the plane of the dislocation loop, then slip dislocations are represented by off-diagonal components of β^P; the three diagonal components correspond to prismatic dislocations (Kroupa 1962).

In a ZSE, the incompatibility is zero and therefore

$$\epsilon_{ikl}\epsilon_{jmn}(\beta^P_{ln})^S_{,km} = 0.$$

This means that there exist classical continuous single-valued functions ϕ_i such that

$$\beta^P_{ij} + \beta^P_{ji} = \phi_{i,j} + \phi_{j,i}. \tag{A.20}$$

Next, suppose that β is distributed throughout a volume V (so that α would have support either over the surface of V or over the whole or part of V). Then, outside V,

$$\phi_{i,j} + \phi_{j,i} = 0,$$

and so, outside V,

$$\begin{aligned} \phi_1 &= \alpha x_3 - \gamma x_2 + \text{constant}, \\ \phi_2 &= -\beta x_3 + \gamma x_1 + \text{constant}, \\ \phi_3 &= \beta x_2 - \alpha x_1 + \text{constant}, \end{aligned} \tag{A.21}$$

for some constants α, β, γ. Since $\beta^P_{11} = \beta^P_{22} = \beta^P_{33} = 0$ in the absence of prismatic dislocations, we have that in V,

$$\phi_1 = f_1(x_2, x_3),\ \phi_2 = f_2(x_1, x_3),\ \phi_3 = f_3(x_1, x_2),$$

for some functions f_1, f_2, f_3. Since the ϕ_i must be continuous, in particular on ∂V, it is not then difficult to see that (A.21) must hold inside V as well as outside, and (A.20) becomes

$$\beta^P_{ij} + \beta^P_{ji} = 0.$$

A.8 Unsteady Conservation Equation

We require the conservation equation for the dynamical situation of Section 5.2. The derivation follows that of the Reynolds Transport Theorem of fluid dynamics (see Acheson 1990, p. 220), and is given in general before being specialised to the case considered in Section 5.2.

Let $V(t)$ be the volume occupied by a 'blob' of dislocations at time t, which we suppose to be dyed in order that one may follow its progress. Suppose also that $\omega(\boldsymbol{x}, t)$ is the dislocation number density at the point $\boldsymbol{x}$ (which moves with the dislocations) and time t. Then

$$\frac{d\boldsymbol{x}}{dt} = \boldsymbol{v}, \tag{A.22}$$

where $\boldsymbol{v}$, the dislocation velocity, is perpendicular to the dislocation lines, so we have $\boldsymbol{v} = A(\sigma_{ij} b_i m_j)\boldsymbol{n}$, where $\boldsymbol{n}$ is the normal to the dislocation lines in their slip planes, A is a mobility constant (Section 1.4.1) and it has been assumed that $a = 1$ in (1.16).

Since we require the total dislocation density in the dyed blob to remain constant in time, we need to show that

$$\frac{d}{dt}\int_{V(t)} \omega(\boldsymbol{x}, t) dV = 0. \tag{A.23}$$

If $\boldsymbol{x} = \boldsymbol{X}$ at $t = 0$, then we may write

$$\frac{d}{dt}\int_{V(t)} \omega(\boldsymbol{x}, t) dV = \frac{d}{dt}\int_{V(0)} \omega(\boldsymbol{X}, t) J dX_1 dX_2 dX_3, \tag{A.24}$$

where the Jacobian J is the determinant

$$J = \frac{\partial(x_1, x_2, x_3)}{\partial(X_1, X_2, X_3)}.$$

The integral on the right in (A.24) is over a fixed volume and so the derivative may be taken inside the integral sign to give

$$\frac{d}{dt}\int_{V(t)} \omega(\boldsymbol{x}, t) dV = \int_{V(0)} \left\{ \frac{\partial}{\partial t}\omega(\boldsymbol{X}, t)\, J + \omega(\boldsymbol{X}, t)\frac{\partial J}{\partial t} \right\} dX_1 dX_2 dX_3.$$

Now

$$\frac{\partial J}{\partial t} = \begin{vmatrix} \frac{\partial}{\partial t}\frac{\partial x_1}{\partial X_1} & \frac{\partial}{\partial t}\frac{\partial x_1}{\partial X_2} & \frac{\partial}{\partial t}\frac{\partial x_1}{\partial X_3} \\ \frac{\partial x_2}{\partial X_1} & \frac{\partial x_2}{\partial X_2} & \frac{\partial x_2}{\partial X_3} \\ \frac{\partial x_3}{\partial X_1} & \frac{\partial x_3}{\partial X_2} & \frac{\partial x_3}{\partial X_3} \end{vmatrix} + \begin{vmatrix} \frac{\partial x_1}{\partial X_1} & \frac{\partial x_1}{\partial X_2} & \frac{\partial x_1}{\partial X_3} \\ \frac{\partial}{\partial t}\frac{\partial x_2}{\partial X_1} & \frac{\partial}{\partial t}\frac{\partial x_2}{\partial X_2} & \frac{\partial}{\partial t}\frac{\partial x_2}{\partial X_3} \\ \frac{\partial x_3}{\partial X_1} & \frac{\partial x_3}{\partial X_2} & \frac{\partial x_3}{\partial X_3} \end{vmatrix}$$

$$+ \begin{vmatrix} \frac{\partial x_1}{\partial X_1} & \frac{\partial x_1}{\partial X_2} & \frac{\partial x_1}{\partial X_3} \\ \frac{\partial x_2}{\partial X_1} & \frac{\partial x_2}{\partial X_2} & \frac{\partial x_2}{\partial X_3} \\ \frac{\partial}{\partial t}\frac{\partial x_3}{\partial X_1} & \frac{\partial}{\partial t}\frac{\partial x_3}{\partial X_2} & \frac{\partial}{\partial t}\frac{\partial x_3}{\partial X_3} \end{vmatrix}$$

$$= J\,\boldsymbol{\nabla}.\boldsymbol{v}.$$

Thus

$$\frac{d}{dt}\int_{V(t)}\omega(\boldsymbol{x},t)dV = \int_{V(0)}\left\{\frac{\partial}{\partial t}\omega(\boldsymbol{X},t)+\omega(\boldsymbol{X},t)\boldsymbol{\nabla}.\boldsymbol{v}\right\}J\;dX_1dX_2dX_3$$

$$= \int_{V(t)}\left\{\frac{d}{dt}\omega(\boldsymbol{x},t)+\omega(\boldsymbol{x},t)\boldsymbol{\nabla}.\boldsymbol{v}\right\}dx_1dx_2dx_3$$

$$= \int_{V(t)}\left\{\frac{\partial\omega}{\partial t}+(\boldsymbol{v}.\boldsymbol{\nabla})\omega+\omega\boldsymbol{\nabla}.\boldsymbol{v}\right\}dV.$$

As this must vanish for all t, if dislocations are to be conserved, then

$$\frac{\partial\omega}{\partial t}+(\boldsymbol{v}.\boldsymbol{\nabla})\omega+\omega\boldsymbol{\nabla}.\boldsymbol{v}=0. \tag{A.25}$$

Equation (A.25) and the equations

$$\alpha_{in,i} = 0 \qquad (\alpha_{in}=\omega b_i\tau_n), \tag{A.26}$$

$$-(\varepsilon_{jmn}\alpha_{in,m})^S = \frac{1}{2\mu}\left(\sigma_{ij,kk}+\frac{2(\lambda+\mu)}{\lambda+2\mu}(\sigma_{kk,ij}-\sigma_{kk,ll}\delta_{ij})\right), \tag{A.27}$$

$$\boldsymbol{v} = A(\sigma_{ij}b_im_j)\boldsymbol{n}, \tag{A.28}$$

together constitute the model for the unsteady case. As mentioned in Section 2.2, (A.26) and (A.27) consist of seven equations for eight unknowns. (A.25) provides one more equation, and $\boldsymbol{v}$ contributes one more unknown (as it is confined to the slip plane, and its direction is known since $\boldsymbol{\alpha}$ is known). Finally, (A.28) represents

one independent equation, and so (A.25)-(A.28) consist of nine equations for nine unknowns.

In Section 5.2 the nonzero components of density are α_{22} and α_{33}, and the dislocations may only move parallel to the x_1-direction. Thus, for the α_{33} dislocations with speed v, (A.25) reduces to

$$\frac{\partial \alpha_{33}}{\partial t} + \frac{\partial (\alpha_{33} v)}{\partial x_1} = 0,$$

and for the α_{22} dislocations with speed v'

$$\frac{\partial \alpha_{22}}{\partial t} + \frac{\partial (\alpha_{22} v')}{\partial x_1} = 0,$$

as required.

References

Acheson, D.J., 1990, *Elementary Fluid Dynamics*, Oxford University Press.

Bailey, J.E., 1963, The dislocation density, flow stress and stored energy in deformed polycrystalline copper, *Phil. Mag.* **8**, 223-236.

Bailey, J.E. and Hirsch, P.B., 1962, The recrystallization process in some polycrystalline metals, *Proc. Roy. Soc.* A**267**, 11-30.

Batchelor, G.K., 1967, *An Introduction to Fluid Dynamics*, Cambridge University Press.

Bardeen, J. and Herring, C., 1952, Diffusion in alloys and the Kirkendall effect, in *Imperfections in Nearly Perfect Crystals*, Wiley, New York, 261.

Bilby, B.A., 1955, Types of dislocation source, in *Report of Bristol conference on defects in crystalline solids*, London:Physical Society, 124-133.

Bilby, B.A., Bullough, R., Gardner, L.R.T. and Smith, E., 1958 Continuous distributions of dislocations IV. Single glide and plane strain, *Proc. Roy. Soc.* A**244**, 538-557.

Burgers, J.M., 1939, Some Considerations of the field of stress connected with dislocations, *Proc. Kon. Ned. Acad. Wet.* **47**, 293-325.

Caffarelli, L.A. and Friedman, A., 1988, A model of dislocations and the associated free boundary problem, *IMA Preprint Series* #391, 1-27.

Chen, H.S., Gilman, J.J. and Head, A.K., 1964, Dislocation multipoles and their role in strain-hardening, *J. Appl. Phys.* **35**, 2502-2514.

Clemmow, P.C., 1973, *Introduction to Electromagnetic Theory*, Cambridge University Press.

Dash, W.C., 1956, Copper precipitation on dislocations in silicon, *J. Appl. Phys.* **27**, 1193-1195.

de Wit, R., 1960, The continuum theory of stationary dislocations, *Solid State Physics*, **10**, 249-292.

Eshelby, J.D., 1949, Edge dislocations in anisotropic materials, *Phil. Mag.* **40**, 903-912.

Eshelby, J.D., 1957, The determination of the elastic field of an ellipsoidal inclusion, and related problems, *Proc. Roy. Soc.* A**241**, 376-396.

Eshelby, J.D., Frank, F.C. and Nabarro, F.R.N., 1951, The Equilibrium of linear arrays of dislocations, *Phil. Mag.* **42**, 351-364.

Frank, F.C., 1948, On slip bands as a consequence of the dynamical behaviour of dislocations, in *Report on Strength of Solids*, Physical Society: London, 46-51.

Frank, F.C., 1955, Hexagonal networks of dislocations, in *Report of Bristol conference on defects in crystalline solids*, London:Physical Society, 159-168.

Furuhashi, R. and Mura, T., 1979, On the equivalent inclusion method and impotent eigenstrains, *Journal of Elasticity* **9**, 263-270.

Gavazza, S.D. and Barnett, D.M., 1976, The self-force on a planar dislocation loop in an anisotropic linear elastic medium, *J. Mech. Phys. Sol.* **24**, 171-185.E

Gay, P., Hirsch, P.B. and Kelly, A., 1954, X-ray studies of polycrystalline metals deformed by rolling. III. The physical interpretation of the experimental results, *Acta Cryst.* **7**, 41-49.

Head, A.K., 1972a, Dislocation group dynamics I. Similarity solutions of the n-body problem, *Phil. Mag.* **26**, 43-53.

Head, A.K., 1972b, Dislocation groups dynamics II. General solutions of the n-body problem, *Phil. Mag.* **26**, 55-63.

Head, A.K., 1973, Dislocation group dynamics VI. The release of a pile-up, *Phil. Mag.* **27**, 531-539.

Head, A.K., Howison, S.D., Ockendon, J.R. and Tighe, S.P., 1992, Mathematical modelling of dislocation plasticity, in *Contributions to Statistical Physics, Elasticity and Dislocation Theory, Festschrift in honour of Jens Lothe on his 60th birthday, 26 November 1991*, pp. 317-321, To be published as a topical issue of *Physica Scripta.*

Head, A.K., Howison, S.D., Ockendon, J.R., Titchener, J.B. and Wilmott, P., 1987, A continuum model for two-dimensional dislocation distributions, *Phil. Mag. A*, **55**, 617-629.

Head, A.K. and Louat, N., 1955, The distribution of dislocations in linear arrays, *Aust. J. Physics,* **8**, 1-7.

Head, A.K. and Wood, W.W., 1973a, Dislocation group dynamics *IV.* General solutions of the continuum approximation, *Phil. Mag.,* **27**, 505-17.

Head, A.K. and Wood, W.W., 1973b, Dislocation group dynamics *V.* Equilibrium revisited, *Phil. Mag.* **27**, 519-530.

Hirth, J.P., 1972, The influence of grain boundaries on mechanical boundaries, *Met. Trans.* **3**, 3047-3067.

Hirth, J.P. and Lothe, J., 1982, *Theory of Dislocations*, Second Edition, Wiley-Interscience.

Hull, D. and Bacon, D.J., 1984, *Introduction to Dislocations*, Third Edition, Pergamon Press.

Jaswon, M.A. and Bhargava, R.D., 1961, Two-dimensional elastic inclusion problems, *Proc. Camb. Phil. Soc.* **57**, 669-680.

Kadić, A. and Edelen, D.G.B., 1982, A Yang-Mills type minimal coupling theory for materials with dislocations and disclinations, *Int. J. Engng. Sci.* **20**, 433-438.

Kanninen, M.F. and Rosenfield, A.R., 1969, Dynamics of dislocation pile-up formation, *Phil. Mag.* **20**, 569-587.

Kröner, E., 1955, Der fundamentale Zusammenhang zwischen Versetzungsdichte und Spannungsfunktionen, *Z. Phys.* **142**, 463-475.

Kröner, E., 1958, *Kontinuumstheorie der Versetzungen und Eigenspannungen*, Springer, Berlin.

Kroupa, F., 1962, Continuous distributions of dislocation loops, *Czech J. Phys.* **B12**, 191-201.

Kuhlmann-Wilsdorf, D., 1987, Energy minimisation of dislocations in LEDs, *Phys. Stat. Sol. (a)*, **104**, 121-144.

Kuhlmann-Wilsdorf, D., 1989, Theory of plastic deformation:- Properties of low energy dislocation structures, *Mat. Sci. Engng.* A**113**, 1-41.

Kuhlmann-Wilsdorf, D. and van der Merve, J.H., 1982, Theory of dislocation cell sizes in deformed metals, *Mat. Sci. Engng.* **55**, 79-83.

Lardner, R.W., 1974, *Mathematical Theory of Dislocations and Fracture*, Univ. of Toronto Press, Toronto.

Leibfried, G., 1953, Versetzungen in Anisotropen Material, *Z. Phys.* **135**, 23-43.

Li, J.C.M., 1963, Petch relation and grain boundary sources, *Trans. AIME* **227**, 239-247.

Lighthill, M.J., 1980, *An Introduction to Fourier Analysis and Generalised Functions*, Cambridge University Press.

Love, A.E.H., 1927, *A Treatise on the Mathematical Theory of Elasticity*, Fourth Edition, Cambridge University Press.

Malis, T. and Tangri, K., 1979, Grain boundaries as dislocation sources in the premacroyield strain region, *Acta Met.* **27**, 25-32.

Mitchell, T.E., Hecker, S.S and Smialek, R.L., 1965, Dislocation pile-ups in anisotropic crystals, *Phys. Stat. Sol.* **11**, 585-594.

Moriguchi, S., 1947, Fundamental theory of the dislocation of elastic bodies, *Oyo Sugaku Rikigaku*, **1**, 29.

Mura, T., 1963, Continuous distribution of moving dislocations, *Phil. Mag.*, **8**, 842-857.

Mura, T., 1989, Impotent dislocation walls, *Mat. Sci. Engng. A* **113**, 149-152.

Nabarro, F.R.N., 1967, *Theory of Crystal Dislocations*, Oxford University Press.

Nye, J.F., 1953, Some geometrical relations in dislocated crystals, *Acta Met.* **1**, 153-162.

Ockendon, H. and Ockendon, J.R., 1983, Dynamic dislocation pile-ups, *Phil. Mag. A*, **47**, 707-719.

Orowan, E., 1934, Zur Kristallplastizität, *Z. Phys.* **89**, 605-659.

Peach, M. and Koehler, J.S., 1950, The forces exerted on dislocations and the stress fields produced by them, *Phys. Rev.* **80**, 436-439.

Pilecki, S., 1977, Analysis of the usefulness of diffusion equations for the description of dislocation mobility and related phenomena, *Arch. Mech.* **29**, 505-517.

Polanyi, M, 1934, Über eine Art Gitterstörung, die einen Kristallplastisch machen könnte, *Z. Phys.* **89**, 660-664.

Rosenfield, A.R., 1971, A continuous distribution of moving dislocations, *Phil. Mag.* **24**, 63-69.

Rosenfield, A.R. and Kanninen, M.F., 1970, The dynamics of dislocation pile-up formation with a nonlinear stress-velocity relation for dislcoation motion, *Phil. Mag.* **22**, 143-154.

Seeger, A., 1955, Theorie der Gitterfehlstellen, in *Handbuch der Physik*, **VII/1**, 383-665, Springer, Heidelberg.

Stein, A.N. and Low, J.R., 1960, Mobility of edge dislocations in silicon-iron crystals, *J. Appl. Phys.* **31**, 362-369.

Taylor, G.I., 1934, The mechanism of plastic distortion of crystals, *Proc. Roy. Soc.*, A**145**, 362-404.

Titchener, J.B., 1988, Continuum models for dislocation distributions, *D. Phil. Thesis*, Oxford University.

Volterra, V., 1907, L'Equilibre des corps élastiques multiplement connexes, *Ann. Sci. Ecole Norm. Sup.* **24**, 401-517.

von Mises, R., 1928, Mechanik der plastischen Formänderung von Kristallen, *Z. ang. Math. Mech.* **8**, 161-185.

Willis, J.R., 1967, Second-order effects of dislocations in anisotropic crystals, *Int. J. Engng Sci.* **5**, 171-190.

Walgraef, D. and Aifantis, E.C., 1985a, On the formation and stability of dislocation patterns - *I*:One dimensional considerations, *Int. J. Eng. Sci.* **23**, 1351-1358.

Walgraef, D. and Aifantis, E.C., 1985b, On the formation and stability of dislocation patterns - *II*: Two-dimensional considerations, *Int. J. Eng. Sci.* **23**, 1359-1364.

Walgraef, D. and Aifantis, E.C., 1985c, On the formation and stability of dislocation patterns - *III*: Three-dimensional considerations, *Int. J. Eng. Sci.* **23**, 1365-1372.

Wood, W.W. and Head, A.K., 1974, The motion of dislocations, *Proc. Roy. Soc.*, A**336**, 191-209.

Wood, W.W. and Head, A.K., 1984, Dislocation pile-ups and stress intensity factors, *Quart. J. Mech. Appl. Math.* **37**, 161-178.

Young, C.T., Headley, T.J. and Lytton, J.L., 1986, Dislocation structures formed during the flow stress recovery of high purity aluminium, *Mat. Sci. Engng.* **81**, 391-407.